Physics – Uspekhi **45** (10) 1019 – 1050 (2002)

REVIEWS OF TOPICAL PROBLEMS PACS numbers: **07.77. – n**, **34.50. – s**, **82.55. + e**

Theoretical aspects of the formation and evolution of charged particle tracks

A M Miterev

DOI: 10.1070/PU2002v045n10ABEH001201

Contents

Abstract. Theoretical ideas on the formation and evolution of charged particle tracks in a condensed medium are discussed. The historical development of the field is briefly reviewed. The distribution of charged particle energies over quantum states and the volume of the absorbing medium are considered, and conditions for the formation of various track structures (entities) are discussed. The structures of extended heavy-ion tracks are compared for some ion parameters and track characteristics under equal conditions. Relaxation processes in the tracks of multiply charged ions are analyzed. Track effects are considered and possible mechanisms for the formation of chemically active defects in a latent track are described.

A M Miterev Obninsk Branch of the State Research Center 'Karpov Institute of Physical Chemistry', 249033 Obninsk, Kaluga Region, Russian Federation
Tel. (7-08439) 9 49 91

Received 15 February 2002, revised 5 June 2002
Uspekhi Fizicheskikh Nauk **172** (10) 1131 – 1164 (2002)
Translated by A S Dobroslavskiĭ; edited by M I Zel'nikov

1. Introduction

Ninety years ago the track of an α-particle was photographed for the first time in a Wilson cloud chamber [1]. First observations of the track confirmed the notion that charged particles trigger changes in physical and chemical properties of the medium, and showed that these changes only affect local microscopic volumes of the medium located along the

path of the particle. Observations of tracks in Wilson chambers became a valuable tool for studying the nuclear processes involving elementary particles. The need for devices capable of studying the nuclear processes involving elementary particles has subsequently led to the invention of bubble chambers [2], photo emulsions [3], also useful for visualization of tracks.

In 1959, long and thin (about 3 nm in diameter) damaged filaments were detected with an electron microscope in mica exposed to fragments of the fission of uranium. Such traces became known as 'latent' tracks [4]. These observations stimulated keen interest in studying the tracks of heavy ions in solids. Direct observations of latent tracks were hindered by the fact that in most materials under an electron microscope they rapidly disappeared. This unfortunate feature could be rectified by chemical etching of the exposed material. It turned out that after treatment of the mica with certain chemicals, the latent tracks of uranium fission products increased to a size at which they became visible through an optical microscope [5].

The class of solids that may host etched tracks is quite broad — glasses, minerals, polymers, and certain semiconductors [4–6]. Numerous studies reveal that etchable tracks may be detected in many crystals with ion bonds (alkaline-haloid crystals, micas), in some crystals with covalent bonds, and in polymers — but only when the parameters of ions exceed certain threshold values [6]. In metals, which feature perfect structure and high electric conductivity, no tracks are usually left even by the high-charge ions. The tracks, however, may appear when the crystal lattice of the metal has defects. An intermittent track is formed in metallic film made up of numerous mosaic blocks. The track is developed in the smaller blocks, but not in the larger ones [7].

Every material capable of hosting etchable tracks has its own detection threshold that depends on the properties of the etching solution. The configuration of pores resulting from chemical etching of dielectric materials exposed to ions depends on the type and parameters of the ions. This correlation was first used for the development of solid state track detectors (SSTD) for identification of charged particles [5, 6]. This requires direct calibrations: the material is exposed to known particles, and the resulting tracks are associated with the parameters of the particles. Such calibration data can then be used for identifying the parameters of unknown particles.

The effect of formation of through channels after chemical etching of polymer film exposed to heavy ions is employed for manufacturing polymer membranes using beams of heavy ions [8] and fragments of fission of nuclear fuel. The *track* method is used for making printed structures on solids and for making separation media for fine filters [8, 9]. Calibration data are also needed for selecting the right ions for obtaining channels of the desired profile and size.

Direct calibrations, however, require accelerators with versatile capabilities. The calibration process is complicated and expensive. Therefore, it would be good to use this procedure only in exceptional cases, and instead forecast the parameters of the tracks from the detailed knowledge of the processes of track formation and development. Unfortunately, this is a very arduous task: the process of track formation and development is very fast, and defies experimental observation.

Many phenomena that occur in a condensed medium irradiated with charged particles are due to the processes that take place in the tracks. First of all, such phenomena include radiation induced in water and water solutions of biologically important substances. It was in these domains that, using the knowledge of the processes taking place in the tracks of charged particles, it was possible to explain the so-called *track effects* — the dependence of the radiation effects on the form of the ionizing radiation [10–16]. Knowledge of the processes of the development and evolution of tracks of charged particles has been used to explain the formation of latent tracks in solids (see, for example, Refs [4–6]). Based on the experimental data on the threshold values of the energy of ions at which a latent track becomes an etchable track, different criteria of track formation were formulated. Notwithstanding certain differences, most of these criteria were derived from the assumption that the disruptions caused by the ion in the medium depend on a particular characteristic of the track — namely, on the linear energy transfer [6]. There were attempts to use the concept of tracks for explaining the inelastic sputtering of solids with ions [17].

A track becomes observable owing to a change in the properties, structure or phase state of matter close to the path of a charged particle. These changes are the reaction of the medium to the disturbance caused by the charged particle. The initial stage of this disturbance is the transfer of energy to the medium by the charged particle. At the initial (*physical*) stage the energy transferred to the medium is shared among the quantum states of the absorbing system. This gives rise to the *primary track*. The description of the spatial dimensions of this track and the spectrum of primary particles resulting from the physical processes of the interaction of a charged particle with matter is the goal of the study of the structure of the primary track.

The time needed to form the complete track depends on the time of deceleration of a charged particle in the medium. The time of deceleration of an ion with an initial energy of 4 MeV $(\text{a.m.u.})^{-1}$ in a condensed medium is 2 to 3 ps. However, this time may be even less for those parts of the track that are still long enough compared to the radial dimension of the track. For example, for a path length of 2 μm, where the ion has an energy of 4 MeV $(\text{a.m.u.})^{-1}$, the redistribution of the energy transferred to the medium within this volume is over in 75 fs. The processes on this time scale defy direct experimental observation, so the only way of studying the structure of the primary track is through theoretical analysis using the methods of mathematical simulation.

Theoretical study of the structure of tracks of charged particles and the processes that take place therein dates back to the earliest observations of tracks. Such studies have been most intensely pursued in radiation chemistry and radiation biology. This review is concerned with theoretical concepts of the processes of formation of primary tracks of charged particles in a condensed medium of molecular composition. In the beginning we give a brief historical account of the development of the concept of charged particle tracks. Then, based on the physics of interaction of charged particles with the molecules of the medium, we consider the distribution of the energy of a charged particle over the quantum states of the absorbing medium, the distributions of the emerging primary active particles over the volume of the medium, the classification of the track entities (shapes, structures) and the conditions of their formation. Special attention is paid to the formation of primary tracks of heavy ions. Some issues related to the

topic under discussion are considered in detail in the reviews [10–16] and in the literature cited in the text.

2. Overview of the development of concepts of charged particle tracks

2.1 Early models of tracks

The earliest model of tracks is probably the notion formulated by Jaffe in 1913, who considered the tracks of alpha-particles in a Wilson chamber as cylindrical ion columns [18]. Assuming Gaussian distribution of ions of each sign in such a column, Jaffe considered the diffusion of ions from the track, with recombination taken into account. This diffusion recombination process is described by a nonlinear differential equation that defies analytical solution. The approximate solution of this problem was obtained under the assumption that the reduction in the concentration of ions in the column is more affected by the diffusion of ions than by the recombination. Such a condition allows one to assume that the distribution of ions remains Gaussian even though the concentration of ions decreases with time. Such an assumption, known as the assumption of prescribed diffusion, was widely used later for calculating the characteristics of chemical transformations in a medium after exposure to charged particles.

In 1934 Lea [19] represented the track in the ionization chamber as a set of isolated *clusters*. Using the approach developed by Jaffe, Lea considered the recombination of ions in different clusters taking into account possible overlapping. These concepts of tracks in ionization chambers were later used for calculating the coefficients of recombination of ions in gases [20], and for measuring the linear energy transfer and the quality coefficient of radiation [21].

The development of nuclear power engineering in the middle of last century stimulated intensive development of radiation chemistry and radiobiology. The construction of nuclear reactors required knowing the radiation stability of water, various water solutions, polymers, hydrocarbons, and many other materials. The study of radiation-induced transformations in water and water solutions of biologically important species was necessary for evaluating the effects of ionizing radiation on living matter. This is why the studies were focused on the radiation chemistry of water and water solutions.

The basics of the theory of interaction of ionizing radiation with matter have already been formulated [22, 23]. The concept of linear energy transfer (LET) was introduced in order to characterize the quality of radiation. Depending on LET, the ionizing radiations were divided into three types: low LET (below 1 eV nm^{-1} in water), medium LET (1 to 100 eV nm^{-1}), and high LET (above 100 eV nm^{-1}). The interpretation of experimentally observed yields of radiolysis products as functions of LET involved the so-called *track effects*, because the degree of inhomogeneity in the distribution of active particles in the tracks had a considerable impact on the overall chemical effects. The quantitative description of chemical transformations in the tracks by chemical kinetics methods required more detailed knowledge of the initial distribution of the reacting particles in the track. The construction of track models was based on the concept of LET and was inseparable from the study of the mechanisms of transformation of the primary particles (ions, electrons, and electron-excited molecules).

Lea was the first to clearly formulate and use diffusion kinetics for tracks of charged particles [19, 24]. According to Lea [19, 24, 25] and Gray [26], in the case of inelastic interactions of charged particles with water molecules, the energy transferred to the medium is used for the formation not only of individual electron-excited molecules or ion-electron pairs, but also of the local regions of ionization and excitation that contain two or more ion pairs. It is these regions that Lea and Gray referred to as *clusters*.

According to Ref. [26], the relative frequency of occurrence of clusters with two, three or more ion pairs shows little dependence on the velocity of the charged particle and the nature of the medium. The nature of the medium, however, has an impact on the ratio of the number of clusters to the number of loose ion pairs. According to Ref. [26], the frequencies of occurrence of clusters of 2, 3, 4 and 8 ion pairs in water are 0.22, 0.11, 0.10 and 0.07, respectively. The frequency of occurrence of a loose pair is 0.45. In the cluster the positive ions are separated by 3 nm, while the mean distance between the ions of opposite signs is 15 nm. The negative ion in this case is the molecule of water that captured a thermalized electron knocked out by ionizing radiation.

In the track of a fast electron the mean distance between the positive primary ions is much greater than 15 nm, and therefore the clusters are isolated from one another. When the energy of the electron is less than 1.5 keV, the clusters start to overlap. The track becomes an ion column. Tracks in the form of ion columns are formed by protons with energy below 3 MeV, and by α-particles with energy below 12 MeV. The distribution of ions in the column was assumed to have the following pattern: the positive ions were located close to the path of the heavy ion, whereas the negative ions occupied a cylinder 15 nm in radius. Platzman [27] advanced these concepts, assuming that the electron, in the process of thermalization, traveled a long way away from the parent ion, and, instead of being neutralized at once, became loose in a sense. Owing to the polarization of the medium it becomes surrounded by the oriented molecules of the liquid. This was the prediction of the hydrated electron in the irradiated water, which was confirmed later on.

Samuel and Magee [28] treated the destiny of the ionized states in a different way [28]. They held that the electron knocked out from the water molecule in the course of ionization cannot leave the Coulombian field of the parent ion and is attracted by the ion after thermalization. The recombination produces an excited water molecule that splits into H and OH. They called the ionization group from one or more ion pairs, located near the unitary act of primary ionization, a *spur*.

By the start of the chemical stage the spur was viewed as a spherically symmetrical formation in which the H and OH radicals are distributed according to Gaussian law with respect to the center of the spur with equal widths. The initial volumes of spurs, and therefore the widths of the initial distributions of radicals, are taken to be proportional to the number of radicals in the spur N_R. The distribution of spurs with respect to the size was described by the analytical expression of the form

$$f(N_R) = 0.65 \exp\left(-\frac{N_R}{4}\right).$$

The mean value of the spur from this distribution corresponds to 2.54 radical pairs per primary ionization. According to

Ref. [28], the track of the fast electron was represented as a set of non-overlapping spurs. The deceleration of the primary particle was not taken into account, and no distinction was made between the tracks of the primary and secondary electrons. The track of the α-particle was considered to be a cylindrical column consisting of overlapped spurs.

2.2 Tracks of particles with low LET

The Samuel – Magee model of the fast electron track [28] was subjected to a rigorous check for its suitability for explaining the dependence of yields of products of radiolysis on the conditions of irradiation. Even the creators of the model, using the reaction of one type of radical, calculated the ratios of molecular yields to the total yield of water decomposition for spurs of different sizes, and obtained values close to those observed experimentally. However, the use of specially fitted parameters in the model compromised its plausibility. At the same time, the model of the spur was used with certain modifications by many researchers for quantitative assessment of the more complicated reaction schemes (the presence of several radicals or an acceptor in the spur) (see the review in Ref. [10]).

Kuppermann and Belford [29] performed a computer analysis of the applicability of different parameters and approximations in the calculations, and came to the following conclusions. For a period of time from 10 to 100 ps the recombination of radicals dominates in the spherical spur. Any initial distribution of radicals becomes Gaussian after 1 ns, and from this time the approximation of prescribed diffusion becomes quite acceptable. The yields of products of radiolysis depend considerably on the width of the initial distribution, the diffusion and the reaction rates.

When the value of LET is assumed to increase as the electron slows down, the model of the electron track had to be modified. Ganguly and Magee [30] considered a model of the electron track consisting of spurs of the same size, the distance between which decreases exponentially as the residual path of the electron decreases. Taking into account the recombination of radicals from adjacent spurs, in this way they studied the effects of the overlapping of spurs as a result of the increase of the electron's LET towards the end of the path.

Mozumder and Magee [31] resolved this problem in a different way. They eliminated the need to take into account the overlapping of spurs by introducing additional track entities. Depending on the energy transmitted by the electron in a single act of interaction, the resulting track structure was attributed to the appropriate class. According to the classification, the energy transmitted by the electron to the medium is used for the formation of spurs with energy from 6 to 100 eV, the so-called *blobs* with energy from 100 to 500 eV, and *short tracks* when the energy transmitted to the medium is in the range from 500 to 5000 eV. A blob is defined as an entity generated by a secondary electron, whose energy exceeds 100 eV but is still not sufficient for the electron to escape from the field of the parent ion. According to the authors, an electron whose energy exceeds 625 eV is capable of escaping recombination with the parent ion in water at room temperature. Based on this estimate, the upper energy limit for a blob was assumed to be 500 eV. Later Magee and Chatterjee [32] used a value of 1.6 keV for the upper energy limit of the blob. They argued that below this limit the deceleration of the electron is much influenced by the process of elastic scattering that facilitates the overlapping of spurs. The blob resembles a pear-shaped drop. However, in the calculations of internal reactions the blob was considered as a large spherical spur [31] or an ellipsoid [32].

In Ref. [31] it was assumed that the initial dimensions of spurs and blobs were proportional to the number of primary particles, or that the initial size of the spur was $r_0 \approx \varepsilon^{1/3}$, which is the same thing. For a spur with $\varepsilon = 100$ eV the initial radius was assumed to be 1.7 nm. Magee and Chatterjee in Ref. [33] treated the dependence of the size of the spur on the number of particles in the spur in a different manner: the size of the spur is supposed to decrease as the number of particles in the spur increases. They came to this conclusion based on the concept of the electron – ion pair as a Rydberg state of the molecule. The size of the electron orbit in this state does not exceed 3 to 3.5 nm before hydratation. When the spur contains several ion pairs, the electron moves in the field of several ion centers, and therefore the radius of its orbit decreases. According to Ref. [33], the initial radius of a spur with one electron – ion pair is of the order of 3 nm, whereas the size of a spur made up of six ion pairs (100 eV) corresponds to the initial radius of 2 nm.

A short track is made up of overlapping spurs. The upper energy limit of the electron forming the short track is determined by the following considerations [31]. The overlapping of spurs affects the reactions in the spurs as long as the mean distance between them does not exceed $10r_0$. This condition is satisfied by an electron with an energy of 5 keV, for which the mean free path between the acts of energy transfer with spur formation is about 10 nm. A secondary electron with energy above 5 keV forms a *branch track*, whose structure is similar to that of the main track. As a rule, it is assumed that the short track has a cylindrical geometry, even though this is not quite consistent with its actual shape. Owing to the processes of elastic scattering, the path of the electron is curved when its energy is below 1.6 keV. In the energy range set in Ref. [32] for the short track, the shape of the short track is practically cylindrical.

The energy distribution of the primary electron between the track structures that make up the main track and its branches was calculated in Ref. [31] by the Monte Carlo method. The calculations indicate that, as the energy of the primary electron increases, the energy share used for the formation of isolated spurs increases mainly at the expense of the energy used for the formation of short tracks. While the energy split between spurs, blobs and short tracks stands as 25 : 10 : 65 (per cent) for an electron with energy 10 keV, the ratio is 67 : 11 : 22 for an electron with energy 1 MeV.

Santar and Bednar [34] carried out a detailed calculation of the energy distribution over the track structures of the electron. In their calculations they assumed that the electron forming a short track has sufficient energy to generate additional short tracks and blobs. They also assumed that each branch track ends with a short track, and each short track ends with a blob. All these assumptions were taken into account by calculating the complete spectrum of degradation of electrons (both primary and secondary). In the complete spectrum of degradation of electrons, the share of spurs is somewhat smaller, and the energy split for the electron with an energy of 1 MeV is 64.7 : 11.9 : 23.4.

The degradation spectrum of charged particles is an important characteristic of ionizing radiation. It is the energy spectrum of the charged particles that actually exist in the irradiated medium. The theory of electron degradation spectrum was developed by Spencer and Fano [35]. They

showed that the spectral intensity is conveniently represented by the quantity $Y(T, E_0)$, which has the dimension of length over energy. With such a representation, $Y(T, E_0)\,dT$ is the total distance traveled in the medium by all electrons (the primary electron with an initial energy E_0, the secondary electron and all the next-generation electrons) with energies in the range of T to $T + dT$. Using the degradation spectrum $Y(T, E_0)$ it is possible to define the total number of primary particles of different types formed in the irradiated medium at the initial stage of radiolysis [36–38]. To find the spatial distribution of primary particles, it is necessary that the spectral intensity be a function of the space variable. Attempts to calculate this characteristic have been made too [39].

Calculating spectral intensity $Y(T, E_0)$ by solving the Spencer–Fano equation is a formidable mathematical task. Therefore some authors have used the method of statistical investigation — the Monte Carlo method — for finding the distribution of electrons with respect to energies [31, 34, 40]. Kaplan and colleagues [40] used the Monte Carlo method for calculating the degradation spectrum in water of the monochromatic electron beam with an energy of 10 keV, assuming classical interaction cross sections. They found that before degrading to $T < I$ (where I is the energy of ionization of a water molecule) the primary electron is engaged in 386 instances of inelastic collisions, losing about 25 eV per collision. In the course of degradation the primary electron knocks out about 150 secondary electrons, more than one half of which (~ 81.5) fall in the energy range of 0 to 10 eV. In turn, the secondary electrons generate ~ 376.5 tertiary and all next-generation electrons.

Simulation of the degradation of a fast electron in Refs [31, 34, 40] has actually been based on the representation of a condensed medium by means of a model of dense gas, ignoring the interaction between the molecules (atoms) in the condensed phase. It was experimentally established that the ionization potential is reduced by $\Delta I \sim 1-2.5$ eV [15] upon transition from the gas to the liquid phase. Even more dramatically changed is the form of the function of energy loss of the fast electron $\mathrm{Im}\left[-1/\epsilon(\omega)\right]$, where $\epsilon(\omega)$ is the dielectric permittivity of the medium [41, 42].

The availability of experimental data on the function $\mathrm{Im}\left[-1/\epsilon(\omega)\right]$ for liquid water [41] opened the door to simulating the primary stage of the radiolysis of water, taking into account the features of the condensed phase. Such simulation by the Monte Carlo method was first done in Refs [43, 44], and then in Refs [45–48]. Simulated in Ref. [44] were the radiation-induced transformations in the electron track with initial energy 5 keV. The coordinates of the acts of ionization and excitation were first calculated. Based on the selected mechanism of transformation of primary particles (H_2O^+, H_2O^* and e^-), the track evolution was then followed up to the onset of the chemical stage of radiolysis — that is, up to the time point of 10 ps. Having thus obtained the distribution of chemically active particles (H_3O^+, OH, H and e_{aq}), the transformations of the latter were further studied owing to the diffusion-controlled reactions up to the time of 0.28 μs.

In Refs [45, 46] the tracks of the electrons were studied by the so-called 'stochastic' approach, which employs the Monte Carlo method for snapshotting the instant pattern of spacial distribution of excitations and ionizations. In this case the tracks are sets of points in the space where the acts of inelastic scattering have taken place. Sets of such tracks allow the calculation of the spectrum of the absorbed energy in the sensitive volumes of the irradiated medium [46], or the calculation of the shapes of lines and the droop of signals of the electron spin echo [47].

Simulation of the primary stage of radiolysis in liquid water and water vapor upon exposure to fast electrons was done in Refs [48–51]. Calculated are the yields of the primary excited and ionized states, the evolution of these states, and the yields of the products of radiolysis. The main results are discussed in Section 4 below.

2.3 Tracks of particles with intermediate values of LET

Intermediate values of LET (from 1 to 100 eV nm^{-1} in water) may be exhibited both by the low-energy electrons and by the ions of light elements (protons, α-particles). Because of this, the tracks of ions in early models were considered in the same way as the tracks of low-energy electrons [26, 28]. It was assumed that in the track of the ion the spurs overlapped so heavily as to produce a cylindrical column. Neglected, however, was the fact that the interaction of heavy charged particles with matter is different from the interaction of electrons. The difference consists mainly in the distribution of secondary electrons with respect to energy and angle. In addition, the recharging processes affect the deceleration of a heavy charged particle in the medium.

Taking these differences into account, Mozumder, Chatterjee and Magee [52] proposed the model of track of heavy nonrelativistic particle composed of two regions. The region in the shape of a cylindrical column with a high value of LET, located near the path of the ion, they referred to as the *core*. The core is formed by the overlapping spurs generated by the primary ion and the track entities (spurs, blobs and short tracks) generated by the secondary electrons passing through the core. The electrons in the low-energy spectrum may completely lose their energy within the core. The high-energy secondary electrons lose part of their energy in the core, and carry the remaining part out of the core, creating a second region of the track with low LET.

For nonrelativistic ions the size of the core was selected based on the following considerations. For ions with velocity $v \leqslant v_0 = 2.28 \times 10^9$ cm s^{-1} the radius of the core was taken to be equal to the path of the electron with energy $E = 100$ eV, which is $r_c = 1.5$ nm. For ions with velocity $v \geqslant v_0$ the radius of the core was defined as $r_c = v/2\omega_{01}$, where $\hbar\omega_{01}$ is the lowest energy of the transition. This expression was derived from Bohr's principle of adiabatic collisions. This principle states that with the impact parameter $b \geqslant r_c$ with respect to the electron excitation with the transition energy $\hbar\omega_{01}$, the collision of an ion with a molecule located at a distance b from the path of the ion is adiabatic and the molecule is not excited. Magee and Chatterjee [53] calculated the radius of the core by the formula $r_c = v/\omega_{pl}$, where ω_{pl} is the plasma frequency. For calculating the radius of the core, Kaplan and Miterev [14, 54] proposed the expression $r_c = \pi v/\omega_{01}$, which is derived from the formula describing the probability of excitation of the molecule as a function of the impact parameter.

These formulas do not take into account the attenuation of the field created by the moving charge because of polarization of the medium. Because of this, at relativistic ion velocities the radii of the core calculated with these expressions with the Lorentz correction are overestimated. In the limit $v \to c$ the radius of the core tends to infinity ($r_c \to \infty$). In order to obtain finite values of the core radius at $v = c$, Mozumder [55] introduced an additional constraint on

the core radius related to the polarization of the medium. The author [56, 57] resolved this problem in the following manner. First, the expression that defines the probability of excitation in a condensed medium as a function of the impact parameter is obtained. Then the principle of adiabatic collisions is used for deriving the formula for calculating the radius of the core with due consideration for the dielectric properties of the medium.

The region of the track surrounding the core was at first called the *sheath*. Then Magee and Chatterjee [53] suggested the term *penumbra* (literally, half-shade) for this part of the track. As a rule, the penumbra is made up of non-overlapping track entities produced by secondary electrons, and, unlike the core, is a region with a nonhomogeneous distribution of active particles. However, this circumstance was ignored in the studies dealing with the calculation of radial distribution of energy in the track of the ion.

The energy distribution in the track of an ion with reference to the description of initiation of visible tracks in bubble chambers was first estimated by Kagan [58]. The distribution of energy of secondary electrons was calculated by the model of continuous deceleration under the assumption that they are emitted from the axis of the track at right angles from the axis. Such assumptions were used in the works of Katz and colleagues [59, 60]. Angular distribution of secondary electrons with respect to the axis of the ion track was done in Refs [61, 62]. Radial distribution of energy in the tracks of ions was also calculated in Refs [63 – 67]. The Monte Carlo method was used for this purpose in Ref. [67].

Numerous theoretical and experimental studies (see, for example, Refs [68, 69]) have been concerned with radial energy distribution in the ion tracks. To understand the detailed structure of the track, however, one needs to know not only the radial energy distribution, but also the distribution of the emerging primary active particles with respect to the volume of the track and the quantum states. For this purpose the Monte Carlo method was used in Ref. [70] for studying the radial distribution of energy losses, the distribution of concentration of emerging ions, the excited molecules, and the energy distribution of the degradation electrons at different distances from the axis of the ion track. As already indicated, if the electron degradation spectrum is known, it can be used for finding the distribution of the primary active particles with respect to the quantum states.

2.4 Tracks of particles with high LET

As a rule, it is the multiply charged ions that display the value of LET in water above 100 eV nm^{-1}. The interest in studying the tracks of such ions arose initially in connection with the fragments of the fission of nuclear fuel. The development of nuclear power engineering stimulated the search for various applications of nuclear energy in energy-intensive industries. One such technology makes direct use of the kinetic energy of the fragments, which constitutes as much as 80% of the total energy of fission, for chemical synthesis in endothermic processes. The radiation chemistry processes that take advantage of the kinetic energy of the fission fragments became known as *chemonuclear* processes [71].

Investigating the radiolysis of methanol exposed to fission fragments, Bulanov and colleagues [72] found that the exposure to the fission fragments, on the one hand, increases the yield of the low-molecular products of radiolysis; on the other hand, however, the yield of ethylene glycol increases not with the higher LET of the fragment, as expected, but, on the contrary, with the lower values of LET. These results could not be interpreted within the framework of existing models of ion tracks. To explain these results it was necessary to understand first that the structure of the track of a multiply charged ion is different from the structure of tracks of protons, α-particles and ions of light elements [73, 74].

Owing to its high ionizing ability, the fission fragment generates a large number of secondary electrons per unit length of track. As a result, the tracks of electrons overlap not only in the core but also beyond — that is, the penumbra becomes a continuous sheath. Taking this into account, Mozumder, Chatterjee and Magee [52] represented the track of a fission fragment as a cylindrical core with radius $r_c = 1.5$ nm surrounded by a cylindrical shell with radius $r_{sh} = 6$ nm. This model was further refined in Refs [73, 74], and in subsequent works by the author.

In concluding our historical overview, we ought to observe that a large number of studies are concerned with tracks in solid dielectrics. These studies advanced as follows. It was experimentally established that etchable tracks did not always appear in dielectrics exposed to particles with different ionizing powers. For quantitative interpretation of this fact the criterion of the formation of tracks was first formulated, and then various mechanisms were proposed to account for the formation of latent tracks. Using the proposed models of formation of latent tracks, various parameters of the particle were tested as the criteria responsible for the rate of etching of the track (see Ref. [5]). For example, the *model of ion explosion wedges* assumes that it is only the initial ionizations and excitations that create those chemically active defects which are responsible for the increased etching rate [6].

These studies, however, failed to give a clear insight into the nature of processes and defects associated with the formation of a track. This is probably because the majority of these studies were designed with a view to immediate practical application of etchable tracks. For identification of particles according to the geometrical dimensions of etched tracks it was sufficient to establish the relation between the etching rate and the selected criterion. The most important result of these studies is the fact that the tracks are formed by the ions in the energy range where the inelastic interactions are the main processes of interaction between the charged particle and the medium [5].

3. Probability of transition from one state to another under time-dependent perturbation. Principle of adiabatic collisions and its implications

3.1 Processes of interaction of a charged particle with the medium and their role in radiation-induced transformations

Passing through a medium, a charged particle loses its energy in collisions with electrons and nuclei and in various associated processes of emission of radiation (bremsstrahlung, transition radiation, Cherenkov radiation). An analysis of the processes of interaction of a charged particle with the medium reveals that the radiation-chemical transformations occur mainly at the expense of the energy of the charged particle transmitted to the medium as a result of *inelastic* collisions. By contrast, radiation physics is mainly concerned with the defects ultimately resulting from *elastic* processes. The role of radiation is assumed to be negligible, not only

because the coefficient of conversion of the energy of a charged particle into radiation is small, but also because the energy of such radiation, as a rule, is weakly absorbed by the medium, and is carried beyond the confines of the exposed volume.

An analysis of the energy dependence of the cross sections of elastic and inelastic scattering of charged particles by a molecule of water reveals that the total cross section of elastic scattering becomes comparable with the total cross section of inelastic scattering and ionization when the energy of ions is less than 1 MeV (a.m.u.)$^{-1}$. However, the elastic collisions that lead to rupture of molecular bonds or to the formation of primary atoms have a low probability (by two orders of magnitude or more) compared to the processes of inelastic scattering down to energies of 10 keV (a.m.u.)$^{-1}$, below which the excitation of the electronic states is not possible. Therefore, the contribution of elastic scattering processes to the formation of a track can be generally neglected when the energy of the charged particle is sufficient for the collisions leading to excitation of the electron levels. It is only when the energy of the ion is less than 10 keV (a.m.u.)$^{-1}$ that the elastic collisions are important for the formation of the track.

To support this argument, Fig. 1 shows the energy dependencies of various cross sections of interaction of oxygen ions with a water molecule. The total cross section of elastic scattering is calculated in accordance with the additivity rule, and is the sum of cross sections of scattering by individual atoms calculated in the approximation of shielded Coulombian potential (see Ref. [23]). For the shielding parameter we used the screening parameter used for the Thomas–Fermi–Firsov potential. The cross section of rupture of the H–OH bond in a water molecule is twice the cross section of elastic collisions of ions with a H atom, at which the energy received by the atom exceeds 5 eV — the energy of the H–OH bond. Cross sections of ionization and inelastic scattering (the sum of the total cross section of excitation and ionization) were calculated by formulas cited in the review [15].

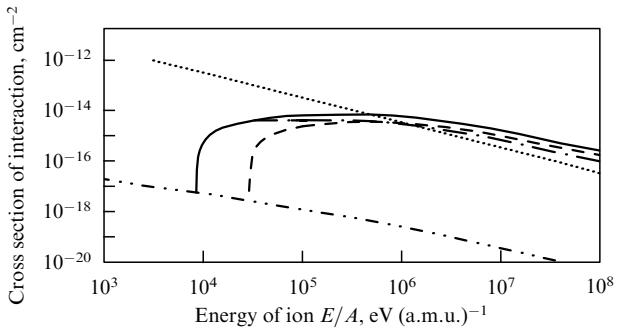

Figure 1. Total cross sections of elastic (· · ·) and inelastic (—) scattering, cross sections of ionization (– – –), excitation (– · –), and rupture of the H–OH bond (– · · –) at the interaction of an oxygen ion with a water molecule.

3.2 Excitation of atoms and molecules

In the course of inelastic processes the charged particle interacts with the electron subsystem of the medium. The result of such an interaction is excitation or ionization of the atom (molecule). In the first-order approximation of perturbation theory, the probability of transition of a quantum system from the initial state (subscript '0') to the jth excited state is [75]

$$w_{0j} = \left| \frac{1}{\hbar} \int_{-\infty}^{+\infty} \langle 0 | V(t) | j \rangle \exp(\mathrm{i}\omega_{0j} t) \right|^2 \mathrm{d}t , \tag{1}$$

where $\langle 0 | V(t) | j \rangle = \int \varphi_j^* V(t) \varphi_0 \, \mathrm{d}\xi$ is the matrix element of the excitation operator $V(t)$, defined using the nonperturbed functions, and $\hbar\omega_{0j}$ is the energy of the transition.

From (1) it follows that if the perturbation $V(t)$ shows little change over the period of oscillation

$$\tau_{\mathrm{qu}} = \frac{2\pi}{\omega_{0j}} , \tag{2}$$

which characterizes the quantum system, then the integrand in (1) oscillates repeatedly over the duration of the interaction, and the value of the integral in (1) is close to zero. Interactions of this type are referred to as *adiabatic*. When the change of the applied perturbation is slow enough (adiabatic), the system that occurs in a particular nondegenerate steady state remains in the same state. The electron subsystem adapts to the perturbation, and the probability of any transition at a nonzero frequency is zero. This is the *principle of adiabatic collisions*.

To study the effects of charged particles on matter, and in particular the formation of space structure of tracks, it is necessary to know not only the probability defined by (1), but also the probability $P_{0j}(b)$ of excitation or ionization of the molecule depending on the distance to the path of the particle (that is, as a function of the impact parameter b). The probability $P_{0j}(b)$ is found in the quasi-classical approximation. Such problems have been solved for particles moving at nonrelativistic velocities (see Refs [75, 76]), and at ultrarelativistic velocities (see, for example, Ref. [77]).

The quasi-classical approximation assumes that the charged particle is moving along a certain path and acts on the ith electron of the molecule with force $\mathbf{F}_i(\mathbf{R}_i) = e\mathbf{E}_i(\mathbf{R}_i)$, where $\mathbf{E}_i(\mathbf{R}_i)$ is the strength of the electric field of the particle, $\mathbf{R}_i(t) = \mathbf{R}_0(t) + \mathbf{r}_i$ is the radius vector from the charge to the electron, $\mathbf{R}_0(t)$ is the radius vector from the charge to the center of the molecule at time t, and $\mathbf{r}_i$ is the radius vector of the ith electron with respect to the center of the molecule. When the path of the particle is a straight line, we have $\mathbf{R}_0(t) = \mathbf{b} + \mathbf{v}t$. At the time of closest approach ($t = 0$) the coordinates of vector $\mathbf{R}$ are $(b, 0, 0)$. The components of the vector of the electric field of the particle $\mathbf{E}(\mathbf{R})$ in the directions $\mathbf{b}$ (transverse) and $\mathbf{v}$ (longitudinal) are given by [78]:

$$\begin{aligned} E_b &= (\gamma Zeb)\left[b^2 + (\gamma vt)^2\right]^{-3/2} , \\ E_v &= (\gamma Zevt)\left[b^2 + (\gamma vt)^2\right]^{-3/2} , \end{aligned} \tag{3}$$

where $\gamma = (1 - \beta^2)^{-1/2}$ is the Lorentz factor. Substituting (3) into (1) and carrying out the integration, for the probability of transition we get

$$P_{0j}(b) = \left(\frac{2Ze^2\omega_{0j}}{\hbar v^2\gamma^2}\right)^2 \left[\left|M_{0j}^v\right|^2 K_0^2(\lambda_{0j} b) + \left|M_{0j}^b\right|^2 \gamma^2 K_1^2(\lambda_{0j} b) \right] , \tag{4}$$

where M_{0j}^v, M_{0j}^b are the components of the matrix elements, and $\lambda_{0j} = \gamma\omega_{0j}/v$, $K_0(\lambda_{0j} b)$, $K_1(\lambda_{0j} b)$ are the modified Bessel functions.

In an isotropic medium we have $|M_{0j}^v|^2 = |M_{0j}^b|^2 = |M_{0j}|^2$. After the introduction, in place of $|M_{0j}|^2$, of the optical strength of the oscillator according to $f_{0j} = (2m\omega_{0j}/\hbar)|M_{0j}|^2$, the expression (4) becomes

$$P_{0j}(b) = \frac{2Z^2e^4\omega_{0j}f_{0j}}{\hbar m v^4\gamma^4}\left[K_0^2(\lambda_{0j}b) + \gamma^2 K_1^2(\lambda_{0j}b)\right]. \qquad (5)$$

When the argument is $\lambda_{0j}b > 1$, we have $K_0(\lambda_{0j}b)$, $K_1(\lambda_{0j}b) \approx (\pi/2\lambda_{0j}b)^{1/2}\exp(-\lambda_{0j}b)$, and the probability $P_{0j}(b)$ decreases exponentially with increasing b. Otherwise, when $\lambda_{0j}b < 0.4$, we have $K_0(\lambda_{0j}b) \sim -\ln(\lambda_{0j}b)$, $K_1(\lambda_{0j}b) \sim (\lambda_{0j}b)^{-1}$. In this case $P_{0j}(b) \sim b^{-2}$.

In the approximation of classical dynamics of collisions, the change in the momentum of the electron after collision is defined by the time integral of the force applied. The longitudinal electric field E_v at the time $t = 0$ changes its sign. The time integral of E_v is zero. Therefore, the changes of momentum and energy of the electron are [78, 79]

$$\Delta p = F_b^{\max}\tau_{\rm coll} = \int_{-\infty}^{\infty} eE(t)\,{\rm d}t = \frac{2Ze^2}{bv}\,,$$
$$\delta E = \frac{(\Delta p)^2}{2m} = \frac{2Z^2e^4}{mv^2b^2}\,. \qquad (6)$$

Since $F_b^{\max} = eE_b^{\max} = \gamma Ze^2/b^2$, the effective time of the interaction is

$$\tau_{\rm coll} = \frac{2b}{\gamma v}\,. \qquad (7)$$

For transition to the new energy state in the discrete or continuous spectrum the molecule (as a quantum system) must receive the energy either $\varepsilon_{0j} = \hbar\omega_{0j} = E_j - E_0$ or $\hbar\omega_{0v}$. In accordance with the principle of *adiabatic* collisions, the transition of a quantum system into the jth state may only take place when the impact parameters satisfy the condition

$$b \leqslant b_{\rm eff}(\omega_{0j}) = \frac{\pi\gamma v}{\omega_{0j}}\,. \qquad (8)$$

From the comparison of the right-hand side of (8) with the argument of Bessel functions it follows that the excitation becomes adiabatic when the argument of Bessel function is $\lambda_{0j}b = \pi$. Indeed, at $\lambda_{0j}b = \pi$ the values $K_0^2(\pi) = (0.0296)^2$, $K_1^2(\pi) = (0.034)^2$ are for all practical purposes close to zero, and therefore the probability $P_{0j}(b = b_{\rm eff}) \approx 0$. From (8) (as an implication of the principle of adiabatic collisions) it follows that the excitations due to the transitions of valence electrons ($\hbar\omega_{0j} \leqslant 10$ eV, $\tau_{\rm qu} \approx 0.413$ fs) may occur rather far away from the path of the charged particle. Transitions with the transfer of electrons from inner shells are only feasible for the molecules that occur near the path of the particle. For states in the continuous spectrum the energy difference between adjacent levels (and ω_{vv_1}) may be infinitesimally small, and therefore the adiabatic condition is not satisfied.

3.3 Excitation in a condensed medium

Because of intermolecular interactions, the spectrum of energy states in a condensed medium becomes continuous. For a continuous spectrum, the analogue of $P_{0j}(b)$ is the function $P(\omega, b)$, which is the density of probability of transmission to the medium of the energy $\hbar\omega = \varepsilon$ at distance b from the path of the particle. The following circumstances have to be taken into account in these calculations. Owing to the high density of the molecules, it is a collective of molecules that is involved in the interaction with the charged particle. The polarization of the medium attenuates the field of the charged particle that acts on the molecule removed from its path. Because of this, it is necessary to use the concept of electrodynamics of a continuous medium for finding the characteristics of the field of a moving charge that acts upon the molecular electron. The author has proposed two approaches for solving this problem: one purely classical [56] and the other semiclassical, using the concepts of quantum mechanics [57].

In the classical approach, the density of probability $P(\omega, b)$ is found from the linkage between the loss of energy of a charged particle $\Delta E(b)$ and $P(\omega, b)$. The loss $\Delta E(b)$ itself was found as a change in internal energy of the dielectric under the action of the field of a moving charge. The components of electric field strengths were found from Maxwell equations [72]. In the semiclassical approach of the first-order perturbation theory, the starting point was the formula for the probability of transitions in a continuous spectrum in a form similar to (1). Then it was assumed that the electrons in the molecule are described by the Dirac equation. The operator of the interaction of the electron with the charged particle was constructed using the potentials of the electromagnetic field created by the moving charge. The potentials were found by solving the Maxwell equations. After some manipulation (described in detail in Ref. [57]), we get the expression for $P(\omega, b)$ that exactly coincides with the formula obtained in the approximation of classical electrodynamics:

$$P(\omega, b) = \frac{Z^2e^2\omega^2}{\pi^2 N\hbar v^4}\,{\rm Im}\left[-\frac{1}{\epsilon(\omega)}\right] \times\left(\left|\frac{K_0(\lambda_\omega b)}{\gamma_\omega^2}\right|^2 + \left|\frac{K_1(\lambda_\omega b)}{\gamma_\omega}\right|^2\right), \qquad (9)$$

where ${\rm Im}\left[-1/\epsilon(\omega)\right] = \epsilon_2(\omega)/\left[\epsilon_1^2(\omega) + \epsilon_2^2(\omega)\right]$ is the function of energy loss, $\epsilon(\omega) = \epsilon_1(\omega) + {\rm i}\epsilon_2(\omega)$ is the dielectric permittivity of the medium without spatial dispersion, $\gamma_\omega = [1 - \beta^2\epsilon(\omega)]^{-1/2}$, $\lambda_\omega = \omega/\gamma_\omega v$, and $K_0(\lambda_\omega b)$, $K_1(\lambda_\omega b)$, as before, are the modified Bessel functions.

By analogy with excitation of individual atoms (molecules), for the condensed state we introduce the '*macroscopic*' forces of an oscillator, such as the spectral density of forces of oscillators

$$F(\omega) = \frac{m\omega}{2\pi^2e^2N}\,{\rm Im}\left[-\frac{1}{\epsilon(\omega)}\right] \qquad (10)$$

and the force of an oscillator of transition of the molecule from the ground state to the jth state of a discrete or continuous spectrum (at ionization)

$$F_{0j} = \frac{m}{2\pi^2e^2N}\int_{\omega_{0j}-\Delta\omega_{0j}}^{\omega_{0j}+\Delta\omega_{0j}} {\rm d}\omega\,\omega\,{\rm Im}\left[-\frac{1}{\epsilon(\omega)}\right], \qquad (11)$$

where $\Delta\omega_{0j}$ is the half-width of the peak of the function ${\rm Im}\left[-\epsilon^{-1}(\omega)\right]$ or $\epsilon_2(\omega)$. Figure 2 shows the energy dependences of the dielectric characteristics of water, the spectral density of forces of oscillators $F(\omega)$, calculated from formula (10), and $f(\omega) = (m\omega/2\pi^2e^2N)\,\epsilon_2(\omega)$. The diagram also shows the effective numbers of electrons, described by the

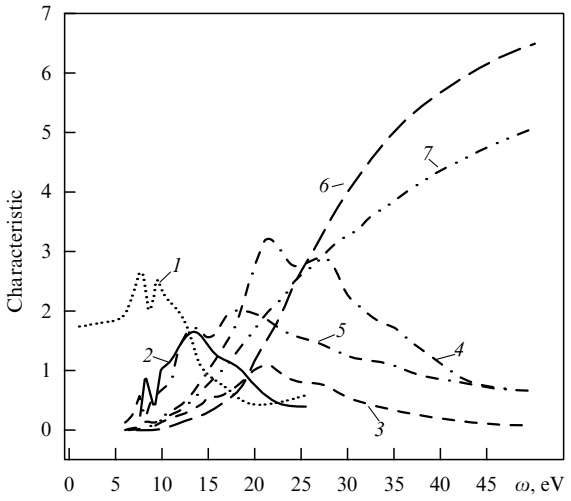

Figure 2. Dielectric characteristics of water $\epsilon_1(\omega)$ (*1*), $\epsilon_2(\omega)$ (*2*), $\mathrm{Im}\left[-\epsilon^{-1}(\omega)\right]$ (*3*), spectral densities of forces of oscillators $F(\omega)$ (*4*), $f(\omega)$ (*5*), and the effective number of electrons $N_{\mathrm{eff}}^{\mathrm{L}}(\omega)$ (*6*) and $N_{\mathrm{eff}}^{\mathrm{G}}(\omega)$ (*7*) for water in condensed and gaseous states vs. the energy.

expressions

$$N_{\mathrm{eff}}^{\mathrm{L}}(\omega) = \int_0^{\omega} F(\omega')\,\mathrm{d}\omega', \qquad N_{\mathrm{eff}}^{\mathrm{G}}(\omega) = \int_0^{\omega} f(\omega')\,\mathrm{d}\omega'.$$

Observe that the normalization conditions hold for the spectral forces of oscillator

$$N_{\mathrm{e}} = \int_0^{\infty} F(\omega')\,\mathrm{d}\omega', \qquad N_{\mathrm{e}} = \int_0^{\infty} f(\omega')\,\mathrm{d}\omega',$$

where N_{e} is the number of electrons in the molecule.

For narrow peaks of the function $\epsilon_2(\omega)$ or function $\mathrm{Im}\left[-\epsilon^{-1}(\omega)\right]$ with the maximums at frequencies ω_{0j} corresponding to the energies of transition of a molecule from the ground state to the jth excited state, the probability of transition $P_{0j}(b)$ can be approximated as

$$P_{0j}(b) = \frac{2Z^2e^4\omega_{0j}}{mv^4}\, F_{0j}\left(\left|\frac{K_0(\lambda_{0j}b)}{\gamma_{0j}^2}\right|^2 + \left|\frac{K_1(\lambda_{0j}b)}{\gamma_{0j}}\right|^2\right), \quad (12)$$

where $\lambda_{0j} = (\omega_{0j}/\gamma_{0j}v)$, $\gamma_{0j} = \left[1-\beta^2\epsilon(\omega_{0j})\right]^{-1/2}$. The probabilities of transition to the continuous spectrum (at ionization) are calculated by integrating $P(\omega, b)$ over the spectrum of energy losses from I to $\hbar\omega$. In doing this, the values corresponding to the transitions to discrete states must be removed from the spectrum.

Collisions in the condensed medium become adiabatic when $\mathrm{Re}\,(\lambda_{0j})\,b_{\mathrm{eff}} = \pi$. In accordance with this restriction, the expression that defines the effective size of the region of distribution of the jth excited state in the condensed medium depending on the energy of transition $\hbar\omega_{0j}$ is [56, 57]

$$b_{\mathrm{eff}}^{\mathrm{c}}(\omega_{0j}) = \frac{\pi\gamma_{0j}v}{\omega_{0j}}, \quad (13)$$

where the coefficient

$$\gamma_{0j} = \sqrt{2}\left\{\left[\left|1-\beta^2\epsilon_1(\omega_{0j})\right|^2 + \beta^4\epsilon_2^2(\omega_{0j})\right]^{1/2} + \left|1-\beta^2\epsilon_1(\omega_{0j})\right|\right\}^{-1/2} \quad (14)$$

plays the role of the *Lorentz factor in a condensed medium*. And indeed, in the vacuum limit it becomes $\gamma = (1-\beta^2)^{-1/2}$. At $\epsilon_1(\omega) = 1$ and $\beta^2\epsilon_2(\omega_{0j}) \ll |1-\beta^2|$, expression (12) becomes (5), and (13) becomes (8).

4. Nature and spectrum of quantum states induced by a charged particle

4.1 Quantum states induced by a charged particle

The energy transmitted to the medium in a single act of interaction is a random quantity distributed in the range from $\varepsilon_{\min}$ to $\varepsilon_{\max}$. For $\varepsilon_{\min}$ we take the energy required for the transition of the molecule to the first allowed electron-excited state. For most substances this state is a singlet state. The maximum energy $\varepsilon_{\max}$ that can be transmitted by the charged particle to the electron subsystem depends on the type of charged particle and its velocity v. For a heavy nonrelativistic particle we have $\varepsilon_{\max} = 2mv^2$, where m is the mass of the electron. In the case of electron–electron collisions for $\varepsilon_{\max}$ we take the energy to be equal to one half of the energy of the electron: $\varepsilon_{\max} = E_{\mathrm{e}}/2$.

The nature and spectrum of the emerging quantum states depend on the structure of the absorbing medium, the type of charged particle and its energy. The value of $\varepsilon_{\max}$ for a charged particle traveling with a high velocity may be much greater than the first ionization potential of the molecule I. Such a particle can excite not only the states associated with the transition of valence electrons to higher discrete energy levels, but also the states associated with electron transitions at the inner shells. The latter processes may generate both the discrete high-energy states in the self-ionization region of the spectrum (the so-called superexcited states) [80], and the states in the continuous spectrum that involve the electrons of ionization of the inner shells of the molecule and lead to the emergence of vacancies (holes). The nature of the high-excitation molecular states and the possible channels of relaxation are discussed in detail in the reviews [13–15].

In a condensed medium the conventional excited states of individual molecules or fragments of the polymer chain are supplemented by the excited states that involve a collective of molecules. Such collective excited states include *plasmons*. A plasmon is a quantum of oscillations of the electron density of plasma. The natural frequencies of plasma oscillations obey the equation

$$\epsilon(\omega) = 0, \quad (15)$$

which holds for conduction electrons in metals. At frequencies ω_{pl} (with $\hbar\omega_{\mathrm{pl}} \approx 15-20$ eV), satisfying equation (15), the function $\mathrm{Im}\left[-1/\epsilon(\omega)\right]$ displays a broad maximum.

In a medium of bound electrons, the collective oscillations occur not in pure form, but always in combination with intramolecular transitions. Because of this, in molecular media the collective excitations of the *plasmon* type take the form of *longitudinal polarization* waves. The energy of excitation of such collective states, as a rule, falls in the range $\hbar\omega_{\mathrm{pl}} \approx 15-25$ eV. In a condensed medium the energy required for the transfer of an electron to the conduction band (the energy of ionization) is, as a rule, less than the energy of ionization of the molecule. Because of this, the majority of excited molecular states and certainly the plasmon states are above the ionization threshold.

4.2 Spectrum of quantum states generated by the primary particle

The probability of occurrence of jth excited state is given by the ratio $p_{0j} = \sigma_{0j}/\sigma_{\text{tot}}$, in which σ_{0j} is the excitation cross section of the jth state, and σ_{tot} is the total cross section of inelastic scattering equal to the sum of the total cross section of excitation $\sigma_{\text{ex}} = \sum_j \sigma_{0j}$ and the ionization cross section $\sigma_{\text{i}} = \int_I^{\varepsilon_{\max}} \mathrm{d}\sigma_{0\omega}$. Analytical expressions for the cross sections can only be found by making considerable assumptions. Their derivation for different types of cross sections based on Bethe's formula can be found in the reviews [15, 81]. Here we reproduce the expressions obtained by the author in the context of the quasi-classical approximation using the functions $P(\omega, b)$ and $P_{0j}(b)$ [57].

Representing the differential cross section of energy transfer $\mathrm{d}\sigma(\omega)$ as a sum

$$\mathrm{d}\sigma(\omega) = \mathrm{d}\sigma_{b>a}(\omega) + \mathrm{d}\sigma_{b<a}(\omega)\,,$$

the following expressions have been derived in Ref. [57] for the relevant cross sections in the nonrelativistic approximation:

$$\mathrm{d}\sigma_{b>a}(\omega) = 2\,\frac{(Ze)^2}{\pi\hbar v^2 N}\,\mathrm{Im}\left[-\frac{1}{\epsilon(\omega)}\right]\ln\frac{1.123v}{a\omega}\,, \qquad (16)$$

$$\mathrm{d}\sigma_{b<a}(\omega) = \frac{2\pi Z^2 e^4}{\hbar m v^2}\,N_{\text{eff}}^{\text{G}}(\omega)\omega^{-2}\,\mathrm{d}\omega\,, \qquad (17)$$

where $N_{\text{eff}}^{\text{G}}(\omega) = \int_0^{\omega}\mathrm{d}\omega' f(\omega')$ is the effective number of electrons participating in the interaction (see Fig. 2). Formula (16) is valid for transitions when the molecular electron receives the small momentum q ($qa < 1$, where a is a value of the order of the size of the atom) — that is, for the excitation of the discrete states by fast particles (at $Ze^2/\hbar v \ll 1$). The applicability of formula (17) is confined to the range of ω from $\omega_1 \approx \hbar/2ma^2$ to $\omega_{\max}$ — that is, to the transitions to the continuum. In the limit of a large $\omega_{\max}$ this formula becomes the Rutherford formula.

The excitation cross section of the jth state with the energy of transition $\hbar\omega_{0j}$ is obtained by integrating with respect to ω formula (16) between the limits corresponding to the maximums of either $\epsilon_2(\omega_{0j})$ or $\mathrm{Im}\left[-1/\epsilon(\omega_{0j})\right]$. As a result of this manipulation, and introducing the oscillator forces, we get the following expression for the cross section:

$$\sigma_{0j} = \frac{4\pi Z^2 e^4}{mv^2}\,\frac{F_{0j}}{\hbar\omega_{0j}}\,\ln\frac{1.123v}{a\omega_{0j}}\,,$$

from which it follows that at $v \gg a\omega_{0j}$ for all states the logarithmic term shows little dependence on $\hbar\omega_{0j}$. As a result, the probability of excitation of the jth state in a condensed medium is $p_{0j} \sim F_{0j}/\omega_{0j}$, and $p_{0j} \sim f_{0j}/\omega_{0j}$ in a gaseous medium (since for a rarefied medium we have $\epsilon_1(\omega) = 1$).

So we see that the highest probability corresponds to the excited states of the discrete spectrum that have the largest ratios (F_{0j}/ω_{0j}), (f_{0j}/ω_{0j}). These are not necessarily the first excited states. In the case of water, the transition in the vapor phase denoted as diffusion bands with $\hbar\omega_{0j} = 13.32$ eV (see Table 1 in Ref. [48]) has the highest oscillator force. The energy of this transition exceeds the first ionization potential ($I_1 = 12.6$ eV), which places this transition into the class of transitions to the superexcited state.

4.3 Role of the phase state of the medium in the distribution of energy over the quantum states

In a condensed medium the level of the conduction band is, as a rule, below the vacuum level. For example, the ionization potential in water vapor is $I_{\text{g}} = 12.56$ eV, whereas in liquid water it is equal to $I_{\text{c}} = 8.79$ eV. On transition from gaseous to liquid state the distribution of forces of oscillators shifts towards the higher energies (see Fig. 2). Because of this, the majority of excited discrete molecular states are above the ionization threshold. Accordingly, all states in water except the first lie above the ionization threshold.

For some substances in the condensed state the high values F_{0j}/ω_{0j} in the spectrum of energy losses have transitions to the plasmon type collective states. In metals, the excitation of such states is practically the only channel of energy loss of a charged particle for excitation. The lifetime of collective excited states is about 0.1 fs. The nature of the decay of plasmon is similar to the decay of a molecule after absorption of a photon with energy $\hbar\omega_{\text{pl}}$. Since $\hbar\omega_{\text{pl}} \approx 2I$, the decay of plasmon generates an electron – ion pair. The electron resulting from the decay of a plasmon is capable of exciting (and even ionizing) a molecule of the medium. Because of this, the formation of plasmons in a condensed medium and their subsequent decay increases the share of ionization in the common spectrum compared to the share of ionization in the gaseous phase. Because of the high probability of excitation of plasmon states (in water the force of the oscillator of the transition $\hbar\omega_{\text{pl}} = 21.4$ eV is $F_{\text{pl}} = 2.03$; see Table 1 in Ref. [48]), a larger share of the charged particle energy is spent for the excitation of these states, thus reducing the yield of the low-lying excited states.

Comparative simulations of the distribution of energy of fast electrons over the quantum states of water and water vapor [48] revealed that *upon transition from the vapor to the liquid phase, owing to the lowering of the ionization potential and the availability of the channel of excitation of plasmon states with a high probability, the share of ion pairs in the spectrum of initial active particles became much higher compared to the excited states.*

The effect of the aggregate state of water on the inelastic energy losses of a charged particle was considered by the author in Ref. [82] using water as an example. The shift of oscillator forces towards higher energies results in a situation where, for the energies of charged particles $E < E_b$ [$E_b = 175$ eV for electrons, $E_b = 320$ keV $(\text{a.m.u.})^{-1}$ for heavy particles], the ionization losses per unit mass in water vapor are higher than in liquid water ($S_\rho^{\text{v}} > S_\rho^{\text{w}}$). At $E > E_b$ the relation between S_ρ^{v} and S_ρ^{w} is reversed ($S_\rho^{\text{v}} < S_\rho^{\text{w}}$). When, however, the energy is reached at which the attenuation of the field of the moving charge by the polarization of the medium is important, the relationship between S_ρ^{v} and S_ρ^{w} again becomes $S_\rho^{\text{v}} > S_\rho^{\text{w}}$ (the density effect [15]).

4.4 Role of secondary electrons in the distribution of energy transmitted to the medium

According to (17), for transitions to the continuous spectrum we have $\mathrm{d}\sigma(\varepsilon) \sim \varepsilon^{-2}$ ($\varepsilon = \hbar\omega$), and the most likely are those transitions involving electrons from valence shells. In the case of a fast particle, when $\varepsilon_{\max} \gg I$, the cross section is $\sigma_{\text{i}} > \sigma_{\text{ex}}$ (see Fig. 1). Such particles generate ionized states with a higher probability than the states of the discrete spectrum. The production of ionized states takes up a considerable part of the energy transmitted to the medium by the primary

particle. According to Refs [48 – 51], this share may be as large as 90% of the energy of the primary electron.

Ionization generates an electron – ion pair. The energy of the electron is in the range $0 < \varepsilon^{\delta} < \varepsilon_{\max} - I$. The electrons with energy $\varepsilon^{\delta} > \hbar\omega_{01}$ may in turn produce excited and ionized states. In this way, the distribution of energy of a charged particle among the quantum states of the electron subsystem of the absorbing medium is fulfilled by the processes of inelastic scattering of both the primary particle and the secondary and next-generation electrons.

For the most part, the secondary electrons generate the same quantum states as the primary particle. However, the distribution of energy of secondary electrons has at least two special features. The first is related to the transfer of energy in space. Although the secondary high-energy electron is generated near the track of the particle, its energy may be distributed in the medium at a considerable distance from the path.

The second feature is due to the fact that low-energy electrons dominate in the spectrum of secondary electrons $N^{\delta}(\varepsilon) \sim \varepsilon^{-2}$ and next-generation electrons. Most of them will be unable to excite the high-excitation molecular states, to say nothing of *plasmon* type collective states. Because of this, in the overall spectrum of excited states the share of states with the lowest excitation energy increases, which increases the share of energy of the primary particle used for the excitation (see Table 1 in Refs [50, 51].

5. Spatial distribution of acts of energy loss. Track entities of fast charged particles

5.1 Distribution of acts of energy loss along the path of a primary particle

Between two consecutive instances of inelastic loss, the particle travels distance l_{in} without interaction. This length is known as the free path with respect to inelastic scattering. The probability of a particle traveling without interaction a distance greater than l_{in} is $P(l_{\text{in}}) = \exp(-N\sigma_{\text{tot}} l_{\text{in}})$, where σ_{tot} is the total cross section of inelastic scattering of particle in the medium. The mean value is

$$\bar{l}_{\text{in}} = \int_0^{\infty} l \, \mathrm{d}P(l) = \frac{1}{N\sigma_{\text{tot}}} .$$

When the velocity of the particle is high, we have $\sigma_{\text{tot}} \sim Z_{\text{eff}}^2/v^2$, and therefore $l_{\text{in}} \sim v^2/Z_{\text{eff}}^2$. Here and further Z_{eff} is the effective charge of the ion. Introduction of Z_{eff} in place of the nuclear charge of ion Z allows the processes of charge exchange that modify the charged condition of colliding particles to be taken into account. The value of Z_{eff} of the ion as a function of its velocity can be expressed as [83]

$$Z_{\text{eff}} = Z\left[1 - \exp\left(-\frac{v}{v_0 Z^{3/4}}\right)\right], \qquad (18)$$

where v_0 is the velocity of the electron on the first Bohr's orbit.

The dependence of $\bar{l}_{\text{in}}$ on the velocity of the particle can be described as follows. When the initial velocity of the ion is $v > 5v_0 Z^{3/4}$, the value of $\bar{l}_{\text{in}}$ decreases as the ion slows down, reaches its minimum, and then slightly increases. For example, for electrons with energy above 0.4 MeV the mean free path in water is 200 to 300 nm. As the electron slows down to $E_{\text{e}} = 10$ keV, the value of $\bar{l}_{\text{in}}$ decreases by an order of magnitude. When the energy of the electron is $E_{\text{e}} = 1$ keV, the value of $\bar{l}_{\text{in}} \leqslant 6$ nm. The pattern of variation of $\bar{l}_{\text{in}}$ for protons and ^{16}O ions in water as a function of the specific energy of the particle reveals that the minimum value of $\bar{l}_{\text{in}} = 0.5$ nm, which is comparable to the size of the molecule, corresponds to the proton energy of $E_{\text{p}} \sim 100$ keV, and the energy of ^{16}O ion 20 MeV (a.m.u.)$^{-1}$. This implies that below this value the process of inelastic energy loss for ^{16}O ion along its path is practically continuous.

The procedure for evaluating $\bar{l}_{\text{in}}$ using σ_{tot} is very arduous and not always feasible owing to the lack of data on σ_{tot} for many substances. Because of this it is more convenient to calculate $\bar{l}_{\text{in}}$ from the mean characteristics of deceleration of the charged particle — namely, $\bar{\varepsilon}_{\text{in}}$ and S_{in}. The first of these

$$\bar{\varepsilon}_{\text{in}} = \frac{1}{\sigma_{\text{tot}}}\left[\sum_j \hbar\omega_{0j}\,\sigma_{0j} + \int_I^{\varepsilon_{\max}} \hbar\omega\,\sigma(\omega)\,\mathrm{d}(\hbar\omega)\right]$$

is the energy lost on average by a particle in one instance of inelastic loss, and the latter

$$S_{\text{in}} = N\left[\sum_j \hbar\omega_{0j}\,\sigma_{0j} + \int_I^{\varepsilon_{\max}} \hbar\omega\,\sigma(\omega)\,\mathrm{d}(\hbar\omega)\right]$$

is the mean energy loss per unit path length of the particle in the case of inelastic scattering. If $\bar{\varepsilon}_{\text{in}}$ and S_{in} are known, then the mean free path may be defined as the ratio $\bar{l}_{\text{in}} = \bar{\varepsilon}_{\text{in}}/S_{\text{in}}$.

The values of S_{in} for many substances are known, and the value of $\bar{\varepsilon}_{\text{in}}$ for fast particles is usually 40 to 60 eV. If in place of $\bar{\varepsilon}_{\text{in}}$ we use the value of the most probable energy loss in one act $\tilde{\varepsilon}$, then, as a result of such a replacement, the ratio $\tilde{l}_{\text{in}} = \tilde{\varepsilon}/S_{\text{in}}$ is the most probable free path length. The most probable value of energy loss corresponds to the energy at which the function $\mathrm{Im}\left[-\epsilon^{-1}(\omega)\right]$ has a maximum — that is, it corresponds to the energy of excitation of the plasmon states ($\tilde{\varepsilon} \approx \hbar\omega_{\text{pl}} \approx 15-25$ eV). These considerations provide a more accurate definition of the energy range of a charged particle in which the distribution of acts of energy loss may be considered continuous.

5.2 Track entities produced by a fast primary particle and their spatial distributions

When the velocity of a particle is high, the acts of energy loss are separated from one another. Consequently, the subsequent processes will take place in isolated microscopic volumes of the medium, which, depending on their shape and size, are referred to as *track* structures (entities) or *tracks*. Transmission of energy $\hbar\omega \leqslant 2I$ (where I is the energy of ionization of the medium) lead to the formation in the medium of the electron-excited molecular states, electron – ion pairs, or plasmon states. In the first two cases the energy transmitted to the medium is localized on an individual molecule (fragment of polymer chain). When a plasmon state is excited, the energy absorbed by the medium is delocalized over an ensemble of molecules. The size of the region of delocalization relative to the distance from the track of the primary particle is given by formula $b_{\text{pl}} = \pi v/\omega_{\text{pl}}$ [see formula (13)]. As a matter of fact, the separated electron-excited states and electron – ion pairs generated in a low-energy act are the *simplest track entities*.

The electron – ion pair is separated by distance r_{th}, which is equal to the thermalization length of an electron with energy $E_{\text{e}} \leqslant \hbar\omega_{01}$. The thermalization length depends on the structure of the medium. The value of r_{th} may vary very

widely — from a few to several hundred nanometers [10]. We set r_{th} equal to 7 nm. This value is commonly used in models of diffusion-controlled reactions in tracks [10].

When $\bar{l}_{in} \leqslant r_{th}$, the pairs cannot be regarded as independent. When the electron energy is $E_e < 1$ keV, the value of $\bar{l}_{in}$ is less than the thermalization length r_{th}. Accordingly, the acts of energy loss $2I < \hbar\omega < 1$ keV give rise to track forms that contain several primary active particles. Using the classification of Mozumder and Magee [10, 31] we shall use the term spur for the entities containing from 2 to 10 primary active particles. We assume that a spur has a spherical configuration with Gaussian distribution of the primary active particles. For the upper energy limit of spur formation we take 100 eV, as done in Ref. [31].

Several overlapping spurs give rise to more complicated track entities — from pear-shaped *blobs* with an energy of formation from 100 to 500 eV [28] to near-cylindrical entities extending along the main track and known as *short tracks*. Considering the overlapping of spurs at the physical stage, we define the energy range of formation of short tracks E_e from 0.5 to 1 keV. Branch tracks are formed when the energy exceeds 1 keV.

Thus, the track of a fast charged particle in the medium is surrounded by a spectrum of track entities ranging from the most simple (individual excited molecules, electron – ion pairs) to more sophisticated forms. The percentage of each particular entity depends on the initial energy of the primary particle. For fast particles, however, this dependence is weak. This is confirmed by the results of mathematical simulation of the primary stage of radiolysis of water by electrons, reported in Refs [50, 51].

According to Refs [50, 51], in the process of degradation the primary electron with energy 10 keV generates 9.24 one-particle excited states, 34.34 collective (plasmon) states, 154.33 ionized states. Out of the total number of ionization acts, 54.86 instances of secondary electrons with energy below 8.4 eV are generated. Such electrons are referred to as or *subexcitation* [84] electrons. Since such subexcitation electrons cannot generate electron-excited states, such ionization acts give rise to individual electron – ion pairs.

As noted above, the collective states live for a short time, and decay with the localization of energy on one of the molecules. Such localization is equivalent to the absorption by the molecule of a photon with an energy of about 21.4 eV. The photo-excited water molecule decays after 0.1 to 1 fs through the ionization channel with quantum yield 1 [85]. The act of ionization releases an electron with an energy of $\varepsilon' = 21.4 - 8.76 = 12.64$ eV. An electron with such energy is capable of producing ionized or excited states. In this way, the relaxation of the collective excited state gives rise to a track entity consisting of several active particles — a spur.

The energy of certain excited states is above the ionization potential. Such super-excited states are engaged in the competitive process of ionization and dissociation. The electron released through the ionization channel is a sub-excitation electron. Accordingly, the decay of electron-excited molecules generates the simplest track entities, comprised of individual electron – ion pairs and pairs of the molecule-radical type.

According to Ref. [48], out of the total number of acts of excitation and ionization (197.91) produced by the primary electron with energy 10 keV, in 98.44 instances we get the simplest track entities, or 49.74% of the total number of acts. *Given the relatively high yield of the simplest track entities, we ought to place them into a separate group, and set the lower energy limit for the formation of a spur at* $E_s = \hbar\omega_{01} + I_c$ *in place of the currently accepted 6 eV. For water this energy value is 17.16 eV.*

The spectrum of energy loss is determined by the structure of the medium and does not depend on the type of charged particle. The relative probability of the loss of energy by the charged particle for excitation and ionization ($p_{0j} = \sigma_{0j}/\sigma_{tot}$) depends on the velocity of the charged particle. *Therefore, charged particles of a different nature produce identical track entities as long as their velocities are equal.* However, the distribution of track entities along the path of the primary particle depends on the type of particle — namely, on Z and m_1. Distribution of the track entities along the path of the primary particle depends on the stochastic nature of the losses. This distribution may be characterized by the mean free path $\bar{l}_{in}$, or by the most probable free path $\tilde{l}_{in} = \tilde{\varepsilon}/S_{in}$. Since $\bar{l}_{in} \sim (v^2/Z_{eff}^2)$, the particle that travels at the same velocity but has a larger Z (and therefore Z_{eff}) travels a shorter distance between the acts of energy loss. Overlapping of track structures occurs for such a particle at a higher velocity.

The effects of mass on the distribution of acts of energy loss of a charged particle work as follows. The cross sections of inelastic loss exhibit no explicit dependence on the mass. However, the length of deceleration of the particle depends on the mass. With the same initial velocities, the initial energy of a heavier particle is greater. If the spectra of energy losses are the same, a light particle will lose a considerable part of its energy in a single act of interaction, whereas for a heavier particle the loss is small compared to its energy before the interaction. The deceleration of the heavier particle takes a greater number of interactions. The continuous track of a heavy ion, resulting from the overlapping of the simplest track entities, will be longer than the track of a light ion, and much longer than the short track of an electron.

The probability of formation of the track entity of energy $\hbar\omega_{0j}$ at distance b from the path of the primary particle is described by the function $P_{0j}(b)$. The maximum value of parameter b does not exceed $b_{eff}^{c}(\omega_{0j})$. The function $b_{eff}^{c}(\omega_{0j})$ characterizes the width of distribution of the track entity with the energy of formation $\hbar\omega_{0j}$ with respect to the straight portion of the path. If the path of the primary particle is not straight, the distribution of track entities with respect to the initial direction of travel will be more complicated.

Figure 3 shows the distributions of various excited states ($\hbar\omega_{0j} = 8.4$, 11.96, 14.1, 21.4 eV) in water as functions of b with the velocity of the particle $\beta = 0.65$. The diagram illustrates the share of various excited states initiated by the primary particle in relation to the distance from the path of the particle. Excitation of the first three states leads to the formation of the simplest track entities, and therefore their distributions characterize the density of such entities at different distances from the path of the primary particle. The distribution of the plasmon states characterizes the distribution of spurs consisting of two particles.

As the particle decelerates, the width of the distribution of states narrows in accordance with the variation of $b_{eff}^{c}(\omega_{0j})$. The analysis of the dependence of $b_{eff}^{c}(\omega_{0j})$ on v reveals that for frequencies ω_{0j}, at which $\epsilon_1(\omega_{0j}) > 1$, the function $b_{eff}^{c}(\omega_{0j})$ in a condensed medium behaves as follows. As the energy increases, the value of $b_{eff}^{c}(\omega_{0j})$ increases, reaches its maximum, and then decreases. The maximum occurs at the

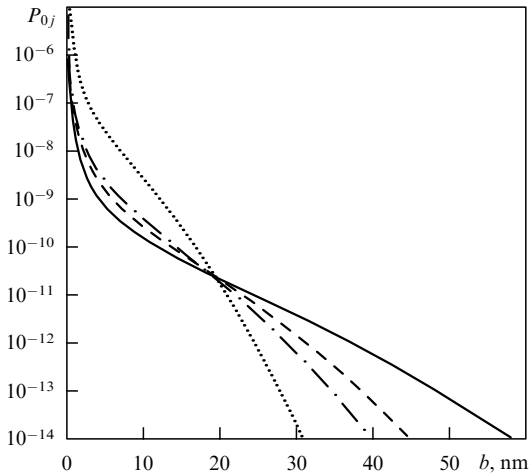

Figure 3. Dependence on the impact parameter of the probability of excitation of states with energies of transition $\hbar\omega_{0j} = 8.4$ eV (solid line), 11.96 eV (dashed line), 14.1 eV (dot-and-dash line), and 21.4 eV (dotted line), formed by the charged particle with unit charge moving at velocity $v/c = 0.65$.

energy value corresponding to $\beta = \epsilon_1^{-1/2}$ — the onset of the Cherenkov radiation. If at this frequency we also have $\epsilon_2(\omega_{0j}) < 2\left[\epsilon_1(\omega_{0j}) - 1\right]$, the actual values of $b_{\text{eff}}^{\text{c}}(\omega_{01})$ exceed the values of $b_{\text{eff}}^{\text{v}}$ obtained at this frequency in a vacuum with due account for the relativistic contraction [that is, according to formula (8)]. It is this situation that is encountered in water for the transition $\hbar\omega_{01} = 8.4$ eV, in polyethylene for the transition $\hbar\omega_{01} = 9$ eV, and in polymethyl methacrylate for the transitions $\hbar\omega_{01} = 5.74$ eV and $\hbar\omega_{02} = 6.23$ eV. The maximum of $b_{\text{eff}}^{\text{c}}(\omega_{01})$ for these transitions occurs at $\beta \approx 0.6$, which corresponds to the energy of the ion of 300 MeV (a.m.u.)$^{-1}$.

Figure 4 shows the dependence of the dimensions of the effective regions of excitation of various electron states in water on the velocity of the charged particle, and the dependence of the kinetic energy of the particle [in units of MeV (a.m.u.)$^{-1}$] on the velocity, and the variation of $b_{\text{eff}}^{\text{v}}$ for the first transition calculated by formula (8). The region of distribution of the track entities narrows as the energy required for its generation increases (from spur to blob, and from blob to short track). Thus, the short tracks will occur near the path of the primary particle, and only the simplest track entities can be found far away from the path of the primary particle. From these curves we also find that the relativistic effects in the values of $b_{\text{eff}}^{\text{c}}(\omega_{01})$ become important at $\beta = v/c > 0.3$ — that is, when the specific energy exceeds 50 MeV (a.m.u.)$^{-1}$.

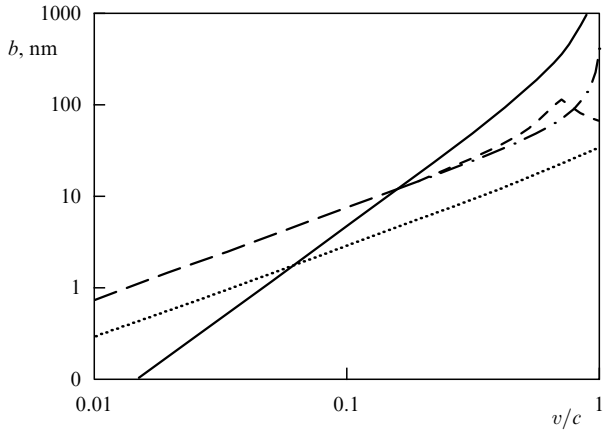

Figure 4. Dependence on the velocity of the effective dimensions of the volumes of distribution of excited states with transition energies $\hbar\omega_{0i} = 8.4$ eV (dashed line) and 21.4 eV (dotted line) formed by the charged particle. The dot-and-dash line in the diagram shows the size of the excitation region for the state $\hbar\omega_{0i} = 8.4$ eV disregarding the dielectric properties of the medium, and the solid line corresponds to the specific energy of the charged particle in MeV (a.m.u.)$^{-1}$.

In a rarefied medium we have $\epsilon_1(\omega) = 1$, and $\epsilon_2(\omega)$ has small but nonvanishing values. From formulas (13) and (14) it follows that at the relativistic velocities, when we have

$$\beta^2\epsilon_2(\omega_{0j}) \gg |1 - \beta^2|\,,$$

the value of $b_{\text{eff}}^{\text{g}}$, unlike $b_{\text{eff}}^{\text{v}}$, in a vacuum linearly approaches the finite limit ($\beta \approx 1$)

$$b_{\text{eff}}^{\text{g}}(\omega_{0j}) = \frac{2\pi c}{\omega_{0j}\sqrt{2\epsilon_2(\omega_{0j})}}\,. \tag{19}$$

Making use of the linkage of the optical power of the oscillator with the imaginary part of permittivity of the medium $\epsilon_2(\omega)$ (per molecule) on the one hand, and on the other hand with the cross section of photoabsorption — namely,

$$f(\omega) = \frac{m}{2\pi^2 e^2 N}\,\omega\epsilon_2(\omega) = \frac{mc}{2\pi^2 e^2}\,\sigma_{\text{ph}}(\omega)\,,$$

the expression (19) can be rewritten as

$$b_{\text{eff}}^{\text{g}}(\omega_{0j}) = \pi a_0\left[\frac{4\,\text{Ry}}{\hbar\omega_{0j}\,\alpha a_0 N\sigma_{\text{ph}}(\omega_{0j})}\right]^{1/2}. \tag{20}$$

From (20) it follows that, as the energy of the particle increases, the effective size of the distribution of excited states in a rarefied medium tends to a finite limit, whose value depends on the density of the medium and the cross section of photoabsorption.

The track entities are formed both by the primary particle itself, and by its δ-electrons. The track entities produced by the δ-electrons may occur at a considerable distance from the track of the primary particle. The spectrum of secondary electrons initiated by the fast electron extends to energy $\varepsilon_{\text{max}}^{\delta} = (E_{\text{e}}/2) - I_{\text{c}}$. The maximum energy of a secondary electron produced by a heavy particle moving at the same velocity as the electron is much higher. In the case of nonrelativistic velocities this energy is greater by a factor of almost 8, because at $I_{\text{c}} \ll E_{\text{e}}/2$ we have

$$\frac{2mv^2 - I_{\text{c}}}{mv^2/4 - I_{\text{c}}} \approx 8\,.$$

According to Refs [50, 51], the yields of the primary active particles show little dependence on the energy of the primary electron. One can expect, therefore, that the increase in the energy range of the secondary electrons initiated by the heavy particle will not have any considerable effect on the percentage of the track entities derived from the mathematical simulation for the electrons in Ref. [51]. It should be noted, however, that the differences in the spectra of secondary electrons will have an effect on the distributions

of the track entities with respect to the path of the primary particle. The higher-energy secondary electrons are capable of producing the track entities at a considerable distance from the path of the heavy particle.

According to Refs [50, 51], in the course of degradation, the secondary electrons initiated by the electron with energy 10 keV create 113 one-particle excited states, 71.7 collective (plasmon) states, and 297.3 ionized states. Out of the total number of ionizations, 209.4 instances produce secondary electrons with an energy below 8.4 eV. In the total number of acts of one-particle excitations, a considerable portion (53.2) leads to the first excited state. The shift of distributions towards the preferential production of the simplest track entities is explained by the large share of low-energy electrons in the secondary spectrum.

Spatial distribution of track entities from the secondary electrons is complicated. Degradation of the energy of secondary electrons in a medium takes place through a cascade of collisions involving the electrons directly knocked out by the primary particle and the next-generation electrons. Such a cascade can only be studied by methods of mathematical simulation. However, the qualitative distribution of the track entities due to the secondary electrons can be pictured as follows. The low-energy electrons degrade near the trajectory of the primary particle. Accordingly, the resulting simplest track entities are located near the track axis of the primary particle. By contrast, the high-energy electrons are capable of producing complicated track entities at a considerable distance from the path of the primary particle. Such a distribution of track entities produced by the secondary electrons smooths out the asymmetry in the spatial distribution of the primary active particles (and track entities) of various natures, created by the primary particle.

6. Structure of extensive tracks of heavy ions of a different nature

6.1 General concepts of ion tracks

The conditions of formation of extensive tracks of heavy ions have not yet been clearly defined. For the energy limit, below which the proton forms a track in the shape of an ion column, Gray [26] proposed the value of 3 MeV. If we accept the upper energy limit of 5 keV, defined for the short track of the electron in Ref. [31], the extensive track of the proton ought to be formed at an energy of about 10 MeV. At this energy, the mean distance between the acts of inelastic loss in water is 10 nm. This value exceeds the size of a spur, and so the spurs overlap only at the chemical stage of the radiolysis.

Overlapping of spurs at the physical stage takes place when the mean free path of a charged particle with respect to inelastic scattering $\bar{l}_{\rm in}$ becomes smaller than the size of the spur. For the radius of an average spur at the physical stage we take $r_{\rm s} \approx 2-3$ nm. The mean free path of 2 or 3 nm of a proton in water corresponds to the energy of 1 or 2 MeV. From these considerations, the track of the proton may be regarded as continuous when the energy of the proton is $E_{\rm p} \leqslant 2$ MeV. From the earlier estimates of the values of $\bar{l}_{\rm in}$ it follows that the continuous track of the ion with nuclear charge Z $(Z > 1)$ will be observed with energy $E_Z \leqslant 2Z_{\rm eff}^2$ MeV (a.m.u.)$^{-1}$.

Owing to the stochasticity of the processes of interaction, the tracks of individual particles, generally speaking, are not similar to one another, and the radiation-induced transformations in each track are unique. Consequently, one may expect fluctuations of radiation effects when the medium is exposed to a small fluence of particles. When the medium is exposed to a large fluence of particles, one might expect that the radiation effect averaged over the number of particles will be the same as the effect for the individual track formed in the model of continuous deceleration.

According to our current views, a heavy ion forms a cone-shaped continuous track, consisting of the *core* and the surrounding *sheath*. The core is filled with the track entities produced both by the primary ion itself and by the secondary electrons. Owing to their azimuthal symmetry and high density, the track entities overlap and lose their individuality. Because of this, the core may be regarded as a region of homogeneous distribution of the primary active particles. Since the path of the heavy ion is practically straight, the distribution of active particles in the core may be characterized by the radial distribution function.

There is no commonly accepted definition of the size of the track core. In radiation chemistry, the radius of the core is the effective value of the impact parameter obtained from the principle of adiabatic perturbations for the transition of the system to the lowest electron-excited state with an excitation energy $\hbar\omega_{01}$, namely

$$r_{\rm c} = b_{\rm eff}(\omega_{01}) = \frac{\pi\gamma_{01}v}{\omega_{01}}\,. \tag{21}$$

The definition of the core radius in formula (21) makes sense for those ions for which the primary activations beyond $r_{\rm c}$ are localized in the individual tracks of δ-electrons. The concentration of primary activations in the core itself does not exceed the value at which the qualitative composition of the core is changed, and the cooperative effects become important. If the tracks of δ-electrons overlap at a distance $r_0 > r_{\rm c}$, it would be reasonable to take r_0 for the radius of the core. Such may be the situation at the end of tracks of heavy ions. If, however, some volume of the track, as will be shown later for multiply charged ions like fission fragments, differs in quality from the rest of the track, then the definition of the core must be based on other principles.

According to Fig. 4, as the velocity increases, the size of the core of the track in water, defined by formula (21) for the first transition to the singlet state ($\hbar\omega_{01} = 8.4$ eV), behaves as follows. In the range of nonrelativistic velocities the radius of the core increases monotonously $(r_{\rm c} \approx \pi v/\omega_{01})$, and decreases after reaching a maximum at $\beta = 0.693$ — that is, we observe the *relativistic compression of the core*.

The spectrum of primary active particles formed by the primary ion and their radial distributions $N_{0j}^{\rm p}(r)$ are defined with the aid of the function $P_{0j}(b)$ using the expression $N_{0j}^{\rm p}(r) = NP_{0j}(r)$ (at $r \equiv b$). For a nonrelativistic particle $N_{0j}^{\rm p}(r)$ is well approximated by the formula

$$N_{0j}^{\rm p}(r) = \frac{2Z_{\rm eff}^2 e^4 F_{0j} N}{mv^2\omega_{0j}r^2}\exp\left(-\frac{\omega_{0j}^2 r^2}{2v^2}\right), \tag{22}$$

which is obtained from (13) at $\gamma_{0j} \approx 1$ if we use the approximate equation [73, 86]

$$x^2\left[K_0^2(x) + K_1^2(x)\right] \approx \exp\left(-\frac{x^2}{2}\right).$$

The spectrum of primary active particles formed by the secondary electrons in the core, and their distribution over the

volume of the core, can only be defined either from mathematical simulation or from the spectrum of degradation of electrons using the expression

$$N_{0j}^{\delta}(r) = N\int_{\varepsilon_{0j}}^{\varepsilon_{\max}(r)} \mathrm{d}\sigma_{0j}(\varepsilon)\, Y(\varepsilon^{\delta}, r)\,.$$

However, the calculation of the degradation spectrum is also a complicated task that can be solved by mathematical simulation [67]. The problem of finding the dependence $\varepsilon_{\max}(r)$ remains quite difficult even in the coarse approximation based on the assumption that the energy distribution of secondary electrons does not change in the radial direction from the axis of the track.

The approximate estimates of the distribution of active particles in the core may be derived under the assumption that the secondary electrons smooth out the asymmetry in the distribution of active particles of various nature created by the primary ion. Taking advantage of this assumption, the radial distribution may be represented as

$$N_{0j}(r) = N_{0j}^{\mathrm{p}}(r) + N_{0j}^{\delta}(r) = \frac{D(r)}{g_j}\,,$$

where $D(r)$ is the radial distribution of energy that is equal to the sum of the radial distributions from the primary particle and from the secondary electrons: $D(r) = D^{\mathrm{p}}(r) + D^{\delta}(r)$. The quantity g_j is the yield of the primary active particle of the jth type. The values of g_j for water, determined from computer simulations, can be found in Refs [48–51].

The distribution of $D^{\mathrm{p}}(r)$ is equal to the integral with respect to energy of the function $P(\omega, b)$, and for the nonrelativistic particles has the form

$$D^{\mathrm{p}}(r) = \frac{2Z_{\mathrm{eff}}^2 e^4 N}{mv^2 r^2}\int_{\omega_{01}}^{\omega_r} F(\omega)\exp\left(-\frac{\omega^2 r^2}{2v^2}\right)\mathrm{d}\omega\,. \qquad (23)$$

The upper limit of integration in (23) is defined from the principle of adiabatic collisions, and is therefore equal to $\omega_r = \pi v/r$. Because of the complexity of the spectral density of oscillator forces $F(\omega)$, the analytical expression for $D^{\mathrm{p}}(r)$ can only be obtained under certain simplifying assumptions. The analysis of $D^{\mathrm{p}}(r)$ indicates that $D^{\mathrm{p}}(r) \sim r^{-k}$ with $k > 2$.

Analytical expressions, however, are available for $D^{\delta}(r)$. Extending the expressions obtained in Refs [59–63, 73], the distribution $D^{\delta}(r)$ can be represented as

$$D^{\delta}(r) = \frac{Z_{\mathrm{eff}}^2 e^4 N N_{\mathrm{eff}}(\varepsilon_{\max})}{mv^2 r^2}\left(1 - \frac{r}{r^{\delta}}\right), \qquad (24)$$

where $N_{\mathrm{eff}}(\varepsilon_{\max})$ is the effective number of electrons in the molecule that may generate secondary electrons, and r^{δ} is the conventional radius of the sheath. Neglecting the angular distribution of the secondary electrons, the radius r^{δ} in the referenced studies was taken to be equal to the linear path of a δ-electron $R_{\max}^{\delta}$ with energy $\varepsilon_{\max}^{\delta} = \varepsilon_{\max} - I$.

If the angular distribution of the secondary electrons is taken into account, the size of the volume of distribution of their energy decreases, and is confined to the radius $r^{\delta} = \eta R_{\max}^{\delta}$. In the model of continuous deceleration of the electrons, the value of the constant η can be found from the condition of the extreme of the dependence $r(\varepsilon) = R(\varepsilon)\sin\theta$, which is determined by the distance from the axis of the track that may be traveled by the electron with energy ε that leaves the axis of the track at angle θ. Since the energy of the electron ε and the direction of travel θ are linked by the relation $\varepsilon = \varepsilon_{\max}\sin(\theta/2)$, we have $r(\varepsilon) = R(\varepsilon)(1 - \varepsilon/\varepsilon_{\max})^{1/2}$. Assuming now that $R(\varepsilon) = \xi\varepsilon^{\gamma}$, from the condition of the extreme we find that the maximum distance away from the axis of the track is traveled by the electron with energy $\varepsilon' = 2\gamma(2\gamma+1)^{-1}\varepsilon_{\max}$. Then the value of $r(\varepsilon') = r^{\delta}$ is

$$r^{\delta} = \frac{(2\gamma)^{\gamma}}{(2\gamma+1)^{\gamma+0.5}}\, R_{\max}^{\delta}\,.$$

For nonrelativistic electrons, the exponent γ in the power-law approximation of the linear electron path versus its energy $R(\varepsilon) = \xi\varepsilon^{\gamma}$ is in the range from 1.5 to 1.75. From the last expression it follows that when γ varies from 1.5 to 1.75 the value of η varies from 0.325 to 0.3. In Ref. [87] it was suggested to take $\eta = 0.31$. Under this assumption $r^{\delta} \approx 0.31 R_{\max}^{\delta}$.

In Ref. [87] the software for computer calculation of radial energy distribution in the track $D(r)$ is developed. Figure 5 shows the results of the calculation for six values of specific energy of radial distribution of the absorbed dose in the track of the fragment of the fission of ^{94}Y in polymethyl methacrylate. Multiplying the values of $D(r)$, corresponding to the specific energy of the ion $E_{\mathrm{Y}}/94$, by $(Z_{\mathrm{eff},Z}/Z_{\mathrm{eff,Y}})^2$ at

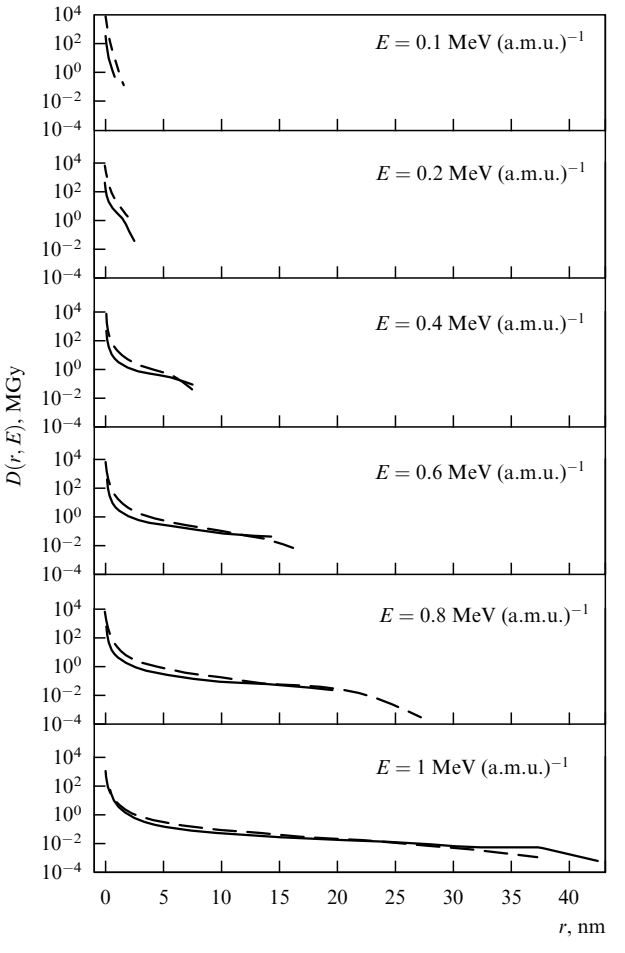

Figure 5. Radial distributions of the absorbed dose in the track of a fragment of fission of ^{94}Y in polymethyl methacrylate for several values of specific energy. Solid lines correspond to computer calculations in Ref. [87], dashed lines are calculated by formula (25).

this value of energy, one can obtain the values of $D(r)$ for an ion with nuclear charge Z, corresponding to the energy of the ion $E_Z/A_Z = E_Y/94$.

First of all, from the diagram we observe a rapid decline in the dose beyond the region of the track confined within the radius $r \approx 4-5$ nm. As the ion slows down, the width of the distribution quickly decreases. At the same time, the values of the dose near the axis of the track increase up to Bragg's peak, and start to decline only after the peak is passed. In this way, as the energy decreases to the value corresponding to the location of Bragg's peak, the density of radiation disturbances increases in the region of the track near the axis.

The distribution of energy between the core and the sheath appears as follows. With the energy of ions $E_Z < 2$ MeV (a.m.u.)$^{-1}$ in light media, less than 25% of the energy spent by the ion for the formation of the track is localized in the sheath, and this share decreases as the ion slows down. At $E_Z \approx 0.15$ MeV (a.m.u.)$^{-1}$ the sheath merges with the core ($r^\delta = r_c$), and the entire energy is localized in the core. Such behavior is due to the fact that, as the ion slows down, the sheath contracts faster than the core. Since $\varepsilon^\delta_{max} \approx 2mv^2$, we have $R^\delta_{max} \sim v^{2\gamma}$, and hence r^δ depends on the velocity of the ion to the power of 3 to 3.5 — that is, $r^\delta \sim v^{(3-3.5)}$. At the same time, the radius of the core, as defined by (21), is practically a linear function of the velocity.

The analysis of distributions $D^p(r)$ and $D^\delta(r)$ indicates that in a broad range of values for r the radial distribution $D(r)$ is determined by $D^\delta(r)$. Because of this, for practical applications the distribution $D(r)$ can be expressed by the approximate formula

$$D(r) = \frac{B}{r^2}\left(1 - \frac{r}{r'}\right), \tag{25}$$

in which the coefficient B is found from the normalization condition

$$\int_a^{r'} 2\pi r\, D(r)\, \mathrm{d}r = S_{in}\,,$$

which states that the total energy absorbed in the volume of the track is equal to the ionization losses. At $r' \gg a$ (where a is the size of the molecule)

$$B \cong \frac{S_{in}}{2\pi \ln (r'/ae)}\,.$$

When the size of the sheath is greater than the size of the core ($r^\delta > r_c$), we have $r' = r^\delta \approx 0.31 R^\delta_{max}$. When the energy of the ion is less than the value at which the sheath merges with the core (that is, $r^\delta \leqslant r_c$), it is natural to take the radius of the core to be r' — that is, $r' = r_c$. Figure 5 shows the results of the calculation of $D(r)$ by formula (25). We see that the best agreement is achieved when the energy of the ion is high — when $r^\delta \gg r_c$, which is rather obvious. At low energies the agreement is somewhat worse, but still not so bad as to prevent one from using the convenient analytical representation of $D(r)$ in formula (25).

6.2 Dependence of characteristics of tracks on the parameters of ions

A charged particle is characterized by three main parameters: rest mass m_Z, velocity v, and charge Z. Other characteristics, such as energy, momentum and ion charge, are derivative. In the model of continuous deceleration the slowdown of a charged particle in the medium is characterized by the following variables: the mean energy loss by the particle over unit path length $-\mathrm{d}E/\mathrm{d}x$, and the length of deceleration (the linear path) of the particle $R(E_0)$.

The qualitative evaluation of the effects of various charged particles on matter in radiation chemistry and radiobiology is based on the characteristic known as the *linear energy transfer* (*LET*). This characteristic only takes into account the loss of energy for inelastic (*ionization losses*) and elastic (*nuclear losses*) interactions. Since it is the inelastic collisions that dominate on most of the particle's path, the LET of the ion on this portion of the track is determined by the energy loss for ionization and excitation of the molecules of the medium.

We represent the ionization loss by a modified Bethe's formula (for nonrelativistic velocities)

$$S_{in} = \left(-\frac{\mathrm{d}E}{\mathrm{d}x}\right)_{in} = \frac{2\pi Z^2_{eff} e^4}{mv^2}\,\frac{N_0 N^*_c \rho}{M}\,\ln\frac{2mv^2}{I^*_c}\,, \tag{26}$$

where N_0 is the Avogadro number, M is the molecular mass of the compound, ρ is the density of matter, N^*_c is the number of electrons of the compound involved in the deceleration process, and I^*_c is the mean excitation potential.

The quantities N^*_c and I^*_c (that enter Bethe's formula as constants) are assumed in (26) to depend on the energy of the incident particle — or, to be more precise, on ε_{max}. With this modification there is no need to introduce any corrections to account for the different bond energies in atoms, due to the distribution of the electrons over different electron shells. In the general case, N^*_c and I^*_c are defined with the aid of the oscillator forces. N^*_c and I^*_c can be approximately calculated using the Thomas–Fermi statistical theory of atoms (see Ref. [88]).

LET depends implicitly on Z via the dependence of the effective charge Z_{eff} on Z [see formula (18)]. The analysis indicates that LET always increases with an increasing Z. LET shows both explicit and implicit dependence on the ion velocity v (via the dependence of Z_{eff}, N^*_c, I^*_c on the velocity). The dependence of LET on the ion velocity appears as follows. If an ion with a nuclear charge Z has an initial velocity $v > 5v_0 Z^{3/4}$, then, as the ion slows down, LET first increases, reaches its maximum and then decreases according to logarithmic law. If the initial velocity of the ion is $v < 0.05 v_0 Z^{3/4}$, then LET decreases steadily as the ion decelerates.

The longitudinal size of the track L in the model of continuous deceleration is determined by the deceleration length, or the linear path of the particle $R(E_0)$:

$$L = R(E_0) = \int_0^{E_0}\left(-\frac{\mathrm{d}E}{\mathrm{d}x}\right)^{-1}\mathrm{d}E\,, \tag{27}$$

where E_0 is the initial kinetic energy of the ion. Since $-\mathrm{d}E/\mathrm{d}x$ depends on Z and v, and E_0 depends on the mass, the longitudinal dimension of the track depends on all three parameters of the ion. The dependence on Z and v comes through the dependence of the derivative $-\mathrm{d}E/\mathrm{d}x$ on Z and v. The dependence on the mass is not so obvious. It comes through the dependence of the upper limit of integration on the mass of the ion.

The dependence of L on the mass of the ion is best illustrated with the example of ions representing isotopes of the same element — for example, hydrogen. With the same

initial v and Z, the value of E_0 of the deuteron is twice that of the proton. Over the long path, the energy losses $-\mathrm{d}E/\mathrm{d}x$ are mainly determined by the losses in inelastic collisions (see Refs [22, 23]), which depend on the specific energy of the ion, and do not practically depend on the mass. Therefore, moving from integration with respect to the kinetic energy to integration with respect to the specific energy, we get

$$L_Z \approx A_Z \int_0^{E_0^Z/A_Z} \left(-\frac{\mathrm{d}E}{\mathrm{d}x}\right)^{-1} \mathrm{d}\left(\frac{E}{A_Z}\right).$$

As applied to our deuteron and proton, the latter expression implies that $L_\mathrm{D} \approx 2L_\mathrm{H}$. Therefore, with the same initial values of v and Z, the proton will slow down to the end energy over a shorter length than the deuteron. From the standpoint of the physics of nuclear collisions, this means that, given that the nature of the energy loss is the same, a deuteron will take twice as many collisions, and travel the path twice as long, in order to exhaust its energy.

The radial dimensions of the track (core, sheath) only depend on the particle velocity v. As the ion slows down, the dimensions of the core and the shell decrease. As noted above, the radial contraction of the track proceeds in such way that the sheath contracts faster than the core.

The local concentrations of the primary active particles depend in the following manner on the parameters of the ion. Firstly, they naturally increase with an increase in Z. The dependence on the velocity is complicated. As the ion slows down, the region of radial distribution narrows, and the distribution transforms as follows. If the velocity of the ion is $v > 5v_0Z^{3/4}$, then, as the ion decelerates, the local concentrations near the axis of the track first increase, reach their maximum, and then decrease — that is, behave similarly to LET.

Further away from the axis of the track, the local concentrations exhibit — as the ion slows down — a sharp decline down to zero on the boundary of the track volume. However, with such a transformation of radial distribution of local concentrations of active particles, it turns out that the mean concentrations both in the core of the track and in the volume of the track increase as the ion decelerates. This means that the intensity of radiation impact on the core and on the total volume of the track increases as these volumes decrease.

For the measure of the intensity of radiation impact on the volume of the track, determined by the size of its core, we may take the mean dose of radiation absorbed in the core of the track D_c. The use of the mean dose in the total volume of the track is not always correct, because the primary active particles in the sheath are usually distributed in the non-overlapping track entities (structures) — that is, in spurs, blobs and short tracks.

The pattern of dependence of the mean dose D_c on the parameters of the ions is as follows. The value of D_c increases with an increasing Z and decreasing velocity. The dependence of D_c on the mass is manifested in the character of the variation of D_c along the path. Other conditions being equal (the initial Z and v are the same), the value of D_c in the track of a heavy ion increases more gradually than in the track of a light ion. The change of D_c from the same initial value to the same end value in the track of a heavy ion takes a longer path length than in the track of a light ion.

From the pattern of radial distribution of the energy of the primary ion absorbed by the medium, as shown earlier (see also Fig. 3), one can see that the highest value of the dose is observed in the central cylindrical region of the track confined within the radius $r \approx 4-6$ nm. Beyond this radius, the dose distribution falls off rapidly (by two orders of magnitude or more). Because of this, it is expedient also to introduce the mean dose in the track region confined to the radius $r_0 = 4$ nm, $D(r \leqslant r_0)$. The author believes (see Ref. [87]) that this characteristic $D(r \leqslant r_0)$ is the measure of intensity of radiation disturbances in the central region of the track, and therefore this characteristic can be used as the argument of the function that describes the rate of etching of the dielectric along the track.

Figure 1 in Ref. [89] shows the results of the calculation of D_c in the tracks of different ions in water, polyethylene and polystyrene as functions of the specific energy of the ion E_Z/A_Z, the values of ionization losses S_in, and the change of r_c. Similar characteristics for the tracks of ions ^{40}Ar, ^{94}Y in polymethyl methacrylate up to an energy of 2 MeV (a.m.u.)$^{-1}$ are shown in Fig. 6. Since the radial size of the track depends on the velocity of the ion, the change in r_c and r^δ will be the same for all ions in such a representation. Such a presentation of characteristics on the same diagram is convenient for analyzing the distinctions in the characteristics of tracks, when not only the specific energies (velocities) are the same, but other parameters are the same as well. For example, projecting the same value of LET from the curves S_in on to the curves D_c and r_c, we can find their values and see how D_c varies in relation to the ion charge Z.

The distinctions in tracks become more clear if the change in characteristics is represented versus the residual path

$$R_r(E) = \int_0^E \left(-\frac{\mathrm{d}E}{\mathrm{d}x}\right)^{-1} \mathrm{d}E.$$

Using this representation, we may trace the changes in characteristics along the path of the ion. Indeed, the

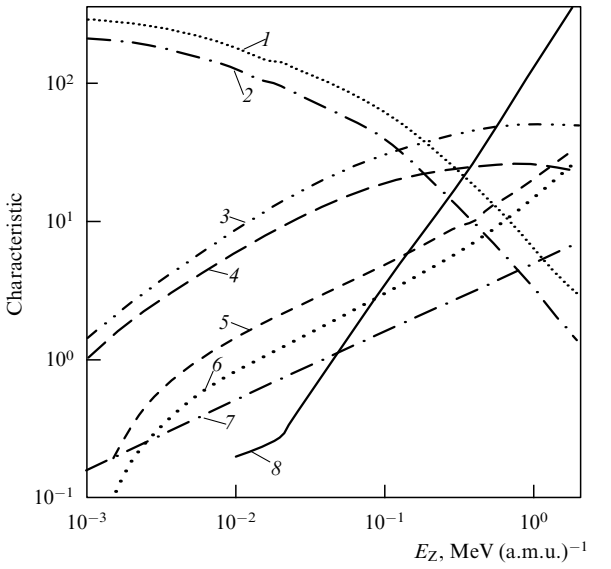

Figure 6. Dependence of the characteristics of the tracks of ions ^{40}Ar, ^{94}Y in polymethyl methacrylate on the specific energy: *1*, *2* — doses D_c in the cores of tracks of ions ^{94}Y and ^{40}Ar, respectively, MGy; *3*, *4* — ionization losses S_in of ions ^{94}Y and ^{40}Ar, respectively, GeV cm^2 g^{-1}; *5*, *6* — residual paths R_Z of ions ^{94}Y and ^{40}Ar, respectively, μm; *7* — radius r_c of the core of the tracks of ions ^{94}Y and ^{40}Ar, respectively, nm; *8* — the path of δ-electron R^δ_max of maximum energy, nm.

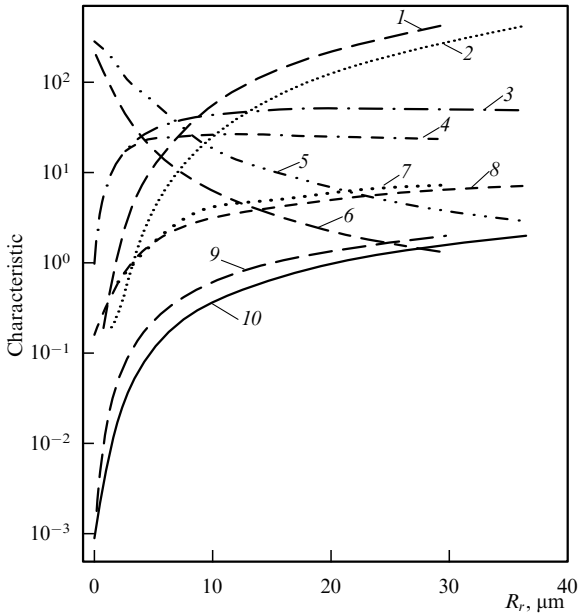

Figure 7. Dependence of characteristics of tracks of ions ^{40}Ar, ^{94}Y in polymethyl methacrylate on the residual path: *1*, *2* — paths of δ-electron $R^{\delta}_{\max}$ of the maximum energy, created by ions ^{40}Ar, ^{94}Y, respectively, nm; *3*, *4* — ionization losses S_{in} of ions ^{94}Y and ^{40}Ar, respectively, GeV cm^2 g^{-1}; *5*, *6* — doses D_{c} in the cores of tracks of ions ^{94}Y and ^{40}Ar, respectively, MGy; *7*, *8* — radiuses r_{c} of the cores of the tracks of ions ^{40}Ar and ^{94}Y, respectively, nm; *9*, *10* — energies of ions ^{94}Y and ^{40}Ar, respectively, MeV (a.m.u.)$^{-1}$.

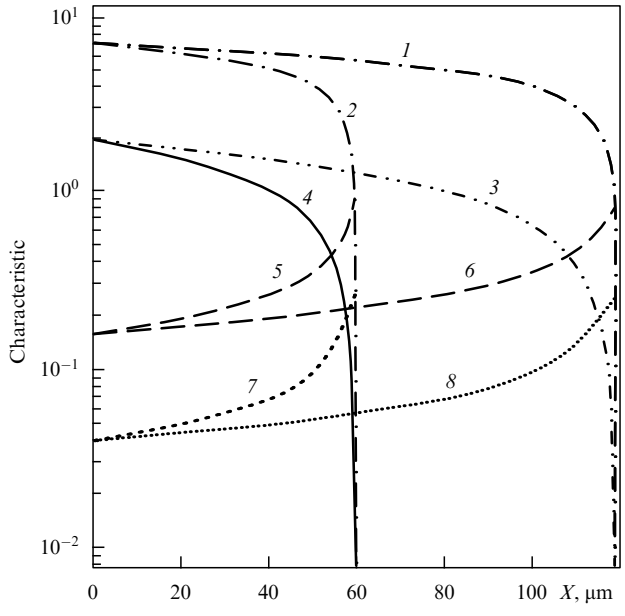

Figure 8. Change in characteristics of tracks along the path of ions H and D with the same initial velocity [$E_Z = 2$ MeV (a.m.u.)$^{-1}$] in PET: *1*, *2* — radiuses of the core r_{c} for ions H and D, respectively, nm; *3*, *4* — energies of ions H and D, respectively, MeV (a.m.u.)$^{-1}$; *5*, *6* — ionization losses S_{in} of ions H and D, respectively, GeV cm^2 g^{-1}; *7*, *8* — doses $D(r \leqslant 4)$ of ions H and D, respectively, MGy.

difference $R_r(E_0) - R_r(E_1) = X(E_0, E_1)$ is the distance traveled by the ion decelerating from initial energy E_0 to energy E_1. Figure 7 shows the characteristics of tracks of ions ^{40}Ar, ^{94}Y with initial energy $E_0^Z/A_Z = 2$ MeV (a.m.u.)$^{-1}$ in polymethyl methacrylate as functions of R_r. If we shift the curves for ^{40}Ar to the right, aligning them with the limit of the residual path of the ^{94}Y ion with the energy 2 MeV (a.m.u.)$^{-1}$, we can then move from right to left to view the changes in the characteristics of tracks of ions ^{40}Ar, ^{94}Y that had the same velocities at the initial time. Let us compare the structures of tracks of different ions in those cases where certain characteristics of particles and tracks are the same. We start with the case where two parameters of the ions are the same: Z and v.

6.3 Differences in the tracks of ions with the same Z and v

As noted above, this situation for heavy ions is possible when the medium is irradiated with different isotopes of the same element. Since the mass of the ion does not explicitly enter the expressions for the cross section and LET, the differences in the tracks are not that clear. When the characteristics of tracks are represented as functions of specific energy, they are all identical with the exception of path length $R(E_0)$. The differences are revealed when the characteristics are represented as functions of the residual path. Let us demonstrate the effects of the mass of a ion on the structure of the track using the example of a proton and deuteron.

Since at $E_0^{\text{H}}/A_{\text{H}} = E_0^{\text{D}}/A_{\text{D}}$ we have $E_0^{\text{D}} = 2E_0^{\text{H}}$, then $L_{\text{D}} \approx 2L_{\text{H}}$. Because of this, the change in characteristics of the deuteron track along the path of the ion is smoother than in the case of the proton. Figure 8 shows the characteristics of a proton, a deuteron and their tracks in lavsan (mylar, PET) as the functions $X(E_0, E) = R_r(E_0) - R_r(E)$ at $E_0^{\text{H}}/A_{\text{H}} = E_0^{\text{D}}/A_{\text{D}} = 2$ MeV (a.m.u)$^{-1}$. From these diagrams we clearly see the difference in the effects of protons and deuterons on matter. Depending on the thickness of the exposed layer of matter, the differences are the following. When the film thickness is $t \simeq R_{\text{D}}$, the thickness of the absorbing layer is $t^{\text{D}}_{\text{rad}} = t \simeq R_{\text{D}}$ for deuterons, and $t^{\text{H}}_{\text{rad}} = t/2 \simeq R_{\text{H}}$ for the protons.

In a film of thickness $t \cong R_{\text{H}} = R_{\text{D}}/2$ the proton will be slowed down completely, while the deuteron will pass through with some loss of energy (see Fig. 8). As a result, we find that the values of LET and the dose, averaged over the thickness of the film, are higher in the core of the proton track and in the cylindrical region of radius $r = 4$ nm than those in the track of deuteron [$\bar{S}^{\text{H}}_{\text{in}} > \bar{S}^{\text{D}}_{\text{in}}$, $\bar{D}^{\text{H}}_{\text{c}} > \bar{D}^{\text{D}}_{\text{c}}$, $\bar{D}^{\text{H}}(r \leqslant 4) > \bar{D}^{\text{D}}(r \leqslant 4)$]. Using the concept of LET, we may say that the irradiation with deuterons manifests itself as exposure to radiation with *low* LET, rather than with protons. Such a situation will be observed when the film is exposed to electrons and protons.

6.4 Differences in the tracks of ions with the same Z and E_0

Since this situation for heavy ions can also be realized when the medium is irradiated with the isotopes of one and the same element, we shall illustrate the differences in the tracks using the example of protons and deuterons. Figure 9 shows the changes in characteristics of particles and tracks along the path of a proton and deuteron with the same initial kinetic energy $E_0 = 2$ MeV. From the diagram we see that the longitudinal and the radial dimensions of the deuteron track are considerably lower than those of the proton, whereas the LET is higher. It turns out that the deuteron acts upon a smaller volume of the medium, but the impact is stronger [$\bar{D}^{\text{H}}(r \leqslant 4) < \bar{D}^{\text{D}}(r \leqslant 4)$] than that of the proton. If we use the concept of LET again, then the irradiation with deuterons appears as exposure to radiation with *high* LET,

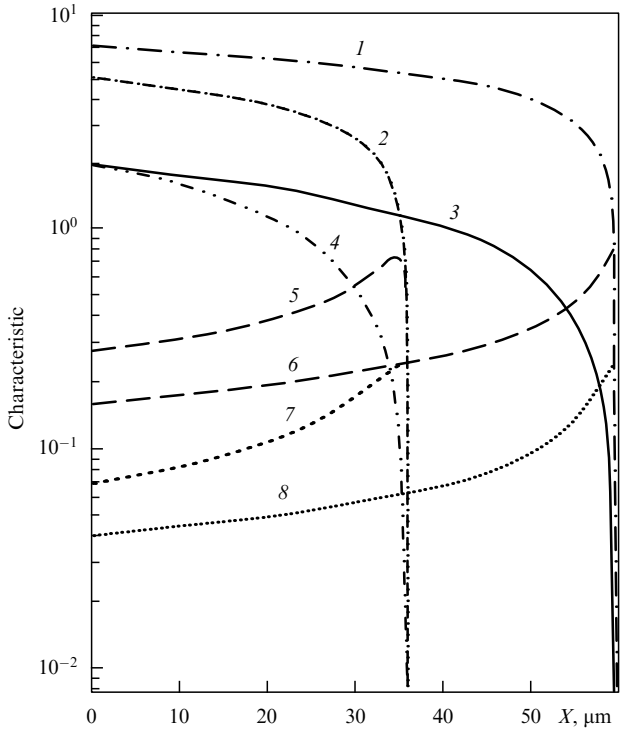

Figure 9. Change in characteristics of tracks along the path of ions H and D with the same initial energy ($E_0 = 2$ MeV) in PET: *1*, *2* — radiuses of the core r_c for ions H and D, respectively, nm; *3*, *4* — energies of ions H and D, respectively, MeV (a.m.u.)$^{-1}$; *5*, *6* — ionization losses S_{in} of ions H and D, respectively, GeV cm^2 g^{-1}; *7*, *8* — doses $D\,(r \leqslant 4)$ of ions H and D, respectively, MGy.

rather than with protons. This difference is due to the fact that the deuteron in this case is a low-velocity particle compared to the proton — and, as noted above, the intensity of the impact of the ion on the medium increases with decreasing velocity.

6.5 Differences in the tracks of ions with the same initial value of LET

When the initial values of LET are the same, all parameters of the particles are different. The relationships between the characteristics of tracks depend on where the initial values of LET are located on the curve of LET versus ion velocity v (to the right or to the left of the maximum). Generally speaking, there are four possible relationships between the velocities of heavy and light ions. The first corresponds to $v_T, v_L > 5v_0Z^{3/4}$, and the values of LET for both ions are located to the right of the maximum. In this case,

$$S_{in} \sim \frac{Z_{eff}^2}{v^2} \ln v^2 \sim \frac{Z^2}{v^2} \ln v^2 .$$

From $S_{in}^L = S_{in}^T$ it follows that $Z_{T,eff}^2/v_T^2 \approx Z_{L,eff}^2/v_L^2$. Since $Z_T > Z_L$, and $m_T > m_L$, we have $v_T > v_L$, $E_T > E_L$, $r_c^T > r_c^L$, $r_T^\delta > r_L^\delta$, $L_T > L_L$, but $D_c^T < D_c^L$. From these relationships we see that in this first case the light ion forms a dense track.

In the second case, when $v_T, v_L < 0.5v_0Z^{3/4}$, the values of LET are located to the left of the maximum. In this case $S_{in} \sim Z^{1/2} \ln v^2$. Since $Z_T > Z_L$, from condition $S_{in}^L = S_{in}^T$ it follows that $v_T < v_L$. Consequently, $r_c^T < r_c^L$, $r_T^\delta < r_L^\delta$, but $D_c^T > D_c^L$. In this case it is the *heavy ion* that forms a dense track along the entire path length.

Two other options correspond to the mixed arrangement of the values of LET. At $v_L > 5v_0Z^{3/4}$, $v_T < 0.5v_0Z^{3/4}$ the values of LET for the light ion fall to the right of the maximum, and those for the heavy ion to the left. Since in this case $v_T < v_L$, we have $D_c^T > D_c^L$, and the *heavy ion* forms a dense track along the path length. In the opposite case, when $v_T > 5v_0Z^{3/4}$, $v_L < 0.5v_0Z^{3/4}$, the value of LET for the heavy ion falls to the right of the maximum, and that for the light ion to the left. In this case $v_T > v_L$. Therefore, $D_c^T < D_c^L$, and it is the *light ion* that forms a dense track along the entire path length.

Observe that these four options are not realized for every pair of ions. For example, for ions ^{40}Ar and ^{94}Y and their tracks, compared in Figs 6 and 7 to the specific energy of $E_Z/A_Z = 2$ MeV (a.m.u.)$^{-1}$, the values for LET can only be equal in cases 2 and 3. Figure 10 shows the characteristics of ions ^{40}Ar, ^{94}Y and their tracks at LET = 24 GeV cm^2 g^{-1}. This value of LET for ^{40}Ar corresponds to the specific energy 1.5 MeV (a.m.u.)$^{-1}$ (to the right of the maximum), while the specific energy for ^{94}Y is 0.06 MeV (a.m.u.)$^{-1}$, and falls to the left of the maximum. Curves shown in Fig. 10 confirm the above conclusion that in this situation it is the *heavy ion* that forms a dense track along the entire path length.

The comparison reveals that there is no direct correspondence between LET and the values characterizing the impact of the ion on the volume of the track — for example, D_c. Because of this, *LET cannot serve as a universal characteristic of the quality of radiation, as assumed in early models of tracks* (see Section 2). Owing to the presence of a maximum on the curve of LET versus energy, there will always be ambiguity in the dependence of the radiation effects on LET even for an individual particle (for more details see Refs [14, 15, 89]).

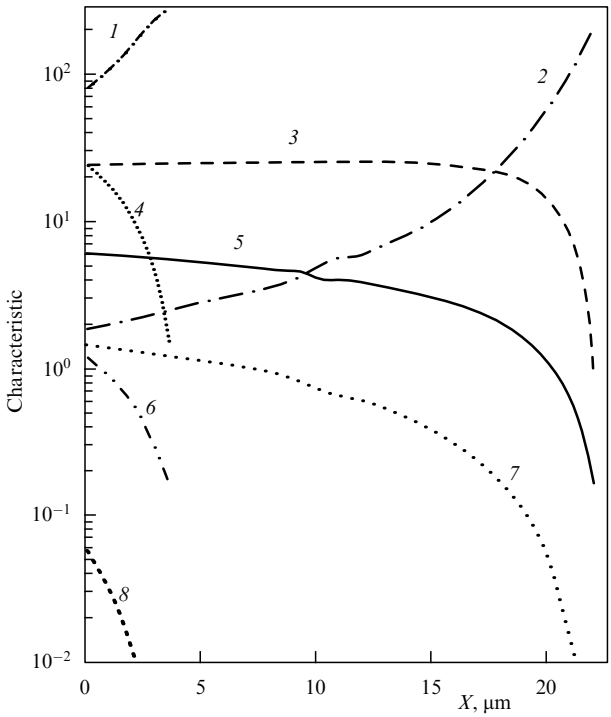

Figure 10. Characteristics of tracks of ions ^{40}Ar, ^{94}Y initially possessing the same values of LET (24 GeV cm^2 g^{-1}) in polymethyl methacrylate: *1*, *2* — doses D_c in the cores of tracks of ions ^{94}Y, ^{40}Ar, respectively, MGy; *3*, *4* — ionization losses S_{in} of ions ^{40}Ar, ^{94}Y, respectively, GeV cm^2 g^{-1}; *5*, *6* — radiuses r_c of the core of the tracks of ions ^{40}Ar, ^{94}Y, respectively, nm; *7*, *8* — energies E of ions ^{40}Ar, ^{94}Y, respectively, MeV (a.m.u.)$^{-1}$.

6.6 Structural features of the track of a multiply charged ion

The concentration of primary active particles (ionized states, electron-excited states) increases with increasing $Z_{\rm eff}^2$. The probability of formation of ionized states is very high near the axis of the track, and their share further increases after the subsequent decay of one-particle high-excitation states lying above the ionization threshold, and states of the plasmon type.

The number of ions generated by the primary ion in close collisions can be estimated by the Rutherford formula [73]

$$N_{\rm i} = \frac{2\pi Z_{\rm eff}^2 e^4}{mv^2}\, NN_{\rm eff}(\varepsilon_{\max})(I^{-1} - \varepsilon_{\max}^{-1})\,. \tag{28}$$

The primary ion, acting upon the electron, changes its energy. This change, depending on the impact parameter, is [the second expression in (6)]

$$\delta E = \frac{2Z_{\rm eff}^2 e^4}{mv^2 b^2}\,.$$

From this expression it follows that the transfer of energy equal to the ionization potential I is possible when the impact parameter does not exceed

$$b_{\rm i}^{\rm c} = \left(\frac{Z_{\rm eff}^2 2e^4}{v^2 mI}\right)^{1/2} = 2a_0\,\frac{Z_{\rm eff} v_0}{v}\left(\frac{\rm Ry}{I}\right)^{1/2}. \tag{29}$$

Therefore, the mean concentration of ions in the cylindrical region of the track confined to the radius $b_{\rm i}^{\rm c}$ is

$$\bar{N}_{\rm i}(r \leqslant b_{\rm i}^{\rm c}) = \frac{N_{\rm i}}{\pi (b_{\rm i}^{\rm c})^2} = NN_{\rm eff}(\varepsilon_{\max})(1 - I\varepsilon_{\max}^{-1})\,. \tag{30}$$

When the velocity of the ion is high, we have $\varepsilon_{\max} \gg I$ and $N_{\rm eff} \gg 1$. Then from (30) it follows that in this region of the track all molecules will be ionized in such way that they will be stripped, at the very least, of all valence electrons. Theoretical analysis and experimental findings confirm the fact that multiply charged ions in close collisions are formed [90–92].

Now let us evaluate the dimensions of this region. According to (29), the quantity $b_{\rm i}^{\rm c}$ depends on the ratio $Z_{\rm eff}/v$. At $v < 0.05 v_0 Z^{3/4}$, the ratio $Z_{\rm eff}/v$ becomes independent of the velocity, and is equal to $Z_{\rm eff}/v = Z^{1/4}/v_0$. We substitute this value into (29), getting as a result the maximal value of $b_{\rm i}^{\rm c}$, equal to $b_{\rm i} = 2a_0 Z^{1/4}({\rm Ry}/I)^{1/2}$. Assuming $I \approx 10$ eV, for Xe ion we get $b_{\rm i}^{\rm c} \approx 0.322$ nm.

The primary ion is capable of also generating ionized states beyond $b_{\rm i}^{\rm c}$ as a result of long-range collisions. The distance from the axis of the track, at which long-range ionization is possible, is found from the expression $b_{\rm eff}^{\rm i} = \pi\gamma v/I$. Although this distance can be much greater than $b_{\rm i}^{\rm c}$, the probability of ionization falls off rapidly as this distance increases. Because of this, the concentrations of ions formed beyond $b_{\rm i}^{\rm c}$ are mainly determined by the ionizations caused by the secondary electrons. The concentrations at different distances from the axis of the track can be approximated from the radial distribution of the dose. Figure 11 shows the mean doses in the track of a ^{54}Xe ion in water for five ranges of distances, obtained from the calculation of $D(r)$ by the technique described in Ref. [87]. In the range $0.5 \leqslant r \leqslant 1$ nm the mean dose is $\bar{D}(0.5 < r < 1) \approx 32-45$ MGy as the ion energy changes from 0.1 to 1.5 MeV (a.m.u.)$^{-1}$.

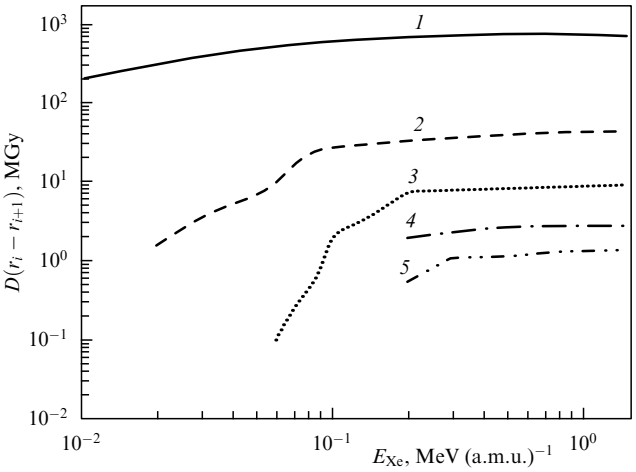

Figure 11. Mean doses vs. energy in the track of a ^{54}Xe ion in water in the range of distances from the axis of the track: *1* — 0–0.5 nm; *2* — 0.5–1 nm; *3* — 1–2 nm; *4* — 2–3 nm; *5* — 3–4 nm.

To evaluate the concentrations of ion pairs, we assume that the energy expended by the secondary electrons for the formation of one pair of ions is $W_{\rm i} \approx 30$ eV. Then we find that in the region of the track $0.5 \leqslant r \leqslant 1$ nm the mean concentration of the ion pairs is $n_{\rm i} \approx 8.3 \times 10^{21}$ cm^{-3}, which corresponds to the degree of ionization $\zeta \approx 0.24$. For the values of r in the intervals 1–2 nm, 2–3 nm, 3–4 nm, the degree of ionization reaches the vales of $\zeta \approx 5.29 \times 10^{-2}$, 1.7×10^{-2}, and 7.83×10^{-3}, respectively. At $\zeta \approx 7.83 \times 10^{-3}$ the concentration of ions is $n_{\rm i} \approx 2.62 \times 10^{20}$ cm^{-3}. The central region of the track ($r < 0.5$ nm), as already indicated, is not only completely ionized, but contains multiply ionized or fragmented ions.

Following the degradation of the energy of the primary ion and its secondary electrons, the track — along with the ions and excited molecules — is populated by the slow (*subexcitation*) electrons with $E_{\rm e}^{\rm sub} < \hbar\omega_{01}$. In water, the energy of such electrons is less than 8 eV. The emergence of subexcitation electrons may be regarded as the end of the *physical* stage of radiation-induced transformation. The fate of subexcitation electrons depends on the degree of ionization of the medium, and hence on their concentration. When the concentration of electrons is low, then, upon collision with the molecule, the kinetic energy of the electron transforms into the energy of vibrational, rotational and translational degrees of freedom of the molecule. As a result of a large number of such collisions, the energy of the electron reduces to the energy of its thermal motion, and the electron is *thermalized*. The time of thermalization of the subexcitation electrons depends on the nature and the aggregate state of the medium, and may range from 0.1 ps to 1 ns [84, 93].

If the concentration of electrons $n_{\rm e}$ is sufficiently high (like, for example, in the track of a multiply charged ion), they at first will very efficiently exchange their energies. As a result, their equilibrium velocity distribution will be established even before thermalization. As indicated above, the initial distribution of the subexcitation electrons with respect to energy is far from equilibrium. According to Ref. [94], the time of relaxation of the electrons to the equilibrium distribution is given by the expression

$$\tau_{\rm ee} = \frac{5}{8}\left[\frac{m(kT_{\rm e})^3}{\pi}\right]^{1/2}(e^4 n_{\rm e} \ln \Lambda)^{-1}\,, \tag{31}$$

in which $\ln \Lambda \approx \ln (r_D/b_{min})$ is the Coulombian logarithm, r_D is the Debye radius, and b_{min} is the minimum value of the impact parameter. Estimates based on the formula (31) indicate that with the mean energy of the electrons $\bar{\varepsilon}_e = (3/2)kT_e \approx 6$ eV and $n_e \approx 10^{22}$ cm^{-3} the electron relaxation time is $\tau_{ee} \sim 10^{-15}$ s. If the concentrations of ions and electrons are the same, the relaxation time of the ions is $\tau_{ii} = (M_i T_i^3/mT_e^3)\tau_{ee}$, and the initial equilibrium distribution of the ions with respect to their velocities is established sooner than that for the electrons, since $T_i \approx 10^{-2} T_e$.

The energy of internal excitation of complex particles (stable molecules) may be represented as the sum of energies of the electron, vibrational and rotational excitations [95]. Each degree of freedom of the molecule (ion) may be regarded as an isolated subsystem. The equilibrium distribution in such a subsystem is established sooner than in the entire system. For example, the probability of $V-V$ exchange is higher than the probability of $V-T$ exchange [95, 96]. This allows the characterizing of the degree of excitation of each state by its own temperature.

When the concentration of electrons is $n_e > 10^{20}$ cm^{-3}, after 10 fs they can be considered as a classical electron gas with temperature T_e, found from the relation $\bar{\varepsilon}_e = (3/2)kT_e$ (where $\bar{\varepsilon}_e$ is the mean energy of slow electrons, and k is the Boltzmann constant). This treatment holds at $kT_e > 4$ eV and concentrations below $n_e \sim 10^{22}$ cm^{-3}. Above this limit the gas degenerates and obeys Fermi–Dirac statistics.

We see that the equilibrium distribution is destroyed in the track of a heavy ionizing particle, and the concept of temperature is no longer applicable. However, one can define the temperature for individual degrees of freedom for each component, including the translational movement. For electrons this exercise has already been done. For heavy particles it is quite obvious that T_h is equal to the temperature of the medium before ionization, because the heavy charged particle loses most of its energy for ionization and electron excitation of the molecules of the medium without affecting the translational, rotational and vibrational degrees of freedom. Only at the end of the path, when the elastic collisions become important, is the equilibrium distribution of heavy particles violated. If, however, the Maxwell distribution of heavy particles is violated, it will be quickly restored within time $\tau_h < \tau_{ee}$ owing to the collisions between particles [94].

The formation of ionized states is dominated by the acts of ionization in which the energy of the released electron is low (which follows, for example, from the Rutherford formula). Such an electron cannot recede far away from the parent ion. Accordingly, most of the ionized states are ion pairs. Because of this, the volume of the track (with the exception of the region next to the axis) is *quasineutral* from the early stage of its formation. When the concentration of ionized states reaches the value at which the *Debye screening radius*, defined by

$$r_D = \left(\frac{kT_e}{4\pi e^2 n_e}\right)^{1/2} \tag{32}$$

for the electron component, becomes smaller than the region of the track under consideration, this region represents the *low-temperature plasma column* [97]. Individual components of such plasma occur in local (owing to the inhomogeneous distribution of particles) quasi-equilibrium states. Since the mean energy of the electrons is of the order of a few electron-volts, and the heavy component is less heated, the plasma is also *nonisothermal*.

Thus, in spite of the similarity of tracks of different ions, the increase in the ion charge leads not only to a *quantitative* increase in the concentration of primary particles (including charged particles), but also to a *qualitative* change in the structure of the track. The track of the ion transforms from the partially ionized region into the *low-temperature nonisothermal plasma*. Such transformation takes place in those regions of the track where the *Debye radius* is small compared to the size of the region. For water at normal conditions, with the degree of ionization 7.83×10^{-3} defined for the range of distances from the axis of the track of 3 to 4 nm, the Debye radius r_D is 0.98 nm — that is, less than the size of the interval. Accordingly, in water the cylindrical region of the track of a Xe ion of about 4 nm in radius is a filament of nonisothermal nonideal and spatially inhomogeneous plasma. This circumstance was first noted in Ref. [98]. Later the same conclusion was made in Ref. [99].

Let us call to mind the description of the system in the quasi-gas approximation, developed in Ref. [98]. This description consists essentially of the following. The relaxation processes in the track were described using the kinetic Klimontovich equation for spatially inhomogeneous plasma [100]. Then the method of Grad moments was used for expressing the transfer equations for the mass, momentum and energy of the components of plasma in the track. After integrating the expressions — which are the components of moments of different order from the collision integrals — the corrections to pressures and energies caused by the interaction of particles were defined. Then the dependence of pressures P_α and energies E_α on the concentration of charged particles and on the relative temperatures of electrons and heavy particles were studied. The medium in this exercise was water at conditions close to critical before passage of the heavy ion. Such are the conditions of the working media in Wilson chambers. The density of water in the near-critical state is 1/3 of the density of the liquid phase at normal conditions. At the same time, a multiply charged ion can create a high concentration of charged particles in such a medium.

The results of calculations presented in the Table indicate that when the heavy component of the system has a low temperature (immediately after ionization), then the pressure and the total energy in the system already become negative at the degree of ionization of 10^{-2}. When the concentration of charged particles is high, and the temperature T_h is low, there are no values for P_i and E_i in the Table, because the parameters η and γ, characterizing the degree of interaction between the charged particles in plasma, are much greater than one, and the quasi-gas approximation is not valid.

Two models were used for evaluating the energy and the pressure for the completely ionized region. The 'jelly' model considers the electrons as a classical gas, and uniformly distributed within its volume are the ions that do not interact with one another because they are shielded by the electron gas [101]. The calculation using this model gives $E = -4.48$ eV for the total energy, and $P = 101P_{cr}$ for the pressure (where P_{cr} is the critical pressure). The other model of the completely ionized region assumes that the classical gas of electrons is uniformly distributed over the volume, and the distribution of ions is point-like [101]. This model gives $E = -6.1$ eV for the energy, and $P = 61.5P_{cr}$ for the pressure.

Table. Pressures (in units of $P_{cr} = 218.4$ bar) and energies (per molecule) of plasma components vs. the degree of ionization (at $T_e/T_h = 10^2$).

Degree of ionization	1	0.5	10^{-1}	10^{-2}	10^{-3}	10^{-4}
P_e	101	92	28.3	3.6	0.39	0.04
P_i			-1.4×10^2	−7.44	−0.4	−0.02
P_n	0	−3.85	−1.13	1.2	1.45	1.47
E_e	−4.4	−0.64	0.33	6.3×10^{-2}	7.4×10^{-3}	7.7×10^{-4}
E_i			−5.4	−0.29	-1.6×10^{-2}	-6.9×10^{-4}
E_n	0	−0.162	-8.85×10^{-2}	-2.45×10^{-2}	-1.8×10^{-2}	-1.74×10^{-2}

The analysis of E and P depending on the degree of ionization reveals that the ionization of a molecular medium by a heavy ion leads — after completion of the physical stage — to an increase in the energy of interaction of the particles. This implies either that bound states are formed in the system (for example, *clusters*) [102, 103], or that there is ordering in the arrangement of particles (for example, the formation of a quasi-metallic structure in the case of complete ionization of the medium). The lifetime of such states depends on the rates of processes energy transfer of electrons and the energy of internal degrees of freedom into the translational degree of freedom of heavy particles — that is, the processes that take place at the second, *physico-chemical* stage of radiation-induced transformations.

7. Relaxation processes in the track of a multiply charged ion

7.1 Processes involving charged particles

Too little is known about the evolution of the primary track. From general considerations the process of development of the primary track may be described by the following scheme. The second — *physico-chemical* — stage of radiation-induced transformations is associated with the transfer of energy to other degrees of freedom and fast chemical reactions — that is, the system moves to a certain equilibrium state that may be considerably different from the initial state. This difference may be concerned with the physical properties (temperature, pressure), as well as with the chemical composition of the medium.

In Section 6 we demonstrated that upon completion of the physical stage the region of the track with a radius of about 4 – 6 nm is a multi-component *low-temperature nonisothermal plasma column*. Individual components of such plasma occur in the local (owing to the inhomogeneous distribution of particles) quasi-equilibrium states. We shall base the analysis of processes of transformation of energy of electron excitation on the classical concepts of local quasi-equilibrium states of plasma components. This treatment is justified by the fact that at a distance of $r > 0.5$ from the axis of the track the concentration of charged particles is such that the classical approximation is valid.

The energy of electrons may dissipate through a number of processes. First of all, electrons may excite the electron states of molecules and ions, including ionization (direct and stepwise). These processes are of a threshold nature [104]. Let us quote some estimates for the rates of these processes in water, using the expressions for the cross sections of excitation and ionization by low-energy electrons. In the case of Maxwell distribution, the mean rate of collisions of electrons with the excitation of molecules at $kT_e \approx 4$ eV is $\nu_{en} \sim 1.7 \times 10^{-9} n_e$ s^{-1}. If $n_e \approx 10^{22}$ cm^{-3}, then the rate of energy loss by this process is $q_{ex} \sim 10^{14}$ eV s^{-1}.

In the case of direct ionization, the mean frequency of collisions of electrons is $\nu_{d.ion} \sim 10^{-9} n_e$ s^{-1}, and at $n_e \approx 10^{22}$ cm^{-3} the rate of energy loss is $q_{d.ion} \sim 10^{14}$ eV s^{-1}. In the case of stepwise ionization these characteristics are greater by several orders of magnitude, and are equal to $\nu_{st.ion} \sim 7.3 \times 10^{-7} n_e$ s^{-1}, $q_{st.ion} \sim 3.7 \times 10^{17}$ eV s^{-1}. The transfer of energy to neutral molecules in the processes of excitation and ionization is highest in that region of the track where the degree of ionization is $\zeta \approx 0.5$. Owing to these processes, the region of excitation and ionization extends until the temperature of the electrons becomes less than the energy required for the transition of the bound electrons of the molecule to the first excited state, or less than the width of the forbidden band of the dielectric. The movement of the excitation boundary caused by the ionization of molecules may appear as the ionization wave. The parameters of such a wave were considered in Refs [105, 106].

Ionization and excitation of the electron states compete with the processes of energy transfer from the electron subsystem to other degrees of freedom, such as the excitation of vibrational and rotational levels and elastic collisions. The cross sections of direct excitation of the vibrational levels fall in the range $\sigma(v \to v') \sim 10^{-17} - 10^{-16}$ cm^2, and in the neighborhood of resonance they are greater by an order of magnitude [107 – 109]. As a result of these processes, the transfer of energy of electrons into the vibrational degree of freedom may occur at rates of $10^{11} - 10^{14}$ eV s^{-1} with the concentrations of particles as indicated above. Excitation of rotations and elastic collisions are less efficient: the transfer rate is about 10^{12} eV s^{-1}. However, elastic collisions are important in plasmas made up of non-bound atoms, as well as in solids — for example, in single-atom semiconductors and dielectrics. The energy exchange through elastic collisions in this case is the only channel available for the equalization of temperatures of electrons and heavy particles. If the rate of energy loss by elastic collisions is $\sim 10^{12}$ eV s^{-1}, the temperatures of electrons and ions are equalized over $\tau_{ei} \geqslant 10^{-12}$ s, and those of electrons and neutral particles over $\tau_{en} \geqslant 10^{-11}$ s.

Observe that various ion-molecular reactions may take place in plasma with the involvement of charged particles (see extensive bibliography in the review [110]). The fastest of these are the reactions of proton transfer. Although the ion-molecular reactions may radically change the composition of ions in the plasma, most of them do not change the degree of ionization of the plasma, and are not efficient in the transport of energy from the electron subsystem to other degrees of freedom. Important from the standpoint of the transfer of

energy of electrons into the translational energy of heavy particles is the dissociative recombination of electrons with complex molecular ions. The coefficient of this process may be as high as $k_{d,r} \sim 10^{-7}$ cm^3 s^{-1} [108, 110, 111], ensuring transfer of energy to the translational degree of freedom at the rate of 10^{15} eV s^{-1} at $n_e = n_i \approx 10^{22}$ cm^{-3}.

We see that a considerable share of the energy of electrons goes to the internal degrees of freedom, and partially to the translational degree of freedom through dissociative recombination. The share of energy spent on the translational movement of the products of dissociation depends on the type of molecular ion. In the case of recombination of the low-atom ions it may constitute several electron-volts.

7.2 Dissipation of energy of electron-excited molecules

Dissipation of energy of electron-excited molecules may also proceed via several channels. The spectrum of electron-excited molecules has a large proportion of superexcited states. The decay of such molecules is most efficient through self-ionization ($k_{a,i} \sim 10^{13}-10^{15}$ s^{-1}), dissociation ($k_d \sim 10^{10}-10^{13}$ s^{-1}), and the processes of internal conversion [112, 113]. In the course of dissociation, part of the internal energy is directly converted into the kinetic energy of the fragment of the dissociated molecule. In the processes of internal conversion (the transition from a highly excited state into the first excited state) the energy of electron excitation is converted into the energy of vibrations. The rate of such processes depends on the type of molecule. In a multiatom molecule, this rate may be $k_{i,c} \sim 10^{11}-10^{13}$ s^{-1}. Internal conversion of the low-atom molecules is only possible in the presence of a solvent. The intercombination conversion (the transition from the first excited singlet state into the first triplet state) is a slower process. In aromatic hydrocarbons, the rate of such conversion is $k_{ic,c} \sim 10^6-10^8$ s^{-1}. In aliphatic hydrocarbons, it is much higher ($k_{ic,c} \sim 10^{10}-10^{11}$ s^{-1}).

The rates of transition from the first excited state to the ground state depend on the energy of excitation of this level. Internal degradation (transition $S_1 \rightarrow S_0$) in molecules with energy $E_{S_1} \leqslant 1.5$ eV may take place at the rate of $k_{i,d} \sim 10^{11}$ s^{-1}. For molecules with $E_{S_1} > 2.5$ eV the rate of internal degradation is just $\sim 10^5$ s^{-1}. Even slower are the processes of intercombination degradation (transition $T_1 \rightarrow S_0$), predissociative and non-adiabatic decays, and radiative transitions [114].

7.3 Exchange of energy between different degrees of freedom

Generally speaking, in the absence of equilibrium all temperatures are different. Exchange of energy between different degrees of freedom facilitates equalization of temperatures. As a result of inelastic collisions, the fastest is the exchange of energy between translational and rotational degrees of freedom. Equalization of the temperatures $T_h = T_\rho$ takes from a few to several hundred collisions [104, 107–109]. From the studies of vibrational relaxation in a condensed medium, it follows that its time exceeds 10^{-12} s, and for small molecules (for example, CH_3I) the rate of vibrational relaxation decreases with increasing temperature [115].

Equalization between translational and vibrational degrees of freedom takes a much greater number of collisions. This applies also to the $E-T$ exchange. The rate of $E-V$ exchange depends considerably on the particular system. Owing to the conversion, in complex molecules the rates of nonradiative transitions of molecules from highly excited electron states to the first excited state may be as high as 10^{11} to 10^{13} s^{-1} [113].

Thus, the rate of conversion of the energy of electron excitation (including the energy of electrons) into thermal energy depends on the efficiency of the processes of decay of molecules and on the rate of the $V-T$ relaxation. Evaluation of the rate of this process indicates that the conversion of the energy of electron excitation through the vibrational degree of freedom into thermal energy is rather extensive in time.

7.4 Processes of energy removal from the track

Apart from the processes considered above, the energy of electron excitation can be removed from the track by the following channel. As is known, the energy of electron excitation in polymers may migrate along the aliphatic chain. Over the anticipated lifetime of the excited state $\tau \geqslant 10^{-12}$ s, the mean path from the place of initial excitation may be greater than a hundred C–C bonds [116]. The intermolecular energy transfer also facilitates the removal of energy from the track, but the rate of this process is 10^9 s^{-1}. However, the more important processes of energy removal from the track are heat conduction and transport by acoustic waves.

The efficiency of the transfer of heat in a medium is characterized by the coefficient of temperature conductivity

$$\chi = \frac{\varkappa}{\rho C_p}, \tag{33}$$

where $\varkappa$ is the coefficient of heat conductivity, ρ is the density of the medium, and C_p is the specific heat capacity at constant pressure [117]. In a multicomponent medium, each component contributes to the transfer of energy, which depends on the type and phase state of the medium. In solid dielectrics, the transfer of thermal energy is accomplished by phonon gas across the lattice, and in metals this is done not only by phonons (lattice conductivity), but also by conduction electrons. As a matter of fact, the heat conductivity of typical pure metals almost completely depends on the conduction electrons. The coefficient of heat conductivity of pure metals may be as high as several hundred watts per meter-kelvin (403 W (m K)$^{-1}$ for silver, 210 W (m K)$^{-1}$ for aluminum) [118]. The coefficient of temperature conductivity of metals lies in the range from 0.21 (iron) to 1.71 cm^2 s^{-1} (silver) [119].

These values of χ are calculated by formula (33) for a metal as a whole — taking into account the lattice heat capacity [$C_V \approx 3R \approx 25$ J (mol K)$^{-1}$] and the density of the metal. The heat capacity of classical electron gas is much lower [$C_V^e \approx (3/2)R$]. The heat capacity for degenerate electron gas is just a few percent of the lattice heat capacity. Because of this, the value of χ_e is much higher than χ. Accordingly, the energy of electron excitation, initially localized in a cylinder of radius $r_0 \approx 4$ nm, is efficiently distributed over the electron gas in a large volume of the medium, without transferring it to the lattice. The efficiency of transfer of energy from a cylinder of radius r_0 is characterized by time $\tau_t = r_0^2/\chi$. In metals the characteristic time of existence of the locally heated electron gas in the cylinder of radius $r_0 \approx 4$ nm is $\tau_t < 10^{-13}$ s.

The lattice conductivity may be rather high in certain dielectrics with rigid bonds. In crystals with a diamond lattice, it is comparable to the heat conductivity of metals (137 W (m K)$^{-1}$ for silicon, 54 W (m K)$^{-1}$ for germanium). The heat conductivity of a diamond is even higher than that of

silver, which has the highest thermal conductivity among all pure metals [$\varkappa_{C_{\text{diamond}}} = 550\text{W (m K)}^{-1}$] [118]. The coefficient of temperature conductivity of such crystals is comparable to χ of metals (0.53 $\text{cm}^2\ \text{s}^{-1}$ for silicon). For $r_0 \approx 4$ nm such dielectrics have $\tau_t \sim 10^{-13}$ s.

Heat conductivity of liquids and polymers is much lower. In water we have $\varkappa = 5.8$ W (m K)$^{-1}$ and in polymers $\varkappa = 0.03-0.8$ W (m K)$^{-1}$. The values of χ for water and polymers are three orders of magnitude lower than for those of metals (1.38×10^{-3} $\text{cm}^2\ \text{s}^{-1}$ for water, $(0.4-1.8) \times 10^{-3}\ \text{cm}^2\,\text{s}^{-1}$ for polymers [120]). Accordingly, in such media the characteristic time of existence of the heated region $r_0 \approx 4$ nm is higher than $\tau_t \sim 10^{-10}$ s.

The efficiency of the hydrodynamic mechanism of energy transfer is characterized by time $\tau_g \sim r_0/s_0$, where s_0 is the speed of sound. In water and polymers $s_0 \sim 1.5 \times 10^3\ \text{m s}^{-1}$ [120], and for $r_0 \approx 4$ nm we have $\tau_g \sim 3 \times 10^{-12}$ s. For these substances, the energy transfer by this mechanism is more efficient than the transport of heat.

We see that the physico-chemical stage in the primary track is characterized by many different processes, whose diversity depends on the type of medium. In pure metals, the main portion of energy from the electron subsystem is rapidly removed from the track, and only part of it is transferred to the lattice. In molecular media, the conversion of the energy of electron excitation into thermal energy is associated, as a rule, with the decomposition of molecules (monodecay, dissociative recombination). Decomposition of the molecules is one of the causes of the increased yield of low-molecular products in radiolysis of liquids by fragments of nuclear fission. In addition, the process of radiolysis by such particles is accompanied by a change in the hydrodynamic parameters of the medium (temperature, pressure), which may also facilitate the decomposition of molecules [121].

8. Features of radiation-chemical reactions in the tracks of particles of a different nature

8.1 Effects of phase state and the role of LET in radiolysis

The stage of formation of the primary track in molecular media is followed by the stage of chemical transformations of matter or structural changes against the background of removal of excess energy from the volume of the track, and the diffusion of active intermediate particles. In a condensed medium the chemical stage is divided into the *track* period, which is characterized by spatial nonuniformity and inhomogeneity in the distribution of chemically active particles, and the subsequent period with uniform distribution of the reactants. Upon completion of the *chemical* stage, chemical equilibrium is established in the system. In a solid dielectric this stage ends with the formation of the latent track. In biological systems there is a fourth (*biological*) stage, characterized by the reaction of the organism to the chemical products created by radiation.

In gaseous media the track structures are separated by large distances and contain, as a rule, a small number of active particles. The diffusion rapidly smooths out the initial inhomogeneity in the distribution of active particles, and by the beginning of the stage of chemical reactions the distribution of intermediate particles in the exposed volume is practically homogeneous. Because of this, the role of tracks in the gaseous phase is negligible. Only the multiply charged ions, like fission fragments, may create spatial inhomogeneity strong enough to affect the development of chemical reactions [122, 123].

Because of the higher density, the spatial inhomogeneity in the distribution of reactants is more articulate in liquids. At the same time, the diffusion processes in liquids are slower. In addition, the phase state of the medium affects the redistribution of the primary active particles, increasing the number of ionized states in the liquid (see Section 4), and also has an impact on the subsequent relaxation processes and the decay of the excited and ionized states [124]. The transition from gas to liquid increases the importance of the inverse processes of recombination of electrons with the parent ion, and decreases the degree of dissociation of molecules into radicals owing to the so-called cell effect [125]. The differences in the kinetics of reactions in the gas and liquid phases depend on many factors, and do not allow for singling out the pure role of the tracks related to the change in the density of the medium. Most fruitful is the study of the dependence of radiation effects on the structure of a track in a situation where the initial physical and chemical properties of the medium are maintained.

Theoretical analysis of radiolysis of liquids is based, as a rule, on solving the diffusion kinetics equations of reactions in the tracks [29, 126 – 130], assuming their spherical or cylindrical symmetry. The stochastic approach has also been used [131]. The discussion of these approaches, as well as any detailed treatment of radiolysis of real systems, falls outside the scope of this review. We only briefly consider the effects of the structure of the tracks on the radiolytic transformations.

The use of diffusion kinetics equations allows for the explanation of many experimental facts observed in the radiolysis of water solutions [127, 130], and especially the dependence of yield on the linear energy transfer (LET). Because of this, LET came to be regarded as a kind of universal characteristic of the quality of radiation. The concentration of active particles in the track was considered as a straightforward function of LET, disregarding the type of charged particle, and the dependence on LET became known as the *track effect*.

However, not all experimental results could be interpreted in a consistent way in the context of such an understanding of the track effect. Such results include the sharp increase in the yield of the low-molecular products of radiolysis at high values of LET [132 – 134]; the increased yield of some products of radiolysis of methanol (for example, ethylene glycol [72]), whose production is associated with the recombination of radicals in the tracks with decreasing rather than increasing LET; and the different yields of hydrogen $G(H_2)$ in the radiolysis of benzene at exposure of protons and α-particles with the same values of LET [133].

Careful studies of the radiolysis of benzene and the dosimetric Fricke system, carried out in Refs [135, 136] using different ions, revealed that the radiation-chemical yields dependence not only on the value of LET, but also on the type of particle is the rule rather than the exception. This becomes clear if we recall the discussion of the detailed structure of the track and its dependence on the type of charged particle (see Sections 4 – 6 above, and Refs [13 – 15]). The role of the structure of the track is especially clear in the radiolysis of liquids by heavy ions. In this case it is possible to vary the geometry of the tracks and the concentrations of active particles in the tracks.

8.2 Effects of the structure of the track on the radiation-chemical processes in liquids

The effects of the structure of tracks of ions have been studied in Refs [134 – 136], as well as in the reviews [13 – 15]. Using the comparative analysis of the tracks of ions, we can offer the following explanation for the dependence of yields on LET. The low values of LET relate to the radiolysis of liquids using high-energy protons. The track of the proton in this case consists of the core and the branches — the tracks of δ-electrons. The higher the energy of the proton, the bigger proportion of its energy is carried away by the δ-electrons. The core itself eventually transforms into separate non-overlapping spurs — in other words, the track of the proton, with the exception of certain features (see Section 6), will resemble the track of the electron. As a result, the nature of the radiolysis will resemble the radiolysis under the action of fast electrons.

As the proton decelerates, both its LET and the number of δ-electrons increase, while the size of the track becomes smaller because the maximum energy of the δ-electron decreases. As a result, we observe a sharp increase in both local and mean concentrations near the axis of the track. This facilitates the increase of yield of the products of recombination of chemically active particles as LET increases — that is, there is a direct correlation between the density of active particles in the track and LET. A similar situation is observed with the track of the α-particle.

High values of LET (above 1 keV nm^{-1}) are observed when the liquid is exposed to multiply charged ions — for example, fission fragments. As already noted in the preceding section, the structure of such tracks has certain special features. One is related to the fact that the mean concentration of active particles increases with decreasing LET. Because of this, the yields of certain products of radiolysis first increase with the decreasing LET of the fission fragment, reach their maximum, and then start to decrease (as the fission fragment further decelerates and the energy loss by elastic collisions becomes considerable). This explains the results of the experiment on the radiolysis of methanol using fission fragments with different initial energies [72].

The second feature of the structure of the track of multiply charged ions (the high concentration of the fragment ions in the core of the track) consists of the fact that it is mainly the low-molecular products of radiolysis that are produced in the core of the track, while the yields of the more complex products decrease. An example is the high yield of H_2, CO, CH_4 in the radiolysis of liquid hydrocarbons under the action of multiply charged ions [72, 132 – 134].

The intermediate values of LET correspond to the radiolysis of liquids exposed to the ions of light elements that are at the beginning of the periodic table. We find that two or more ions may exhibit the same value of LET. As demonstrated in Section 6.5, even though the values of LET are the same, all other parameters of the ions are different. The relationships between the radiation-chemistry yields for different ions will depend on which of the four possible relations between their velocities is realized. If it is the first option (the value of LET is to the right of the maximum), then the light ion forms a dense track. The size of this track is the smallest, while the local and mean concentrations of chemically active particles are the highest. Therefore, the yield of recombination products will be higher for the light ion than for the heavier ions. Radiolysis in the track of the heavier ions (with higher Z) corresponds essentially to the process that takes place in the track of a light ion (with lower charge) with a lower value of LET. This is the behavior of the curves $G(H_2)$ versus LET, obtained for the radiolysis of benzene under the action of different ions (see Fig. 5 in Ref. [135]).

8.3 Thermochemical action of ionizing particles

The appearance of point heat in the wake of an ionizing particle was first indicated in Ref. [137]. The concept of point-heat is based on the assumption that the energy initially transmitted by the particle for the excitation of the electron states of molecules is immediately transformed into energy of vibrations of molecules in a small region located near the path of the particle. Early theories of the chemical action of ionizing radiation, using the model of *thermal spike* (a later synonym for point-heat), attempted to explain chemical transformations taking place in the irradiated medium [138, 139] (see also the review [10] on this). Later it was demonstrated that for the track entities (spurs) formed by charged particles with low LET, the temperature increase was insignificant. On top of that, the lifetime of the heated region is short.

According to Mozumder (see Ref. [10]), the temperature rise of a spur of radius ~ 2 nm, in which an energy of ~ 30 eV is localized, is just 30 K, while the characteristic relaxation time is about 6×10^{-12} s. According to the Arrhenius equation, the reaction of free radicals with a characteristic energy of activation ~ 8 kcal mol^{-1} and a pre-exponential coefficient of $\sim 10^{-11}$ cm^3 $(mol\ s)^{-1}$, requires that the region heated to 400 K should exist for at least 2×10^{-6} s. This implies that for such reactions, the thermochemical action of γ-radiation and fast electrons is too weak. The review [140] states, however, that for certain reactions the temperature jump in the spur may reverse the direction of the primary reaction processes. For example, using the normal specific radical reaction rate of $\sim 5 \times 10^9$ dm^3 $(mol\ s)^{-1}$ at 300 K, then with the energy of activation ~ 6 kcal mol^{-1}, it is sufficient for certain reactions (for example, for the reaction of a solvated electron with an acceptor) that the heated region persists for $\sim 10^{-10}$ s.

In the case of multiply charged ions, the density of energy absorbed near the track (in a cylinder of radius 4 – 6 nm) is high. If this energy were adiabatically transformed into heat, the heat in this region could be considerable (above 10^4 K). Based on this assumption, Goldanskiĭ and Kagan [141] considered the general characteristics of the thermochemical effect of ionizing radiation. In some papers [10, 132, 142], the model of the thermal spike was used for explaining the increased yield of the low-molecular products of radiolysis by the fission fragment. The yields of low-molecular products in radiolysis of methanol were estimated in Ref. [142]. Calculations indicate, however, that for this medium the thermochemical effect is low, even notwithstanding the lag of energy transfer from the electron subsystem to other degrees of freedom (see Section 7). This weak effect of the thermal spike on chemical transformations is due to the smallness of the heated region and the short lifetime of the thermal spike.

To evaluate the heating of the medium within the thermal spike, the authors of Ref. [143] conducted the following experiment. Gaseous propane and a mixture of methane with ammonia (6%) and propane (4%) of varying densities were exposed to irradiation by fission fragments. The yields of isopropyl radicals and normal propyl radicals were measured.

The heat of formation of isopropyl radicals and normal propyl radicals differ by 3.6 kcal mol^{-1}. Accordingly, the change in the relative yields of these radicals, produced in radiolysis by fission fragments, as compared to the ratio of the same radicals produced in γ-radiolysis, could be used for assessing the heat in the track. The results of this experiment also indicate that the heating effect is much smaller than predicted by the model of the thermal spike.

8.4 Hydrodynamic action of radiation

Hydrodynamic effects of radiation in stable liquids are associated with the excitation of hydrodynamic radiation from the tracks of charges particles. The theory of this radiation was proposed in Ref. [144]. It derives from the assumption that the jerky movements of ionic complexes, the microexplosive creation of nucleation cavities by local heating near the tracks of the particles, are accompanied by intensive, local, pulsed emission of ultrasonic and hypersonic waves, which at the initial stage have the nature of quasi-microspheric shock waves. This phenomenon is characterized by the fact that the zone of the strong radiation field is much larger than the region of primary ionization. If such radiation actually exists, it must have a strong destructive action on the substance. The effect ought to be similar to the effect of shock waves or to exposure to powerful ultrasound.

Today there is no doubt that fast charged particles excite acoustic waves in the medium. A new science of radiation acoustics emerged from the combined studies in acoustics and radiation physics. Many papers treat various mechanisms of sound generation by penetrating radiation (see Refs [145–147]). They are usually associated with the different physical possibilities of transforming the energy of penetrating radiation into acoustic energy [146]. Many of the proposed mechanisms make just a small contribution to the total sonic field created by radiation. According to the thermoradiative (thermoelastic) mechanism, the sound is generated by thermal expansion of the region of the medium that has absorbed the energy of the charged particle. This corresponds to the moderate densities of the absorbed energy when there are no phase transitions.

The emergence of a shock wave in the track of a single particle has not been finally established, although there have been some quantitative estimates of the parameters of such a wave. In Ref. [148] the generation of shock waves was defined as the consequence of the explosive expansion of microscopic volumes of liquid (thermal spikes) overheated with δ-electrons. The calculation indicates that a δ-electron with an energy of 1.23 keV can create a microscopic spherically shaped region of radius 0.664 nm, the pressure in which is as high as 8.21×10^5 atm. This forms the basis for the conclusion regarding the destructive action of the 'hydrodynamic radiation' on living tissues and structural materials.

In Ref. [121] the model of an infinitely long 'filament' source with a given energy release per unit length of the filament was used for calculating the parameters of the shock wave generated in water by a fission fragment under the following assumptions. The energy of the fragment is instantaneously converted into heat in the cylindrical region of the track with radius $r_0 \approx 6$ nm. Adiabatic heating in this cylinder creates a pressure $P \approx 60$ kbar. The time evolution of the shock wave, whose front was concentric with the cylindrical surface of the source, was described using the equations of the macroscopic theory of explosions in water. The velocity of propagation of the shock wave front (in cm s^{-1}) varies as $D \approx 0.34/\sqrt{t}$, and its radius as $r(t) = r_0(1 + t/t_0)^{1/2}$, where $t_0 \approx 10^{-12}$ s. Based on these pressure estimates, the effect of the shock wave on chemical transformations in the track is evaluated. The shock compression of matter increases the concentration of electrons, ions and radicals, which stimulates various chemical processes.

The instantaneous increase in pressure in the track has not been convincingly substantiated. After the ionization of the molecules, the short-range forces of intermolecular interaction are replaced with the long-range shielded Coulombian interaction. The transition to the new (plasma) state may be accompanied not by an increase in pressure, but — at certain degrees of ionization — by a pressure drop owing to the change in the potential energy of interaction. The rise in pressure and heating of the medium are only possible as a result of the subsequent conversion of the energy of electron excitation (monodecay, dissociative recombination), and not the other way round as stated in Ref. [121]. As demonstrated earlier, the rates of individual processes of energy transfer from the electron subsystem are comparable to the rate of the hydrodynamic mechanism of energy transfer, and in some processes they are even lower (for example, $\tau_{ei} \approx \tau_g$, and $\tau_{en} < \tau_g$). Therefore, the estimates obtained in Ref. [121] ought to be regarded as exaggerated. Even these vales, however, imply that at $t \approx 5 \times 10^{-12}$ s, the velocity of the front of the shock wave will slow down to the velocity of sonic waves in water $s = 1.5 \times 10^5$ cm s^{-1}, having traveled $r = 14.7$ nm. Thus, the shock wave rather soon becomes a sonic wave. It ought to be expected, therefore, that the effects of the hydrodynamic mechanism of energy transfer will take the form of an impact of an acoustic wave mainly at a rather large distance from the track.

The author pointed out this circumstance as early as 1980 (see Ref. [98]). However, recently published papers [149, 150] again assume the generation of shock waves in the tracks, and the parameters of the shock wave are calculated from the macroscopic theory of underwater explosions [151]. The calculation of the parameters of the shock wave in Ref. [149] is practically identical to the approach used earlier in Ref. [121]. Accordingly, all our comments on the results of Ref. [121] completely apply also to Ref. [150].

The authors of Ref. [149] postulate the generation of a shock wave in a spur by a single water molecule occurring in the high-energy vibration-excited state. Such molecules result from the geminate (pairwise) recombination of electron – ion pairs in the spurs (see Refs [50, 51]). In Ref. [149] it is assumed that during the time $\sim 10^{-12}$ s the energy of vibrational excitation of one molecule is transmitted to its nearest environment, and a spherical thermal spike of radius ~ 0.75 nm is formed. Trivial estimates demonstrate that the assumptions made in Ref. [149] are not strictly reasonable.

The concentration of molecules in water under normal conditions is $n = 3.345 \times 10^{22}$ cm^{-3}. The volume per molecule, and the radius of the sphere of this volume are, respectively, $v = 1/n = 3 \times 10^{-23}$ $cm^3 = 3 \times 10^{-2}$ nm^3 and $r = (3v/4\pi)^{1/3} = 0{,}192$ nm. Accordingly, the mean distance between the molecules is $d = 2r = 0.384$ nm, and the spherical volume occupied by the initial molecule and its nearest environment (in one layer) is $V = 4\pi(3r)^3/3 = 27v$. The adiabatic heating of this volume of radius ~ 0.576 nm by the energy of the vibration-excited molecule of 6.26 eV will raise the temperature by $\Delta T \simeq 295$ K, which is not much even under such assumptions.

The formation of an equilibrium ensemble of 27 molecules takes $\sim 4 \times 10^{-12}$ s (given that the time of one collision is $\sim 1.5 \times 10^{-13}$ s, as assumed in Ref. [149]). Therefore, the time of vibration-translational relaxation is greater than accepted in Ref. [149]. The characteristic time of propagation of hydrodynamic disturbance from this volume, calculated using the method of authors of Ref. [149], is $\tau_g \approx 6r/a_0 = 0.79 \times 10^{-12}$ s. According to these estimates, the rate of the hydrodynamic mechanism of energy transfer is higher than the rate of vibration-translational relaxation. Because of this, a sharp increase in the pressure, and hence the formation of a shock wave, is hardly possible. The formation of a shock wave is more likely to occur through the mechanism of splitting the vibration-excited molecule into two fragments, because in this case the kinetic energy of the fragments will be distributed over the ensemble of molecules sooner than through the mechanism proposed in Ref. [149].

Experimental study of the acoustic waves in the frequency range 0.2 to 1.0 MHz in liquids (acetone, ethyl alcohol, glycerin, carbon tetrachloride) generated by the solitary heavy nuclei (fission fragments) was the subject of Refs [152, 153]. Only in carbon tetrachloride, with the minimal distance of $\sim$ 1 mm between the source and the hydrophone, observed in the amplitude spectrum of noise of the acoustic channel, were significant changes attributable to the change in the intensity of the source of fission fragments. According to Ref. [152], this effect, even though it was only discovered in one liquid, may serve as an indirect indication of the generation of hypersonic pressure waves, postulated in Ref. [121]. This observation, however, does not yet prove that the shock wave is the primary source of this wave. Shock waves have certain important distinctions from sonic waves [117]. The velocity of a shock wave is always higher than the speed of sound in the unperturbed medium, and depends on the intensity of the shock wave. Shock waves are accompanied by a motion of the medium in the direction of travel of the front. The parameters of state and motion of the medium change abruptly in the front of the shock wave. A shock wave is not periodical, and propagates as a solitary compression shock.

8.5 Problem of equivalence of radiation impact of different types of ionizing radiation

The problem of equivalence arises in at least two situations. One is the use of known data on radiation effects of some type of ionizing radiation for predicting radiation effects caused by a different type of radiation. This problem is closely related to the applicability of dosimetric systems (especially liquid chemical dosimeters). The other relates to the possibility of simulating one source of radiation (which may be difficult to control, like cosmic rays) with a different source.

As a rule, the radiation effect from the majority of radiations is a superposition of the effects caused directly by the primary radiation, and the effects of the secondary (and maybe tertiary) radiation, in which part of the energy of the primary radiation is transformed. Because of this, if the secondary radiation is definitive for some radiation effect, it may be regarded as the primary source. As follows from our knowledge of the tracks of charged particles, this assumption is correct as long as the spatial distribution of track entities in the exposed volume is close to the distribution resulting from the primary radiation. In accordance with this basic principle, exposure to X-rays and gamma radiation may be replaced with irradiation with fast electrons with the appropriate energy spectrum, while exposure neutrons may be equivalent to exposure to the ions of the elements that comprise the medium.

The use of fast electrons for simulating the radiation effects of heavy ions is only possible in principle for high-velocity ions. When the velocity is high (recall the conditions of formation of continuous extensive tracks), the ion generates non-overlapping track entities similar to those created by fast electrons. Simulation of continuous tracks of heavy ions runs into difficulties. It might seem that the availability of high-current electron accelerators has made it possible to create in the medium such concentrations of active particles that are close to those realized in the tracks of heavy ions (see Ref. [154]). Such simulation, however, does not reproduce the spatial distributions of active particles. Electrons from high-current accelerators realize the high concentrations of active particles in macroscopic volumes. The large size of the region with a high concentration of charged particles is not good for energy transfer. Because of this, the temperature in the exposed volume will rise higher than in the individual track. With the high concentrations of charged particles in macroscopic regions we encounter new effects due to the collective properties of the dense electron – ion system [155].

For a long time, LET was used for characterizing the quality of ionizing radiation. However, the analysis of the track structure on the radiation-chemical processes brings us to an important conclusion: there is no direct correlation between the value of LET and the local and mean concentrations of active particles in tracks. *For this reason, LET cannot serve as the universal characteristic of quality of radiation, notwithstanding the particular types of particles.*

Attempts have been made to find some other characteristic of quality of radiation to replace LET — for example, the ratio Z^2/v^2 [156, 157]. However, a comprehensive description could not be achieved in terms of Z^2/v^2 [158], which is quite understandable. The ratio Z^2/v^2 is a certain approximation of LET, and therefore all our criticism of LET as a universal characteristic of the quality of radiation entirely applies to this parameter.

With reference to ions, the authors of Refs [89, 136] investigated the possibility of using the mean specific energy absorption D_c in the core of the track as the measure of equivalence. This selection was based on the following considerations. Firstly, D_c reflects the three-dimensional nature of energy absorption in the microscopic volume of the exposed medium, and it is the microscopic volume that hosts the majority of all primary transformations. Secondly, out of all quantities that characterize the structure of the track, it is D_c that exhibits the strongest dependence on the type of primary ion. Finally, unlike LET, the curves of D_c versus the velocity and the residual path do not show any extremes.

It was found that neither in the representation of $G(H_2)$ as a function of D_c in Ref. [136], nor in the representation of $G(Fe^{3+})$ as a function of D_c in Ref. [89], was it possible to eliminate the dependence of the effect on the type of ion. The differences in yields for different types of ions are inevitable and are related to the fact that they have the same value of D_c, while the size of the core is different. Because of this, the competing action of the diffusion processes on the physico-chemical and chemical transformations of the reactants is different, which tells on the magnitude of the effect.

It appears that the attempts to introduce a universal characteristic of the radiation-chemical impact of radiation are futile. The nature of radiation transformations depends on the spatial distribution of the active particles in the track. The shape of the latter for a large part of the track of the particle depends on all three parameters of the particle (charge Z, velocity v, and mass m). Useful for the comparative analysis of the effects of different radiations, however, are the characteristics averaged over the volume of the track, like the mean energy density, the mean concentration of active particles, etc. Despite the difference in the effects for different ions with the same D_c, this characteristic can be used as the approximate parameter of equivalence. As demonstrated in Ref. [89], the functions $G(Fe^{3+})$ versus D_c are free from ambiguities for yields of the same ion, while similar functions $G(Fe^{3+})$ versus LET have a range of values of LET that correspond to two values of $G(Fe^{3+})$. This ambiguity is related to the presence of a maximum (Bragg's peak) on the LET curves.

To end this section, let us pay attention to the fact that this discussion has straightforward implications for liquid dosimeters of ionizing radiation. Since the radiation effect in such systems generally depends on the structure of the track of charged particles, the dependence of readings of liquid dosimeters only makes sense for one type of radiation, and only either to the left or to the right of Bragg's peak. A dosimeter calibrated for one type of radiation can only be used for measuring the absorbed dose of a different radiation if it has been corrected for the specific track effects. Because of this, the recommendation given in the monograph [84] on the use of curves of $G(Fe^{3+})$ versus LET, obtained in Ref. [159], for measuring exposure to heavy ions, is not correct.

9. Models of formation of latent tracks

9.1 Model of an electronic thermal spike

Using the concept of point-heat introduced in Ref. [137], Seitz [160] developed the theory of thermal spikes of two kinds (corresponding to spherical and cylindrical symmetry) in solids. Spikes of the first kind result from elastic collisions. The knocked-out atom, having slowed down to an energy which is not sufficient for displacing atoms from lattice points, shares its remaining energy with the nearest neighboring atoms. As a result, the temperature of the lattice increases. Experimental studies reveal, however, that latent tracks do not form in dielectrics when the energy of the ions facilitates the predominance of elastic scattering of ions by the atoms of the medium.

According to Seitz's classification, the formation of a thermal spike of cylindrical symmetry is due to the processes of energy absorption by the electron subsystem. Today such spikes are referred to as electronic thermal spikes [161, 162]. The simplest model of the electronic thermal spike assumes that the energy localized initially in the electron subsystem is instantaneously transmitted to the lattice. Calculations of the temperature field in the track (as a rule, in metals and metallic films) in some papers have been made, accounting for different relaxation times [163, 164].

The concept of the electronic thermal spike was used for explaining the formation of latent tracks by fission fragments in dielectrics (see Refs [4–6]) in thin films of siliconand germanium, magnesium oxide of varying thickness [165], and metallic films comprised of numerous mosaic blocks [7, 166]. The main conclusion of these studies can be formulated as follows. The thermal mechanism for generating defects in the latent track operates when the removal of energy of electron excitation from the track is impeded. In such a case the lattice can be heated above the melting point. The heating creates a region of recrystallization around the path of the ion. This explains the formation of tracks even in metallic thin films and mosaic blocks [7, 164, 165].

In the opposite case, owing to the high electron conductivity in metallic samples with a highly ordered structure, or owing to the high lattice conductivity in crystals with rigid bonds (diamond, silicon), the lattice is heated only slightly. There are no structural changes in the lattice, and no tracks from fission fragments.

In materials with poor thermal conductivity, the contribution of the thermal mechanism to the generation of defects becomes important, and in some cases definitive (in a solid atomic dielectric in the absence of direct radiation-induced transformations). The situation with polymers is different. We know that chemical reactivity increases in polymers after exposure to fast electrons or γ-radiation. It was demonstrated that the formation of tracks correlates with the number of broken molecular chains. It is quite possible that the defects are mainly produced as a result of radiation-induced transformations, and the thermal mechanism accompanies the radiation mechanism. A thermal wedge may extend the zone of distribution of defects. The thermal wedge may also be primarily responsible for the excitation of acoustic waves, which may generate additional defects at a considerable distance from the path of the ion.

9.2 Model of an ion explosion wedge

The mechanism of an ion explosion wedge was proposed in Ref. [167], based on the following idea. The charged particle creates along its path a narrow region of positively charged ions in high concentration. Mutual repulsion of these ions may displace them from the interstices, which gives rise to vacancies. Subsequent elastic relaxation reduces local stresses and extends the region of deformation. The resulting deformations of the lattice can be observed with the transmission electron microscope.

The model of the ion explosion wedge is semi-quantitative. It has been used for deriving a number of quantitative criteria of formation of a latent track. The most important criterion derives from the assumption that the formation of the track requires that the forces of electrostatic repulsion between the ions should exceed the mechanical strength of the medium. Based on such parameters as the lattice constant, dielectric permitivity and Young's modulus, the 'coefficient of stress' of matter — the measure of relative sensitivity of various track-forming media — was defined. According to this theory, tracks are especially easily formed in those materials for which the above three parameters are low.

Another criterion, known as the continuity criterion, derives from the assumption that at least one ion has to be formed in each atomic plane. This requirement is more stringent than the condition of formation of a extended track (see above). Moreover, for the region of positive ions to exist for more than 10^{-13} s, the density of electrons must be low. Obviously, it is only dielectrics that satisfy this condition. Finally, to facilitate the process of deformation of the lattice, the mobility of vacancies must not be high. Otherwise the ions may be neutralized sooner than they are pushed apart by the

electrostatic forces. This implies that tracks will not form in good semiconductors.

The model of an ion explosion wedge gives an adequate description of the sensitivity of media used for registration of tracks, and explains the absence of tracks in metals and good semiconductors. This circumstance has led many researchers to the conclusion that this model is fairly adequate for crystalline solids [4]. Detailed analysis of the formation of tracks of multiply charged ions reveals, however, that the idea of separation of charges, on which the model is based, is not correct. As demonstrated earlier, the central region of the primary track is a quasineutral plasma filament [98, 99]. The separation of charges in a plasma does not exceed the Debye radius. If neutrality is violated, it will be restored within less than 10^{-14} s [99]. Quasineutrality can only be violated at the boundaries of the exposed medium (at the points of entry and exit of the ion). Because of this, the model of an ion explosion wedge has the right to exist for explaining sputtering of matter from surfaces exposed to ions [17, 168].

9.3 Models of shock waves and acoustic waves

Generation of a shock wave in the track of a heavy ion is represented in different ways. The most common theory views the formation of the shock wave as a result of a thermal electron spike — in accordance with the ideas of Ref. [121]. The instantaneous heating of matter in the limited volume of the track generates a pressure jump that sets the particles of the medium in motion. If the velocity of this movement is faster than the speed of sound, a shock wave is created in the medium. It is this mechanism of the shock wave that has been used for explaining the hollow channels in the surface tracks produced by heavy ions in single crystals of gypsum, in LiF, in carbon and in glass [169 – 173].

An important drawback of this model consists of the use of the classical theory of heat conductivity. This theory is based on the Fourier law for heat flux that holds as long as the scale of space-time inhomogeneities exceeds the free path length and the time between collisions. Formal application of these concepts to the fast processes in the track is not quite correct. A more consistent description of the nonequilibrium processes must be based on the relaxation equations, or at least on the Fourier law modified to take into account the relaxation of thermal flux (see Ref. [164]).

Some authors (see Ref. [162]) consider the generation of a shock wave as a consequence of electrostatic repulsion of ions produced in the core of the track. Since the plasma in the track is quasi-neutral, this mechanism of formation of shock waves is not likely to operate in the bulk tracks. Finally, in Ref. [174] the effect of heavy ions on metal was viewed as the 'instantaneous impact' of electron pressure. According to the author, in metals with a sufficiently low coefficient of temperature conductivity, the stress near the ion path may reach the yield point, which may cause local changes in the crystal lattice.

Such diversity of the processes of conversion and transfer of energy of electron excitation implies that there are many mechanisms that contribute to the formation of defects in the latent track. The relative role of a particular mechanism in the generation of defects depends on the structure of the medium and the spatial arrangement of these defects. The establishment of the mechanism responsible for the generation of defects in a latent track calls for a careful analysis of the processes that take place in the track at the physico-chemical stage.

10. Conclusions

This review is concerned primarily with the formation stage of the primary track. The processes that take place at the stage of radiation disturbances receive more attention, and theoretical interpretations of this stage have been more successful. This is due to the fact that for some problems, it suffices to understand the process of energy release near the path of the ion in order to explain the radiation effect and to predict the behavior of the effect when one source of radiation is replaced by another. The use of such considerations in applying radiation chemistry is demonstrated in Section 8. Problems of this kind include, for example, the interpretation or prediction of the shape of hollow channels produced after chemical etching of solid dielectrics exposed to heavy ions.

It is an experimental fact that the rate of etching along a track is only determined by that part of the energy loss of the ion which is localized along the axis of the track in the cylindrical region of radius 4 to 6 nm. Concentrated in this region are most of the disturbances of the medium created by the ion. From these considerations, the value of $D(r < 4)$ (see Ref. [87]) is a good characterization of the measure of the magnitude of disturbances in the central portion of the track, and can serve as the argument of the function that describes the rate of etching along the track.

The results concerning the structure of the primary track throw new light on the operation of the Wilson chamber [175] and bubble chambers [176] used for the registration of tracks of ions. The high degree of ionization in the Wilson chamber may by itself be the cause of condensation even in a non-supersaturated vapor. The lifetime of the track in the condensed form may be increased by using simple monoatomic media in the Wilson chamber. In such media there are no fast channels of energy transfer from the electron subsystem to the heavy components.

The situation with the bubble chambers is different. At the early stage, the bubble chamber, like the Wilson chamber, operates according to the ion mechanism. As energy is removed from the electron subsystem, the ion mechanism is replaced with a thermal mechanism, which leads to the formation of gas bubbles. In the case of the bubble chamber, the ion mechanism increases the lag of the instrument before registration. To reduce this lag, it is necessary to speed up the processes of energy removal from the electron subsystem. This means that the best media are polyatomic substances with poor thermal conductivity.

Finally, let us once again emphasize that the interpretation of a particular radiation effect requires careful analysis of the distribution of energy transferred to the medium. As demonstrated above, it is often not enough to know the value of LET or the ionization losses. Such a correlation is the exception rather than the rule. This conclusion is brilliantly supported by the results obtained at the Physical Institute of the Academy of Sciences in the 1960s and 70s concerning ionization effects in the detectors of relativistic charged particles (see the review [177]). The main conclusion of these studies is that the ionization effect produced by charged relativistic particles is not always correlated with the ionization energy losses, but is determined by the spectrum (differential cross section) of inelastic losses in the medium of the detector. The introduction of the detector response function $R(\omega)$, which also depends on energy ω, transmitted by the particle in the single act of inelastic collision in the detector medium, was also very important. The response

function characterizes the efficiency of use of this energy for the formation of a fragment of the track. Such an approach allows for describing the measured relativistic growth of the density of tracks of proportional detectors, as well as other ionization effects, in the Wilson chamber.

This study was sponsored by the Russian Foundation for Basic Research and the Government of the Kaluga Region (Grant 01-02-96-013).

References

1. Wilson C T R *Proc. R. Soc. London Ser. A* **85** 285 (1911)
2. Glaser D A *Phys. Rev.* **87** 665 (1952)
3. Powell C F, Fowler P H, Perkins D H *The Study of Elementary Particles by the Photographic Method* (London: Pergamon Press, 1959)
4. Fleischer R L, Price P B, Walker R M *Nuclear Tracks in Solids. Principles and Applications* (Berkeley: Univ. of California Press, 1975)
5. Durrani S A, Bull R K *Solid State Nuclear Track Detection: Principles, Methods and Applications* (Oxford: Pergamon Press, 1987) [Translated into Russian (Moscow: Energoatomizdat, 1990)]
6. Marennyĭ A M *Dielektricheskie Trekovye Detektory v Radiatsionno-Fizicheskom i Radiobiologicheskom Eksperimente* (Dielectric Track Detectors in Radiation Physics and Radiobiology Experiment) (Moscow: Energoatomizdat, 1987)
7. Geguzin Ya E, Kaganov M I, Lifshitz I M *Fiz. Tverd. Tela* **15** 2425 (1973)
8. Flerov G N, Barashenkov V S *Usp. Fiz. Nauk* **114** 351 (1974) [*Sov. Phys. Usp.* **17** 783 (1975)]
9. Fischer B E, Spohr R *Rev. Mod. Phys.* **55** 907 (1983)
10. Mozumder A, in *Advances in Radiation Chemistry* Vol. 1 (Eds M Burton, J L Magee) (New York: Wiley-Interscience, 1969) p. 1
11. Kaplan I G *Khim. Vys. Energ.* **17** 210 (1983)
12. Byakov V M, Nichiporov F G *Vnutritrekovye Khimicheskie Protsessy* (Chemical Processes Inside Tracks) (Moscow: Energoatomizdat, 1985)
13. Kaplan I G, Miterev A M *Khim. Vys. Energ.* **19** 208 (1985)
14. Kaplan I G, Miterev A M *Usp. Khim.* **55** 713 (1986)
15. Kaplan I G, Miterev A M, in *Advances in Chemical Physics* Vol. 68 (Eds I Prigogine, S A Rice) (New York: Wiley-Interscience, 1987) p. 255
16. Miterev A M *Ross. Khim. Zh.* **42** (4) 40 (1998)
17. Baranov I A et al. *Usp. Fiz. Nauk* **156** 477 (1988) [*Sov. Phys. Usp.* **31** 1015 (1988)]
18. Jaffe G *Ann. Phys.* (Leipzig) **42** 303 (1913)
19. Lea D E *Proc. Cambr. Philos. Soc.* **30** 80 (1934)
20. Booz J, in *Charged Particle Tracks in Solids and Liquids* (Inst. of Physics and the Phys. Soc., Conf. Series, No. 8, Eds G E Adams, D K Bewley, J W Boag) (London: Inst. of Physics & the Phys. Soc., 1970) p. 19
21. Dennis I, in *Proc. of the Symp. on Microdosimetry, Ispra, Italy, November 13–15, 1967* (Ed. H G Ebert) (Brussels: European Communities, 1968) [Translated into Russian: in *Mikrodozimetriya* (Microdosimetry) (Eds of translation A N Krongauz, V I Ivanov) (Moscow: Atomizdat, 1971) p. 251]
22. Bethe H A, in *Handbuch der Physik* Bd. 24. Tl. 1 (Hrgs. H Geiger, K Scheel) (Berlin: Springer, 1933) p. 273
23. Bohr N *Det. Kgl. Danske Vidensk. Selskab. Math.-Fys. Medd.* **18** 8 (1948) [Translated into Russian: *Prokhozhdenie Atomnykh Chastits cherez Veshchestvo* (Moscow: IL, 1950)]
24. Lea D E *Actions of Radiations on Living Cells* (Cambridge: Univ. Press, 1946) [Translated into Russian (Moscow: Gosatomizdat, 1963)]
25. Lea D E *Br. J. Radiol. Suppl.* **1** 59 (1947)
26. Gray L H *J. Chim. Phys.* **48** 172 (1951)
27. Platzman R L, in *Basic Mechanisms in Radiobiology* Pt. 2 (National Research Council (U.S.) Publ., No. 305, Nucl. Sci. Ser., Rep. No. 15) (Washington: National Acad. of Sciences, National Research Council, 1953) p. 51
28. Samuel A H, Magee J L *J. Chem. Phys.* **21** 1080 (1953)
29. Kuppermann A, Belford G G *J. Chem. Phys.* **36** 1412, 1427 (1962)
30. Ganguly A K, Magee J L *J. Chem. Phys.* **25** 129 (1956)
31. Mozumder A, Magee J L *Radiat. Res.* **28** 203 (1966)
32. Magee J L, Chatterjee A *J. Phys. Chem.* **82** 2219 (1978)
33. Magee J L, Chatterjee A *Radiat. Phys. Chem.* **15** 125 (1980)
34. Santar I, Bednar J *Int. J. Radiat. Phys. Chem.* **1** 133 (1969)
35. Spencer L V, Fano U *Phys. Rev.* **93** 1172 (1954)
36. Platzman R L *Int. J. Appl. Radiat. Isotopes* **10** 116 (1961)
37. Platzman R L, in *Radiation Research: Proc. of the Third Intern. Congress of Radiation Research, Cortina d'Ampezzo, Italy, June-July, 1966* (Ed. G Silini) (Amsterdam: North-Holland Publ. Co., 1967) [Translated into Russian: in *Sovremennye Problemy Radiatsionnykh Issledovaniĭ* (Ed. of translation L Kh Eĭdus) (Moscow: Nauka, 1972) p. 13]
38. Douthat D A *Radiat. Res.* **64** 141 (1975)
39. Berger M J, in *Proc. of the 4th Symp. on Microdosimetry* (Eds J Booz, H G Ebert, R Eickel, A Wacker) (Luxembourg: Commission of the European Communities, 1974) p. 695
40. Kaplan I G, Popova L V, Khadzhibekova L M *Khim. Vys. Energ.* **7** 241 (1973)
41. Heller J M et al. *J. Chem. Phys.* **60** 3483 (1974)
42. Kutcher G J, Green A E S *Radiat. Res.* **67** 408 (1976)
43. Turner J E et al. *Radiat. Res.* **92** 47 (1982)
44. Turner J E et al. *Radiat. Res.* **96** 437 (1983)
45. Tregub V A, Raĭtsimring A M, Moralev V M, Preprint No. 7, No. 8 (Novosibirsk: Institute of Chemical Kinetics and Combustion, Siberian Branch of the USSR Academy of Sciences, 1980, 1981)
46. Pitkevich V A, Duba V V *Radiobiologiya* **21** 829 (1981)
47. Raitsimring A M, Tregub V V *J. Chem. Phys.* **77** 123 (1985)
48. Kaplan I G, Miterev A M, Sukhonosov V Ya *Khim. Vys. Energ.* **20** 495 (1986)
49. Kaplan I G, Miterev A M, Sukhonosov V Ya *Radiat. Phys. Chem.* **27** 83 (1986)
50. Kaplan I G, Miterev A M, Sukhonosov V Ya *Khim. Vys. Energ.* **23** 392 (1989)
51. Kaplan I G, Miterev A M, Sukhonosov V Ya *Radiat. Phys. Chem.* **36** 493 (1990)
52. Mozumder A, Chatterjee A, Magee J L, in *Radiation Chemistry* Vol. 1 (Advances in Chemistry Series, Vol. 81) (Washington: Am. Chem. Soc., 1968) p. 27
53. Magee J L, Chatterjee A *J. Phys. Chem.* **84** 3529 (1980)
54. Kaplan I G, Miterev A M *Dokl. Akad. Nauk SSSR* **280** 127 (1985)
55. Mozumder A *J. Chem. Phys.* **60** 1145 (1974); **62** 4585 (1975)
56. Miterev A M *Khim. Vys. Energ.* **21** 332 (1987)
57. Miterev A M *Khim. Vys. Energ.* **28** 17 (1994) [*High Energy Chem.* **28** 11 (1994)]
58. Kagan Yu K *Dokl. Akad. Nauk SSSR* **119** 247 (1958)
59. Butts J J, Katz R *Radiat. Res.* **30** 855 (1967)
60. Kobetich E J, Katz R *Phys. Rev.* **170** 391 (1968)
61. Vaĭsburd D I, Volkov Yu V, Kol'chuzhkin A M, in *Radiatsionnye Narusheniya v Tverdykh Telakh i Zhidkostyakh* (Radiation-Induced Disturbances in Solids and Liquids) (Ed.-in-Chiefs V V Generalova, O R Niyazova) (Tashkent: FAN, 1967) p. 83
62. Baum J W, Stone S L, Kuehner A V, in *Proc. of the Symp. on Microdosimetry, Ispra, Italy, November 13–15, 1967* (Ed. H G Ebert) (Brussels: European Communities, 1968) p. 269
63. Kudryashov E I et al. *Kosmich. Biol. Meditsina* **4** (5) 35 (1970)
64. Chatterjee A, Maccabee H D, Tobias C A *Radiat. Res.* **54** 479 (1973)
65. Miller J H, Green A E S *Radiat. Res.* **57** 9 (1974)
66. Fain J, Monnin M, Montret M *Radiat. Res.* **57** 379 (1974)
67. Paretzke H G, in *Proc. of the 4th Symp. on Microdosimetry* (Eds J Booz, H G Ebert, R Eickel, A Wacker) (Luxembourg: Commission of the European Communities, 1974) p. 141
68. Varma M N, Baum J W, Kuehner A V *Radiat. Res.* **62** 1 (1975)
69. Wingate C L, Baum J W *Radiat. Res.* **65** 1 (1976)
70. Kaplan I G, Miterev A M, Khadzhibekova L M *Khim. Vys. Energ.* **11** 409 (1977)
71. Kazazyan V T et al. *Fizicheskie Osnovy Ispol'zovaniya Kineticheskoĭ Energii Oskolkov Deleniya v Radiatsionnoĭ Khimii* (Physical Foundations of the Use of Kinetic Energy of Fission Fragments in Radiation Chemistry) (Ed. A K Krasin) (Minsk: Nauka i Tekhnika, 1972)
72. Bulanov L A, Starodubtseva E V, Borisov E A *Khim. Vys. Energ.* **6** 476 (1972)

73. Miterev A M, Kaplan I G, Borisov E A *Khim. Vys. Energ.* **8** 537 (1974)
74. Borisov E A, Kaplan I G, Miterev A M, in *Proc. of the Fourth Tihany Symp. on Radiation Chemistry, Keszthely, Hungary, June 1–6, 1976* (Eds P Hedvig, R Schiller) (Budapest: Akadémiai Kiadó, 1976) p. 1043
75. Davydov A S *Kvantovaya Mekhanika* (Quantum Mechanics) (Moscow: Fizmatgiz, 1963) [Translated into English (Oxford: Pergamon Press, 1965)]
76. Kabachnik N M, Kondrat'ev V N, Chumanova O V, Deposited at VINITI No. 5958-V86 (Moscow: VINITI, 1986)
77. Yudin G L *Zh. Eksp. Teor. Fiz.* **83** 908 (1982) [*Sov. Phys. JETP* **56** 523 (1982)]
78. Jackson J D *Classical Electrodynamics* (New York: Wiley, 1962) [Translated into Russian (Moscow: Mir, 1965)]
79. Ritchi R H *Nucl. Instrum. Methods* **198** 81 (1982)
80. Platzman R L *Radiat. Res.* **17** 419 (1962)
81. Inokuti M *Rev. Mod. Phys.* **43** 297 (1971)
82. Miterev A M *Khim. Vys. Energ.* **28** 105 (1994) [*High Energy Chem.* **28** 83 (1994)]
83. Miterev A M, Borisov E A *At. Energ.* **36** 320 (1974)
84. Pikaev A K *Sovremennaya Radiatsionnaya Khimiya. Osnovnye Polozheniya. Eksperimental'naya Tekhnika i Metody* (Modern Radiation Chemistry. Main Principles. Experimental Technique and Methods) (Moscow: Nauka, 1985)
85. Berkowitz J *Photoabsorption, Photoionization, and Photoelectron Spectroscopy* (New York: Academic Press, 1979)
86. Jahnke E, Emde F, Lösch F *Tafeln Höherer Funktionen* (Stuttgart: Teubner, 1960) [Translated into Russian: *Spetsial'nye Funktsii* (Special Functions) (Moscow: Nauka, 1968)]
87. Miterev A M *Khim. Vys. Energ.* **31** 197 (1997) [*High Energy Chem.* **31** 173 (1997)]
88. Miterev A M *Khim. Vys. Energ.* **30** 98 (1996) [*High Energy Chem.* **30** 86 (1996)]
89. Miterev A M, Mamed'yarov D Yu, Kaplan I G *Khim. Vys. Energ.* **26** 20 (1992)
90. Yudin G L *Zh. Tekh. Fiz.* **57** 1714 (1987)
91. Matveev V I, Musakhanov M M *Zh. Eksp. Teor. Fiz.* **105** 280 (1994) [*JETP* **78** 149 (1994)]
92. Pivovar L I, Krivonosov G A, Tubaev V M *Zh. Eksp. Teor. Fiz.* **53** 1872 (1967) [*Sov. Phys. JETP* **26** 1071 (1968)]
93. Garin B M, Byakov V M *Khim. Vys. Energ.* **22** 195 (1988)
94. Ramazashvili R R, Rukhadze A A, Silin V P *Zh. Eksp. Teor. Fiz.* **43** 1323 (1962) [*Sov. Phys. JETP* **00** (1962)]
95. Landau L D, Lifshitz E M *Statisticheskaya Fizika* (Statistical Physics) Pt. 1 (Moscow: Nauka, 1976) [Translated into English (Oxford: Pergamon Press, 1980)]
96. Slovetskiĭ D I *Mekhanizmy Khimicheskikh Reaktsiĭ v Neravnovesnoĭ Plazme* (Mechanisms of Chemical Reactions in Nonequilibrium Plasma) (Moscow: Nauka, 1980)
97. Kudrin L P *Statisticheskaya Fizika Plazmy* (Statistical Physics of Plasma) (Moscow: Atomizdat, 1974)
98. Miterev A M *Khim. Vys. Energ.* **14** 483 (1980)
99. Ritchie G G, Claussen C *Nucl. Instrum. Methods* **198** 133 (1982)
100. Klimontovich Yu L *Kineticheskaya Teoriya Neideal'nogo Gaza i Neideal'noĭ Plazmy* (Kinetic Theory of Nonideal Gas and Nonideal Plasma) (Moscow: Nauka, 1975) [Translated into English: *Kinetic Theory of Nonideal Gases and Nonideal Plasmas* (Oxford: Pergamon Press, 1982)]
101. Kittel Ch *Quantum Theory of Solids* (New York: Wiley, 1963) [Translated into Russian (Moscow: Nauka, 1967)]
102. Kulik P P, Norman G É, Polak L S *Khim. Vys. Energ.* **10** 203 (1976) [*High Energy Chem.* **10** 185 (1976)]
103. Kulik P P, Norman G É, Polak L S *Khim. Vys. Energ.* **11** 195 (1977)
104. Hochstim A R (Ed.) *Kinetic Processes in Gases and Plasmas* (New York: Academic Press, 1969) [Translated into Russian (Moscow: Mir, 1972)]
105. Ivanov A A, Parail V V, Soboleva T K *Zh. Eksp. Teor. Fiz.* **64** 1245 (1973) [*Sov. Phys. JETP* **37** 631 (1973)]
106. Katin V V, Martynenko Yu V, Yavlinskiĭ Yu N *Pis'ma Zh. Tekh. Fiz.* **13** 665 (1987)
107. Eletskiĭ A V, Palkina L A, Smirnov B M *Yavleniya Perenosa v Slaboionizovannoĭ Plazme* (Transfer Phenomena in Weakly Ionized Plasma) (Moscow: Atomizdat, 1975)
108. Mitchner M, Kruger Ch H (Jr) *Partially Ionized Gases* (New York: Wiley, 1973) [Translated into Russian (Moscow: Mir, 1976)]
109. Gordiets B F, Osipov A I, Shelepin L A *Kineticheskie Protsessy v Gazakh i Molekulyarnye Lazery* (Kinetic Processes in Gases and Molecular Lasers) (Moscow: Nauka, 1980) [Translated into English (New York: Gordon and Breach Sci. Publ., 1988)]
110. Smith D, Adams N G *Pure Appl. Chem.* **56** 175 (1984)
111. Smirnov B M *Zh. Eksp. Teor. Fiz.* **72** 1392 (1977) [*Sov. Phys. JETP* **45** 731 (1977)]
112. Makarov V I, Polak L S *Khim. Vys. Energ.* **4** 3 (1970) [*High Energy Chem.* **4** 1 (1970)]
113. Plotnikov V G, Ovchinnikov A A *Usp. Khim.* **47** 444 (1978)
114. Turro N J *Molecular Photochemistry* (New York: W.A. Benjamin, 1965) [Translated into Russian (Moscow: Mir, 1967)]
115. Pogorelov V E et al. *Usp. Fiz. Nauk* **127** 683 (1979) [*Sov. Phys. Usp.* **22** 248 (1979)]
116. Kaplan I G, Plotnikov V G *Khim. Vys. Energ.* **1** 507 (1967)
117. Landau L D, Lifshitz E M *Gidrodinamika* (Hydrodynamics) (Moscow: Nauka, 1988) [Translated into English (Oxford: Pergamon Press, 1987)]
118. Epifanov G I *Fizika Tverdogo Tela* (Solid State Physics) (Moscow: Vysshaya Shkola, 1977)
119. Vedenov A A, Gladush G G *Fizicheskie Protsessy pri Lazernoĭ Obrabotke Materialov* (Physical Processes at Laser Treatment of Materials) (Moscow: Energoatomizdat, 1985)
120. Novichenok L N, Shul'man Z P *Teplofizicheskie Svoĭstva Polimerov* (Thermophysical Properties of Polymers) (Minsk: Nauka i Tekhnika, 1971)
121. Gol'danskiĭ V I, Lantsburg E Ya, Yampol'skiĭ P A *Pis'ma Zh. Eksp. Teor. Fiz.* **21** 365 (1975) [*JETP Lett.* **21** 166 (1975)]
122. Meisels G G et al. *J. Am. Chem. Soc.* **97** 987 (1975)
123. Meisels G G et al. *J. Phys. Chem.* **82** 2231 (1978)
124. Lipsky S *Chem. Education* **58** 93 (1981)
125. Freeman G R, in *Advances in Radiation Research. Physics and Chemistry: 4th Intern. Congress of Radiation Research, Evian-les-Bains, France, 1970* Vol. 2 (Eds J F Duplan, A Chapiro) (New York: Gordon and Breach, 1973) p. 351
126. Dyne P J, Kennedy J M *Can. J. Chem.* **36** 1518 (1958); **38** 61 (1960)
127. Vereshchinskiĭ I V, Pikaev A K *Vvedenie v Radiatsionnuyu Khimiyu* (Introduction to Radiation Chemistry) (Moscow: Izd. AN SSSR, 1963)
128. Freeman G R *Int. Radiat. Phys. Chem.* **4** 237 (1972)
129. Naumann W, Stiller W *Int. Radiat. Phys. Chem.* **8** 407 (1976)
130. Buxton G V, in *The Study of Fast Processes and Transient Species by Electron Pulse Radiolysis* (NATO Adv. Study Inst. Series, Ser. C, Vol. 86, Eds J H Baxendale, F Busi) (Dordrecht: D. Reidel Publ. Co., 1982) p. 241
131. Hummel A *Can. J. Phys.* **68** 859 (1990)
132. Matsui M, Imamura M *IPCR Cyclotron Prog. Rept.* **5** 93 (1971)
133. Kil'chitskaya S P, Petryaev E M, Kalyazin E P *Khim. Vys. Energ.* **13** 213 (1979)
134. Burns W G, in *Charged Particle Tracks in Solids and Liquids* (Inst. of Physics and the Phys. Soc., Conf. Series, No. 8, Eds G E Adams, D K Bewley, J W Boag) (London: Inst. of Physics & the Phys. Soc., 1970) p. 143
135. La Verne J A, Schuler R H *J. Phys. Chem.* **88** 1200 (1984)
136. La Verne J A, Schuler R H *J. Phys. Chem.* **91** 5770 (1987)
137. Dessauer F *Z. Phys.* **38** 12 (1923)
138. Magee J *Ann. Rev. Phys. Chem.* **12** 389 (1961)
139. Burns W G, Barker R, in *Aspects of Hydrocarbon Radiolysis* (Eds T Gäumann, J Hoigné) (New York: Academic Press, 1968) p. 33
140. Hunt J W, in *Advances in Radiation Chemistry* Vol. 5 (Eds M Burton, J Magee) (New York: Wiley-Interscience, 1976) p. 185
141. Goldanskii V I, Kagan Yu M *Int. J. Appl. Radiat. Isot.* **11** 1 (1961)
142. Borisov E A, Bulanov L A, Starodubtseva E V *Khim. Vys. Energ.* **4** 550 (1970)
143. La Verne J A, Meisels G G *Radiat. Phys. Chem.* **21** 329 (1983)
144. Askar'yan G A *At. Energ.* **3** 152 (1957)

145. Zalyubovskiĭ I I, Kalinichenko A I, Lazurik V T *Vvedenie v Radiatsionnuyu Akustiku* (Introduction to Radiation Acoustics) (Khar'kov: Vyshcha Shkola, 1986)
146. Lyamshev L M, Chelnokov B I, in *Radiatsionnaya Akustika* (Radiation Acoustics) (Ed.-in-Chief L M Lyamshev) (Moscow: Nauka, 1987) p. 8
147. Lyamshev L M *Usp. Fiz. Nauk* **162** (4) 43 (1992) [*Sov. Phys. Usp.* **35** 276 (1992)]
148. Anoshin A I *Zh. Tekh. Fiz.* **47** 2186 (1977)
149. Sukhonosov V Ya, Kaplan I G *Khim. Vys. Energ.* **28** 214 (1994) [*High Energy Chem.* **28** 183 (1994)]
150. Seregin A A, Seregina E A *Khim. Vys. Energ.* **35** 305 (2001) [*High Energy Chem.* **35** 274 (2001)]
151. Yakovlev Yu S *Gidrodinamika Vzryva* (Hydrodynamics of Explosion) (Leningrad: Sudpromgiz, 1961)
152. Baranov I A et al. *At. Energ.* **52** 335 (1982)
153. Golubnichiĭ P I, Kudlenko V G, Yakovlev V I, in *Radiatsionnaya Akustika* (Radiation Acoustics) (Ed.-in-Chief L M Lyamshev) (Moscow: Nauka, 1987) p. 35
154. Vaĭsburd D I et al. *At. Energ.* **39** 366 (1975)
155. Vaĭsburd D I et al. *Vysokoenergeticheskaya Elektronika Tverdogo Tela* (High-Energy Electronics of Solids) (Ed. D I Vaĭsburd) (Novosibirsk: Nauka, 1982)
156. Katz R *Health Phys.* **18** 175 (1970)
157. Paretzke H G, in *Proc. of the 3rd Symp. on Microdosimetry, Stresa, Italy, October 18–22, 1971* (Ed. H G Ebert) (Luxembourg: Commission of the European Communities, 1972) p. 141
158. Katz R, in *Proc. of the 7th Symp. on Microdosimetry* Vol. 1 (Eds J Booz, H G Ebert, H D Hartfiel) (Brussels, Luxembourg: Harwood Acad. Publ. for the Commission European Communities, 1981) p. 583
159. Bibler N E *J. Phys. Chem.* **79** 1991 (1975)
160. Seitz F, Koehler J S, in *Solid State Physics* Vol. 2 (Eds F Seitz, D Turnbull) (New York: Academic Press, 1956) p. 305
161. Baranov I A, Krivokhatskiĭ A S, Obnorskiĭ V V *Zh. Tekh. Fiz.* **51** 2457 (1981)
162. Thompson D A *Radiat. Eff.* **56** 105 (1981)
163. Goland A N, Paskin A *J. Appl. Phys.* **35** 2188 (1964)
164. Ronchi C *J. Appl. Phys.* **44** 3575 (1973)
165. Kazuhiko I *J. Phys. Soc. Jpn* **20** 915 (1965)
166. Vorob'eva I V, Geguzin Ya E, Monastyrenko V E *Fiz. Tverd. Tela* **22** 2253 (1980)
167. Fleischer R L, Price P B, Walker R M *J. Appl. Phys.* **36** 3645 (1965)
168. Bitenskiĭ I S, Paralis É S *At. Energ.* **46** 269 (1979)
169. Vorob'eva I V et al. *Fiz. Tverd. Tela* **26** 1964 (1984)
170. Vorob'eva I V, Geguzin Ya E, Monastyrenko V E *Fiz. Tverd. Tela* **28** 163, 2402 (1986)
171. Vorob'eva I V, Geguzin Ya E, Monastyrenko V E *Fiz. Tverd. Tela* **31** 1 (1989)
172. Vorob'eva I V, Ter-Ovanes'yan E A *Fiz. Tverd. Tela* **34** 414 (1992) [*Sov. Phys. Solid State* **34** 222 (1992)]
173. Vorob'eva I V *Fiz. Tverd. Tela* **36** 653 (1994) [*Phys. Solid State* **36** 360 (1994)]
174. Borin I P *Fiz. Tverd. Tela* **30** 2222 (1978)
175. Das Gupta N N, Ghosh S *Rev. Mod. Phys.* **18** 225 (1946) [Translated into Russian: *Kamera Vil'sona i Ee Primeneniya v Fizike* (Wilson Chamber and Its Applications in Physics) (Moscow: IL, 1947)]
176. Aleksandrov Yu A et al. *Puzyr'kovye Kamery* (Bubble Chambers) (Ed. N B Delone) (Moscow: Gosatomizdat, 1963) Pt. 1 [Translated into English (Bloomington: Indiana Univ. Press, 1968)]
177. Asoskov V S et al. *Tr. Fiz. Inst. Akad. Nauk SSSR* **140** 3 (1982)